



Ghent University

Faculty of Engineering

Department of Flow, Heat and Combustion

Academic Year 2011-2012

**OPTIMIZATION OF SMOKE CONTROL SYSTEMS IN UNDERGROUND SUBWAY STATIONS**

Nicholas Bartlett

Promoter: Bart Merci

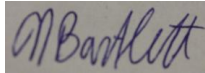
Master thesis submitted in the Erasmus Mundus Study Programme

**International Master of Science in Fire Safety Engineering**

## DISCLAIMER

This thesis is submitted in partial fulfillment of the requirements for the degree of *The International Master of Science in Fire Safety Engineering (IMFSE)*. This thesis has never been submitted for any degree or examination to any other University/programme. The author declares that this thesis is original work except where stated. This declaration constitutes an assertion that full and accurate references and citations have been included for all material, directly included and indirectly contributing to the thesis. The author gives permission to make this master thesis available for consultation and to copy parts of this master thesis for personal use. In the case of any other use, the limitations of the copyright have to be respected, in particular with regard to the obligation to state expressly the source when quoting results from this master thesis. The thesis supervisor must be informed when data or results are used.

April 30, 2012,  
Nicholas Bartlett

A handwritten signature in blue ink, appearing to read "N Bartlett", is placed over a grey rectangular background.

## **Summary/Abstract**

History has shown that fires in underground subway stations pose a severe threat to the life safety of occupants. The purpose of this thesis is to analyze various smoke control strategies in underground subway stations, starting from an existing subway station. Strategies implemented include passive only, mechanical only, and hybrid methods of smoke control. Each case is studied by means of CFD, using FDS V5.0. Cases are ranked based on ability to maintain a smoke free environment on both levels of the station. Platform screen doors and longitudinal ventilation are found to be most useful in controlling smoke spread at platform level. Extraction and stairwell enclosures are seen to control smoke spread to the upper level. Hybrid methods of smoke control result in tenable conditions on both levels for the longest average period of time. Sufficient exit capacity and proper location within the station are critical to ensuring safe occupant egress. Some conclusions drawn can be applied to general fire safety design of subway stations.

# Contents

1. List of Abbreviations & Definitions .....	5
2. List of Tables and Figures .....	6
3. Introduction & Objective .....	9
3.1 Need .....	9
3.2 Objectives.....	10
3.3 Limitations of Research.....	10
4. Literature Review .....	11
4.1 Small Scale Material Tests.....	11
4.2 Heat Release Rates of Subway Trains .....	14
4.2.1 Real-Scale Tests.....	15
4.2.2 Alternate Methods of HRR Prediction .....	18
4.2.3 Previously Proposed Design Fires .....	19
4.2.4 Carry-on Luggage .....	22
4.2.5 Miscellaneous Issues Related to the HRR .....	23
4.2.6 Design Fire Proposal.....	24
4.3 Risk Assessment Discussion .....	24
5. Current Practices in Station Fire Safety .....	25
5.1 Results of Questionnaire.....	25
5.2 Methods of Smoke Control.....	26
5.2.1 Smoke Control Methods – Mechanical Ventilation .....	26
5.2.2 Smoke Control Methods – Natural Ventilation .....	29
5.2.3 Smoke Control Methods – Passive.....	30
6. Case Study Subway Station .....	32
6.1 Station & Tunnel Description .....	32
6.2 Train Geometry .....	33
7. Evacuation Calculations .....	34
7.1 Prescriptive Approach.....	34
7.2 FDS+Evac Approach .....	34
8. CFD Simulations .....	36
8.1. Choice of FDS .....	36

8.2 Organization of Simulations.....	36
8.3 Input Parameters .....	37
8.3.1 Geometry .....	37
8.3.2 Material Selection .....	38
8.3.3 Window Properties .....	39
8.3.4 Soot Production .....	39
8.3.5 Heat Release Rate & Combustion Parameters .....	41
8.3.6 Boundary Conditions.....	41
8.3.7 Radiation Model.....	42
8.4 Tenability Criteria.....	42
9. Results.....	44
9.1 Grid sensitivity .....	44
9.2 Material sensitivity.....	46
9.3 Boundary Condition Sensitivity.....	47
9.4 Resulting HRR.....	49
9.5 Simulation Results – Concourse Level Visibility.....	54
9.5.1 Passive Smoke Control.....	56
9.5.2 Mechanical Smoke Control .....	60
9.6 Simulation Results – Platform Level Visibility.....	68
9.7 Simulation Results - Temperature .....	71
9.8 Simulation Results – Small Fire .....	71
9.9 Ranking of Methods.....	71
9.10 Simulation and Ranking Comments.....	72
10. Conclusions .....	74
11. Acknowledgements.....	76
12. References .....	77
Appendix A: NFPA 130 Calculations.....	81
Appendix B: Ventilation Calculations.....	84
Appendix C: Survey Questions .....	87
Appendix D: Relevant Statistics for Subway Fires.....	89
Appendix E: Obscuration – Visibility Calculations.....	93

Appendix F: Literature Review of Window Failure .....	94
Appendix G: Effect of PSD design on smoke spread .....	96
Appendix H: Calculations for Dynamic Pressure Boundaries.....	98
Appendix I: Visibility Comparison, Stairwell Pressurization vs. Push-Pressurization .....	100
Appendix J: Slices of specific cases and miscellaneous images .....	101
Appendix K: Temperature plots .....	104
Appendix L: Screen shots of Case V and II .....	106

## 1. List of Abbreviations & Definitions

Carriage: The carriage is considered to be comprised of the exterior (skin, windows, and undercarriage components) and all interior components. Carriage is used for consistency when referring an individual subway ‘car’.

Guideway- The portion of the station in which the carriage moves. Not including platforms.

Critical velocity – the minimum rate of airflow necessary to prevent backlayering of smoke at the fire site.

Tenable conditions – conditions which are considered to support human life for a period of time.

Hybrid ventilation – ventilation incorporating mechanical and passive methods of smoke control

Kpc- Thermal inertia (product of conductivity, density, and specific heat)

ASTM – American Society for Testing and Materials

CRF – Critical Radiant Flux

FDS – Fire Dynamics Simulator

CFD – Computational Fluid Dynamics

ASET – Available Safe Egress Time

RSET – Required Safe Egress Time

LES – Large Eddy Simulation

FED – Fractional Effective Dose

HRR – Heat release rate. Energy released from a fire as a function of time.

HRRPUA – Heat release rate per unit area.

## 2. List of Tables and Figures

Figure 1-Peak HRR vs Flame Spread Index. R2coefficient =.13 (Peacock R. B., 2001) .....	12
Figure 2- Eureka Fire Test Results, Rail & Subway Carriages, (Ingason H. , 2006).....	15
Figure 3-HRR curves, EUREKA fire tests (Ingason H. , 2005).....	16
Figure 4- Proposed HRR curves, (Ingason H. , 2006).....	17
Figure 5- UPTUN WP2 Proposal (Ingason H. , 2006).....	17
Figure 6 -Design Fires in Vienna, Munich, Frankfurt (Haack, 2011).....	20
Figure 7 - HRR from carry on luggage. METRO Project (Kumm, 2010) .....	23
Figure 8 - Transverse Ventilation (ASHRAE, 2011).....	27
Figure 9 - Semi - Transverse Ventilation in a Tunnel, Supply and Exhaust (ASHRAE, 2011).....	27
Figure 10 - Zoned Semi Transverse Ventilation (Levy, 1999).....	28
Figure 11 - OTE and UPE ventilation systems ( Tabarra, 2004) .....	29
Figure 12 - Platform screen doors in Dubai Metro (photo taken by author) .....	31
Figure 13 - Station Design with UPE, PSD, and Pressurized Stairwell (Wahlström, 2011) .....	32
Figure 14 - Platform Level, Top View .....	33
Figure 15 - Concourse Level, Top View .....	33
Figure 16 - Queuing at platform exits in FDS+Evac seen at 228 seconds. ....	35
Figure 17 - Front station view, XZ plane, cut at Y=45, platform level.....	37
Figure 18 - Isometric station view (concourse ceiling clipped for clarity) .....	38
Figure 19 - Soot Yields of various materials (Tewarson A. ).....	40
Figure 20 - FRP Polyester properties (Chiam, 2005) .....	40
Figure 21 - Front view of carriage and burner .....	41
Figure 22 - Mesh Specifications .....	45
Figure 23 - Grid Sensitivity, All Meshes, Temperature vs. Station Height. Location 14 meters from fire source along station centerline. Averaged over 30 seconds from 390 to 420 seconds. Very fine and fine meshes converge. ....	46
Figure 24 - Temperature vs. Height. Concrete and Brick vs inert station material properties.....	47
Figure 25 - Dynamic Pressure vs. Height for OPEN and Dynamic Pressure BCs Taken 20 meters from tunnel portal and averaged over 30 seconds from 70 to 100 seconds .....	48
Figure 26 - Visibility at V1 & V3, Open vs. dynamic pressure BCs. 10 meter tenability criteria. See Figure 32/33 for location. ....	49
Figure 27 – Resulting HRR & Burn Rate verse time. Burn rate windows simulated not seen as it is identical and thus overlapped by the yellow curve. Yellow curve follows right Y-axis. Green curve (windows breaking), follows theoretical HRR curve most closely/ .....	50
Figure 28 - Glass temperature vs Time, base case, fine mesh. 8 thermocouples representing 8 window panes. Fallout at 600 Celsius.....	51
Figure 29 - Temperature vs Height, Window breakage vs. no window breakage. 15 meters from fire source. Averaged over 30 seconds from 200-230 and 390-420. ....	52
Figure 30- Oxygen Mass Fraction vs. Time. Data points along the length of the carriage, just outside. Each vertical section represents the length of the carriage on fire, proceeding in averaged time from left	

to right. First vertical box is averaged from 90-95, second from 95-100, and so on. Spikes represent the three doors of the car. The change in the first spike in each subsequent vertical section represents fluctuations in oxygen mass fraction just outside the carriage, as flames leave and then return to the carriage via one door. Only small fluctuations are seen during this time interval as station is well ventilated and fire is small..... 53

Figure 31 - Oxygen Mass Fraction vs. Time. Data points along the length of the carriage, just outside. Each vertical section represents the length of the carriage on fire, proceeding in averaged time from left to right. First vertical box is averaged from 300-305, second from 305-310, and so on. Spikes represent the three doors of the car. The change in the first spike in each subsequent vertical section represents fluctuations in oxygen mass fraction just outside the carriage, as flames leave and then return to the carriage, of one door. Large fluctuations are seen in this chart as the fire is large and station less well ventilated. .... 53

Figure 32 - Locations of visibility and temperature detectors in FDS, Side View ..... 54

Figure 33 - Location of visibility and temperature detectors in FDS, Top View, Concourse Level ..... 54

Figure 34- Smoke Screens as seen in Smokeview ..... 56

Figure 35 - Stairs 1 & 3 Enclosed..... 57

Figure 36 - Stairs 2/4 & Escalators 1/2 enclosed (concourse not shown) ..... 57

Figure 37 - Top view of platform level with platform screen doors (seen in green). Platform B clear after 300 seconds. .... 58

Figure 38 - Multiple smoke screen design. Additional screens bisect longitudinal screens..... 58

Figure 39 - Visibility at point V1 (see figure 32/33 for location) .Tenability exceeded under 10 meters... 59

Figure 40 - Visibility at V3 (see figure 32/33 for location).Tenability exceeded under 10 meters ..... 59

Figure 41 - Push Only, Smoke spread at 180 seconds ..... 60

Figure 42 - Pull Pull, Smoke spread at 180 seconds..... 60

Figure 43 – Pull Only, Smoke spread at 180 seconds ..... 61

Figure 44 – Pull-Pull, 180 seconds..... 61

Figure 45 – Visibility at V1 (refer to Figure 32/33 for location). All cases longitudinal ventilation only. ... 62

Figure 46 – Visibility at V3 (refer to Figure 32/33 for location). All cases longitudinal ventilation only. ... 62

Figure 47 - Atrium Vents, 240 Seconds..... 63

Figure 48 - Exhaust ports for ceiling vents..... 63

Figure 49 -10 exhaust ports (some exhaust ports seen not extracting), 240 seconds ..... 64

Figure 50 - Side Extraction, 240 seconds ..... 64

Figure 51 - Visibility at V1 (refer to Figure 32/33 for location), all mechanical extraction methods ..... 65

Figure 52 - Visibility at V3 (refer to Figure 32/33 for location), all mechanical extraction methods ..... 65

Figure 53 - Visibility at V1 (refer to Figures 32/33 for location). All hybrid methods of smoke control. Pull-Pull with revised PSD+ Windows not shown as tenability not exceeded in 420 seconds. .... 67

Figure 54 - Visibility at V3. (refer to Figures 32/33 for location). All hybrid methods of smoke control. Pull-Pull with revised PSD+ Windows not shown as tenability not exceeded in 420 seconds. .... 68

Figure 55 - Placement of beam detectors V4, V5, V6, and V7. Top view. Platform level..... 68



Figure 56 - Visibility at V4. No cases with platform screen doors are shown as smoke does not spread to platform B. The best case is where smoke is pushed and exhausted, mitigating backlayering and thus spread to Y=75. ....	69
Figure 57 - Visibility at V5. Cases with “Push” and with the revised platform screen doors perform well. When ‘Push’ is combined with platform screen doors, the ‘push’ only prevents smoke from backlayering within the PSDs. Smoke that is not caught by the PSDs is free to spread on the platform and therefore tenability at V5 is lost quicker with PSDs. ....	69
Figure 58 - Visibility at V6. Pull-Pull with PSDs is seen as the best case scenario. This is due to a higher pressure region which prevents flow to this area of the platform. Instead, smoke which has previously entered the platform is actually pulled back into the guideway through the open doors in the PSDs. Appendix K details this phenomenon. Push-Push configuration not shown at tenability is maintained for longer than 420 seconds. ....	70
Figure 59 - Visibility at V7. All hybrid methods of smoke control. Two of the three best cases use platform screen doors. The other of the top three pulls from the portal opposite V7, permitting V7 to maintain tenable conditions for longer. ....	70
Figure 60 - 1999-2005 Fire Incidents, Korea (Yoon, 2009) .....	89
Figure 61 - Rail fires in the US -2003-2007 .....	90
Figure 62 - Rail Accidents, 2006-2008, Europe (Agency, 2010) .....	90
Figure 63 - Fire Causes (Chiam, 2005).....	91
Figure 64 - Rail Fire Sources USA, 2005-2009 (Hall, 2011).....	92
Figure 65 - Gas Temperature at Fallout (Brabrauskas).....	94
Figure 66 - Pane Temperature at Fallout (Brabrauskas).....	95
Figure 67 - Revised PSD, 300 seconds, platform B clear .....	97
Figure 68 - Smoke Spread and visibility at X=2.6 m. Stairwell pressurization only, 180 seconds .....	100
Figure 69 - Smoke Spread and visibility at X=2.6 m. Stairwell Pressurization + Push of 3 m/s from left tunnel portal., 180 seconds Less smoke spread seen at platform level, more spread at concourse level. ....	100
Figure 70 – Pressure slice. For Push, Ceiling Exhaust, Revised PSD, Stairs Enclosed configuration. Top view. Z=3 (.8 meters above platform height). Time=30 seconds Pressure difference seen on platform which drives flow to right. Causing V7 to be exceeded quicker and V1 and V3 (not shown, at concourse level) to be tenable for much longer. ....	101
Figure 71 - Pressure slice for push, side exhaust, revised PSD, stairs enclosed configuration. Top View Z=3 (.8 meters above platform height). Time=30 seconds. Little pressure difference seen, therefore flow is not directed to the right as much and thus smoke flow occurs quicker to V1/V3 on the concourse.....	101
Figure 72 - Velocity vectors stairwell 2. Side view. Push, Side Exhaust, Revised PSD, Stairs Enclosed. It is seen that velocity vectors move from platform to concourse, allowing smoke spread. Time=83 seconds. ....	102
Figure 73 -Velocity vectors stairwell 2. Side view. Push, Ceiling Exhaust, Revised PSD, Stairs Enclosed. It is seen that velocity vectors move from concourse to platform, delaying smoke spread to concourse. Time=83 seconds. ....	102

Figure 74 - Pull - Pull with PSD Revised. Left tunnel portal shown. Top-view shows platform level only. Visibility maintained in higher pressure region on platform (corresponding to where V6 is located). Time=160 seconds. Concourse visibility also maintained due to make-up air entering from concourse level.....	103
Figure 75 - Push-Push Side Exhaust Stairs Enclosed. Smoke Spread. Platform ends kept clear. Shot at 240 seconds .....	103
Figure 76 –Side View of smoke spread. 500 kW Fire. 420 Seconds. Side Exhaust, Revised PSD, Stairs Enclosed.....	103
Figure 77 - Top View of smoke spread. 500 kW Fire. 420 Seconds. Side Exhaust, Revised PSD, Stairs Enclosed .....	103
Figure 78 - Temperature vs Time at point T3. No case exceeds 60 degrees Celsius. ....	104
Figure 79 - Figure 76. Temperature vs Time at point T5 (half of the cases from Table 6 shown) .....	104
Figure 80 - Temperature vs Time, Point T5. Half of the cases from Table 6.....	105
Figure 81 - Smoke spread at 4 minutes. Case V. Side view.....	106
Figure 82 – Smoke spread at 4 minutes. Case V. Top View .....	106
Figure 83 – Smoke spread at 4 minutes. Case II. Side view. ....	106
Figure 84 - Smoke spread at 4 minutes, Case II. Top view.....	106

### 3. Introduction & Objective

#### 3.1 Need

Mass transit systems are a prominent form of transportation in many countries throughout the world. The number of mass transit systems has increased dramatically since the 1970s and this trend is continuing. As of April 2012, there were 183 worldwide metro systems, containing more than 8,500 stations and more than 10,500 kilometers of track length, representing more than 112 million passenger rides daily (Metrobits.org, 2009). While not all of these stations and distances are necessarily contained underground, the fact is that the quantity of underground systems and thus ridership is ever increasing. As a result, extra attention must be given to safety. Of particular interest is fire safety, in light of the history of catastrophic fires that have occurred in subway stations. Recent fires in London’s Kings Cross station (1987, 31 deaths), Baku Underground (Azerbaijan, 1995, 289 deaths), and Daegu (South Korea, 2003, 198 deaths), reiterate that fire safety must not be taken lightly due to the potentially devastating consequences.

Subway stations present a unique challenge for fire safety. In case of a fire, large numbers of people may need to be evacuated from several floors below grade. Exits may be limited, and occupants may be unfamiliar with the station layout. Fires that originate in carriages are very large and grow rapidly, especially if the origin is due to arson. The result of these factors is that a station will be quickly filled with toxic smoke, preventing passengers from escaping. Ultimately, injuries and death may result.

Globally, there are many different approaches to smoke control in underground subway stations. Furthermore, each underground station is a unique design, making it difficult for a set of prescriptive

requirements to cover all possible cases. This work first aims to investigate the various existing approaches through a literature study and industry survey. It then seeks, via CFD modeling, to provide general recommendations and ideas for smoke control strategies which will help make underground subway stations safer in case of fire.

### **3.2 Objectives**

The objectives of this research are:

- 1) To make a literature study on "good practice" for dimensioning smoke control systems for upgrading existing underground subway stations.
- 2) To classify acceptable safety levels in different countries.
- 3) To perform a sensitivity study (CFD) on several parameters for an existing subway station and compare different strategies to control the smoke spread and allow for tenable conditions to be maintained.
- 4) To propose recommendations for optimizing the smoke control systems in existing subway stations.

In considering these objectives, safe egress of occupants is paramount. Thermal response of structures or access for firefighters is not directly considered.

### **3.3 Limitations of Research**

The physical dimensions of the carriages and station used in this study are based on engineering drawings provided to the author by the metro system, unless changed as noted. Attempts were made to replicate these drawings in all computer modeling as accurately as possible. No testing has been conducted to validate the results. The assumptions made during the course of the study may substantially affect the results and conscious efforts were made to ensure assumptions were as accurate and realistic as possible. Some major assumptions made include:

- a) Design fire (Carriage HRR, growth, and location)
- b) Simulation boundary conditions
- c) Smoke production rate
- d) Ventilation conditions via windows breaking
- e) Thermal properties of materials

The study is further limited by the inherent approximations made as a result of choosing CFD to model the station. These include combustion models, radiation models, heat transfer models, sub-grid models, and other models used in the chosen CFD package. Finally, grid sensitivity studies have not been conducted on all scenarios. Thus, the CFD study as a whole can be considered qualitative.

## 4. Literature Review

### 4.1 Small Scale Material Tests

Prescriptive requirements have been put in place in many countries to ensure a minimum level of fire safety for carriage materials. Thus, oftentimes materials are judged as being safe for use in carriage construction in that they comply with various material performance standards such as those contained in ASTM 162, ASTM D3675, ASTM C 542, DIN 5510, EN 45545, BS 476-6, and BS 476-7. Such tests, while permitting for relative ranking of materials, are conducted in such a way that they do not consider factors which have been repeatedly stated to be of utmost importance in fire safety design, such as the heat release rate. Furthermore, they do not properly assess the material's performance and its interaction with the environment in its proposed configuration. Thus, it can be said that the current approach to material selection is on a component-based approach, not a systems-based approach. Some legitimate questions to be asked then are: does performance in these individual material tests actually correlate with full-scale performance? For design considerations, can materials compliant with these tests be used to promulgate the selection of less severe design fires?

One relevant study by NIST & Volpe National Transportation Systems Center contained in (Peacock R. B., 2001) examines this question. The study focused on establishing a correlation between the results of several component level tests to pertinent full-scale fire behavior attributes. This included ASTM 162, ASTM E 648, and ASTM E 662.

ASTM 162 & ASTM D 3675 measure material flammability in terms of vertical flame spread. The result of this test is a numerical value, the "flame spread index",  $I_s$ .  $I_s$  is a combination of two test variables: the flame spread factor and the heat generation factor. NFPA 130 (NFPA, 2010), as an example, prescribes a maximum  $I_s$  value depending upon the part of the carriage. Less than 25 for cushioning, less than 100 for windows, less than 35 for seat and mattress frames, etc. Figure 1 shows test results which plot various items' peak HRR, as measured in the cone calorimeter, to the prescriptive value obtained for the flame spread index,  $I_s$  (Peacock R. B., 1999). The prescriptive thresholds, depending upon carriage part, are superimposed as dotted horizontal lines.

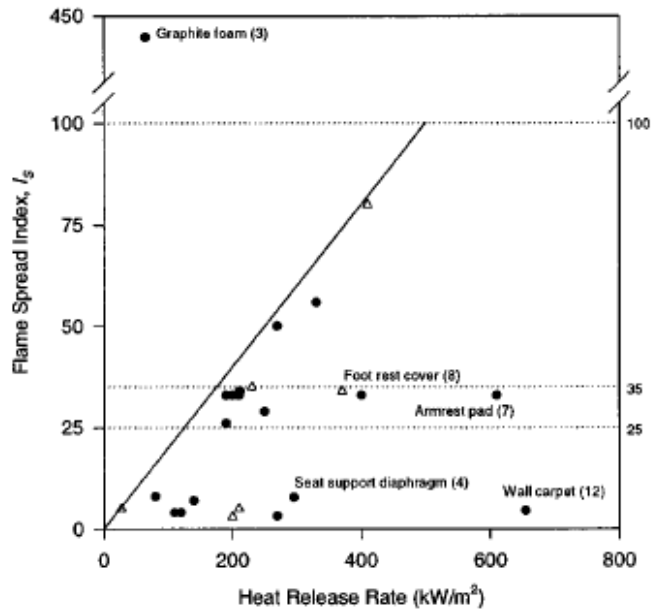


Figure 1-Peak HRR vs Flame Spread Index. R2coefficient =.13 (Peacock R. B., 2001)

The superimposed diagonal line in Figure 1 establishes a correlation between  $I_s$  and actual HRR, as obtained in via cone calorimeter testing. One can see from the data set that the  $I_s$  value is primarily an indicator of *minimum* HRR. Only one tested material lies above the curve, indicating that it had a lower tested HRR than expected for its  $I_s$  value. The remaining materials lie below the curve, indicating higher HRRs than expected for the given  $I_s$ . The data implies then that ASTM 162 and the  $I_s$  value may be used only as an indicator of best-case performance. It is of use to note that the points on the chart represent a wide range of materials used in trains, from plastics to elastomers & foams.

ASTM E 648 measures the response of a floor covering to an imposed radiant flux that varies along 1 m sample length from 11 kW/m<sup>2</sup> to 1 kW/m<sup>2</sup>. The result of the test is a CRF (critical radiant flux) value; that is, after the sample length is ignited, the flux at the distance which the burning floor self-extinguishes. NFPA 130 requires a CRF greater than or equal to 5 kW/m<sup>2</sup>. Two floor coverings were tested in (Peacock R. B., 1999), at flux of 50 kW/m<sup>2</sup> (concluded to be more representative than that specified in the test procedure). The result was CRF values of 7 kW/m<sup>2</sup> and 11 kW/m<sup>2</sup>. Cone calorimeter values were 250 kW/m<sup>2</sup> and 300 kW/m<sup>2</sup>. Due to limited test data, no conclusions were drawn. It would be of value for future test work to expand on this data set to develop a correlation with peak HRR to determine the test validity.

Finally, (Peacock R. B., 1999) examines ASTM E 662. This measures smoke generation from small specimens exposed to both flaming and non-flaming heat fluxes. The result is a value called  $D_s$ , which is described as the specific optical density and is measured in a closed chamber. The measurement method is through a polychromatic light beam, and values for  $D_s$  are taken at 1.5 and 4 minutes into the test. The first conclusion drawn was that the results of the ASTM E 662 test method and the cone calorimeter method for measuring smoke (per ASTM E 1354) were not directly comparable due to variation in measurement techniques. Therefore, an alternative approach was taken. The values of  $D_s$

per ASTM E 662 at 4 minutes were found to have good correlation with cone calorimeter smoke measurement at 1 minute. There is value in this approach, in that establishing a correlation with cone calorimeter data provides a potential link to HRR data, a much more indicative index in assessing full-scale performance.

A more recent study was conducted in the United States by the National Association of State Fire Marshals (NASFM) and FTA (Federal Transit Administration), in conjunction with Underwriters Laboratories (UL). The study researched the adequacy of existing rail carriage and bus fire safety standards and investigated potential improvements in test methods and performance criteria (UL, 2008). One major conclusion from the study was that bench-scale material tests do not predict real-world fire performance of materials used in rail carriages and buses. The study proposed upgrades to existing guidelines in order to improve fire safety criteria. The major recommendations included the addition of small-scale cone calorimeter testing according to ASTM 1354-99 and testing according to BSS 7239, to attempt to limit smoke toxicity. These recommendations were taken in the context of the needs of NFPA 130 (for example, toxicity requirements in EU45545-2 were also considered, however the BSS test setup better fit the existing testing infrastructure as well as the market of those clients using NFPA 130).

The UL testing demonstrated a correlation between the ASTM 1354-99 cone calorimeter testing and real-scale testing according to NFPA 286 (Room Corner Test). Materials were ranked by their performance in ASTM 1354 and separated based on whether they did or did not cause a flashover in the NFPA 286 test. The recommendations of additional test criteria according to ASTM 1354 are as follows:

*“For wall and ceiling panels, partitions, shelves, opaque windscreens, end caps, roof housings, and HVAC ducting, add criteria of Avg. HRR@180 seconds  $\leq$  120 kW/sq. m. and Max HRR  $\leq$  140 kW/sq. m. These numbers are derived from the ASTM E1354-99 @ 50 kW/m<sup>2</sup> applied heat flux with a retainer frame.”*

Finally, specific recommended test criteria in regards to BSS 7239 are as follows:

HCN  $\leq$  150 ppm  
CO  $\leq$  3500 ppm  
NO/NO<sub>2</sub>  $\leq$  100 ppm  
SO<sub>2</sub>  $\leq$  100 ppm  
HF  $\leq$  200 ppm  
HCL  $\leq$  500 ppm

Further details regarding these recommendations are extensive and a presentation on such information here is outside the scope of this work. Reference should be made to (UL, 2008) for test data and detailed explanations of conclusions and recommendations.

If current bench-scale test methods are indeed an unreliable method of assuring acceptable fire performance of train carriage interiors, then new methods must be considered for material selection. While amending existing standards to include additional tests is one option as proposed in (UL, 2008),

one recent study provides an alternative approach which could prove promising if investigated in further detail. In (Lautenberger, 2009), a reverse engineering approach is taken. One current method of material design & selection is to construct a computer model, using material properties derived from cone calorimeter tests as inputs, and use this to predict real-scale performance. If real-scale performance is known (or standards are set defining acceptable performance levels), it might be possible to use modeling to predict material properties which would result in acceptable performance levels. Coles, Lautenberger, and Wolski (Lautenberger, 2009) conducted real-scale tests on two transverse double seats, resulting in transient curves for HRR, gas temperature, heat flux, and mass loss. Then, using FDS 5.0, they attempted to estimate material properties which would result in similar performance. In order to avoid performing cone calorimeter tests on the materials as input to the CFD calculations, they used a genetic algorithm to guess hundreds of combinations of material properties. The desired result of the simulation is a combination of material properties resulting in an HRR curve that is a good match with the experimental data generated. In this case, the shapes of the curves matched well, but the CFD modeled peak HRR over-predicted the experimental value by 15% and also occurred 45 seconds later. Peak temperature and heat fluxes agree, but the time at which they occur did not.

This approach provides an alternative method of arriving at acceptable materials. If an HRR curve is known, or parameters are prescribed which describe an acceptable curve (such as growth rate and peak HRR), then combinations of acceptable material properties could be specified. This method would need to be well validated, as testing is not necessary on any scale. The interaction between material properties, material geometry, and item orientation can also be evaluated in this manner to achieve the best performing curve. This method has the potential to minimize costs as manufacturers would not need to conduct testing. However, without this additional testing, the review and acceptance of such modeling would require a high level of technical competence in CFD modeling for third-party reviewers and approving agencies.

Material selection, be it based on prescriptive codes or alternative methods, should result in a safer carriage in the event of a fire. In design terms, this should lead to selecting a design fire with a lower HRR, slower growth, less toxic byproduct & soot production, or at least a combination of the above. Unfortunately, design fires cannot easily be extrapolated simply from compliance with prescriptive material requirements. Therefore, it is necessary to conduct full scale and model-scale tests to assist in design fire predictions.

## **4.2 Heat Release Rates of Subway Trains**

In a subway fire, the most important variables controlling the necessary level of safety and ventilation are the peak heat release rate (HRR), and the fire growth rate (Colella, 2010). The fire growth rate will determine whether individuals in the vicinity have sufficient time to escape. The HRR, depending upon the combustibles being burned, will determine the required size of the smoke control system to assist in providing tenable conditions for evacuation.

In fire safety engineering, the design fire is an attempt at quantifying a real world phenomenon into an engineering concept for practical use. This is typically accomplished by representing the fire life cycle as

a combination of three distinct phases: the growth, peak HRR, and decay. As previously mentioned, the growth and the peak HRR are the primary variables which will control the required level of safety.

#### 4.2.1 Real-Scale Tests

Real-scale testing has been one attempt to quantify the design fire. One of the major series of tests that has been conducted which provides insight in to real-scale HRR's of subway and rail vehicles was the EUREKA 499 test series (Ingason H. , 2006). The results are based on the burning of single carriages. The time to peak HRR varied between tests from 5 to 80 minutes, and the peak HRR varied from 7 to 43 MW. Results from both rail cars and subway carriages are shown in Figure 2 for completeness. For the subway carriages and two German IC rail cars, the tests were conducted with the doors closed and one of the glass windows open. The aluminum roof skin on the 35 MW subway carriage melted (which increased ventilation during the test) (Cutonilli, 2010). Details of the tests, including train construction (exterior & interior), ignition source, and calorimetry methods are found in (Chiam, 2005).

Type of vehicle, test series, test nr, u=longitudinal ventilation m/s	Calorific value (GJ)	Peak HRR ( $\dot{Q}_{max}$ ) (MW)	Time to peak HRR (min)	Peak temperatures in tunnel ceiling (°C)	Reference
<i>Rail</i>					
A Joined Railway car; two half cars, one of aluminium and one of steel, EUREKA 499, u=6-8/3-4 m/s	55	43	53	980	Steinert [20]
German Intercity-Express railway car (ICE), EUREKA 499, u=0.5 m/s	63	19	80	830	Steinert [30]
German Intercity passenger railway car (IC), EUREKA 499, u=0.5 m/s	77	13	25	720	Ingason et al [30]
British Rail 415, passenger railway car <sup>*)</sup>	NA	16	NA	NA	Barber et al. [31]
British rail Sprinter, passenger railway car, fire retardant upholstered seatings <sup>*)</sup>	NA	7	NA	NA	Barber et al. [31]
<i>Metro</i>					
German subway car, EUREKA 499, u=0.5 m/s	41	35	5	1060	Ingason et al [30]
German metro steel car, EUREKA 499, u=0.3 m/s	33	NA	NA	630	[16]

Figure 2- Eureka Fire Test Results, Rail & Subway Carriages, (Ingason H. , 2006)

The detailed HRR curves are shown in Figure 3. The 35 MW peak for the subway carriage is reached in approximately 5 minutes.



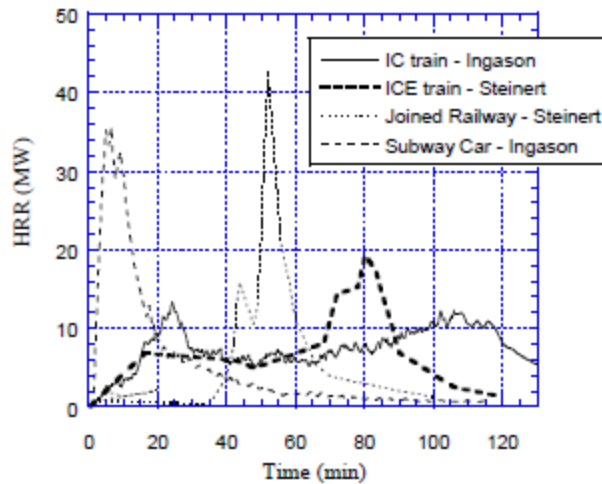


Figure 3-HRR curves, EUREKA fire tests (Ingason H. , 2005)

Recognition to further define design fire scenarios was made during the UPTUN project. The goal of the UPTUN project was to provide a methodology for upgrading tunnels in terms of fire safety (Marlair, 2008). One part of this project included a literature study which would lead to the proposal of design fire curves. Additional parts of this project included collaboration with real-scale tests conducted in the Runehamar tunnel with heavy goods vehicles. Ingason (Ingason H. , 2006) pointed out that based on the results of these tests, it is possible for the HRR in a tunnel fire to reach very high heat release rates, up to 100 MW, in less than 10 minutes. And although these results are not for subway carriages, it is clearly shown in Figure 3 that the subway carriage had the fastest growth rate of all the EUREKA fire tests, reaching 35 MW in just over 5 minutes. With this in mind, it is not safe to assume passengers have time to evacuate safely without additional measures.

In selecting a design fire, the fire growth rate is essential. Ingason (Ingason H. , 2006) developed design fire equations based on a quadratic model of fire growth, a constant peak, and an exponential decay. He proposed, for a subway carriage of aluminum construction, a peak HRR of 35 MW with a growth factor ( $\alpha_{g,q}$ ), of  $1.08 \text{ MW}/\text{min}^2$  and a decay factor ( $\alpha_{d,q}$ ) of  $.06 \text{ min}^{-1}$ . The values are proposed on the basis of the EUREKA fire test results. The equations and time intervals are shown below. With a peak HRR of 35 MW and growth of  $1.08 \text{ MW}/\text{min}^2$ , the proposed subway design fire will peak at 5 minutes and 40 seconds.

Method Reference	HRR as a function of time t (s)	Time interval (s)	Time to maximum HRR (s)	Time to decay starts, $t_D$ , and/or fire duration, $t_d$ (s)	Other conditions
Quadratic growth  Ingason [33]	$HRR = \alpha_{g,q} t^2$	$0 \leq t_{max}$	$t_{max} = \sqrt{\frac{\dot{Q}_{max}}{\alpha_{g,q}}}$	$t_D = \frac{2E_{tot}}{\dot{Q}_{max}} + \frac{2}{3}t_{max} - \frac{1}{\alpha_{D,q}}$	If $t_D \leq t_{max}$ no constant period, then  $\dot{Q}_{max} = X\alpha_{D,q}E_{tot} \left(1 - \frac{\alpha_{D,q}^{3/2}}{6} \sqrt{\frac{2E_{tot}}{\alpha_{D,q}}}\right)^2$ and  $t_{max} = \sqrt{\frac{\dot{Q}_{max}}{\alpha_{g,q}}} = t_D$
	$HRR = \alpha_{g,q} t_{max}^2 = \dot{Q}_{max}$	$t_{max} < t < t_D$			
	$HRR = \dot{Q}_{max} e^{-\alpha_{D,q}(t-t_D)}$	$t \geq t_D$			

Figure 4- Proposed HRR curves, (Ingason H. , 2006)

UPTUN, based on their literature review and real-scale tests, proposed slightly different recommendations. They leave the decision to the designer whether to select a design fire in which the subway vehicle is considered “low combustible”, “normal combustible”, or consider a scenario with two or more carriages on fire. The growth rate is treated linearly. With a HRR equal to or less than 30 MW (classification of “low” or “normal” combustible”), a growth rate of 10 MW/minute is proposed. With a HRR greater than 30 MW (for two carriages), a growth rate of 20 MW/minute is proposed. This means that if a single, normal combustible carriage is assumed as the design fire, the suggested design will reach its peak of 20 MW in two minutes. Whereas the EUREKA tests show a single subway vehicle with aluminum construction had a peak HRR of 35 MW, the UPTUN conclusions slightly contradict this in saying a fire of such a size would actually be represented as two carriages. In this case, two carriages should have a HRR of at least 30 MW, and with the proposed growth rate, the peak HRR would be reached in 3 minutes, several minutes shorter than the 5 minutes and 40 seconds proposed by Ingason.

HRR MW		Road, examples vehicles	Rail, examples vehicles	Metro, examples vehicles	At the fire boundary
Risk to life structure	5	1-2 cars			ISO 834
	10	Small van, 2-3 cars, ++	Electric locomotive	Low combustible passengers carriage	ISO 834
	20	Big van, public bus, multiple vehicles		Normal combustible passengers carriage	ISO 834
	30	Bus, empty HGV	Passengers carriage	Two Carriages	ISO 834
	50	Combustibles load on truck	Open freight wagons with lorries	Multiple carriages (more than two)	ISO 834
	70	HGV load with combustibles (approx. 4 tonne)			HC

Figure 5- UPTUN WP2 Proposal (Ingason H. , 2006)

Real scale tests were performed in 2011 under the METRO project, in an abandoned tunnel in Arvika, Sweden. Two subway carriages from the Stockholm metro were used in the test. One car was tested as-received, while another car was retrofitted with aluminum paneling on the interior to represent a more modern carriage. The maximum HRR of each test was very similar, with values of 76.7 and 77.4 MW. The old carriage reached its peak HRR in 12.7 minutes. The retrofitted carriage burned with a very low HRR

for about 110 minutes. After this time, two liters of diesel fuel was ignited, and a fire growth very similar to the other test was seen. This indicates that the newer style carriage with the aluminum paneling gives passengers a longer time to react to a developing fire. It is very important to note that one reason why the HRRs were much higher than those seen in the EUREKA tests was that luggage was placed in the carriages to more realistically represent the actual contents on board during a fire. In total, 79 pieces of luggage were placed throughout the carriage, with a weight of 351 kg (they were filled with clothes and papers). (Lonnermark, 2012). Also of note in these tests is that the doors fell out during the tests.

Real-scale tests were conducted at Carleton University on a subway carriage. The doors on one side were left open (four total). The maximum HRR of this test was 52.5 MW, reaching this about 9 minutes after ignition (Hadjisophocleous, 2012). It is interesting to note that the fire grew from 1 MW to 52.5 MW in only 140 seconds. The initial 7 minutes of the test showed very little fire growth.

Additional real-scale tests are referenced in a literature review by Chiam (Chiam, 2005). These were of Japanese train cars compliant with Japanese regulations. The details of the tests are not known, but the values of HRR range between 10 and 20 MW.

#### **4.2.2 Alternate Methods of HRR Prediction**

Although real-scale tests are the preferable and best method of predicting the HRR, alternate methods of predicting the HRR of a subway carriage exist, based mostly on small scale testing of individual car components, computer modeling, model-scale tests, or a combination of the aforementioned. These methods, though they contain inherent uncertainty, are necessary, as conducting real-scale tests are expensive and not practical (Cutonilli, 2010).

Hughes & Associates (Cutonilli, 2010) developed a method to predict the HRR of a rail car based upon computer fire modeling and calorimetry tests. The small scale calorimetry tests are used to generate input for two computer fire models (which they call HAIFGMRail and HAICFMRail) in the form of material properties such as ignition temperatures, thermal properties, and smoke and species yields. The combination of the two programs results in heat and smoke generation rates. According to Hughes, these models have been validated by comparison with available data, and have been used in the design of ventilation systems in various rail systems. One advantage of the HAIFGMRail program is that it simulates fire spread pre-flashover. This is important to consider as not all ignition sources will lead to a flashover. The HAICFMRail program is used to determine the smoke and heat production rate in the fully-developed fire. Window failure, which is found to change HRR predictions substantially due to changes in ventilation (Beyler), is included based on the results of experiments. Additionally, the model does not rely solely on user input for burning rate. Rather, it models an interrelationship between compartment temperature, airflow rates, and burning rate. Modeling of burning rates from several different materials is considered.

Using the two aforementioned programs and small scale test data, Hughes & Associates (Cutonilli, 2010) tried to simulate three of the full-scale EUREKA fire tests, namely, the 35 MW subway carriage, and the two German IC rail cars. First, they used HAIFGMRail to determine an ignition source size that would lead the car to flashover. Then, they modeled the HRR under several different ventilation conditions.

Results are stated as being similar to the subway carriage, with a peak HRR of 25 MW after only several minutes. Full details are contained in the source Cutonilli, 2010. An interesting claim is also made that newer railcars may produce higher heat release rates when compared to older rail cars, due to replacement of metals with plastic composites and glass with polycarbonate. Regarding the growth rate, the quick two-minute rise is also supported by newer real-scale test results from 2005 in Australia (White, 2005), in which a rail car resulted in flashover conditions between 140 and 175 seconds (fire was fuel-controlled, as test was conducted outdoors) . In general, the work by Hughes & Associates appears to support the use of higher heat release rates as design fires, in the order of at least 15-35 MW, based on the output of their program and when compared favorably with real-scale fire test results.

A peak HRR of 5 MW was proposed by Chiam (Chiam, 2005) for subway carriages in stations, and 10 MW for subway carriages in tunnels. Chiam conducted extensive cone calorimeter tests to evaluate interior materials' reaction to fire (for items such as seats, flooring, wall panels, etc.), obtaining properties such as ignition temperature, *kpc*, and HRR curves. The information derived from these tests was used as input in FDS to simulate a total subway carriage fire. This study did not take into account the added fuel load of carry-on luggage, which could substantially increase the HRR. These values lie on the low end of most available real-scale and model-scale predictions.

Arup developed a model to predict the HRRs of train cars (non-subway). A newer train with fire retardant seats resulted in an HRR of 7 MW, whereas an older train resulted in an HRR of 16.3 MW. The model used results from furniture calorimeter tests for upholstered car seats and lining materials. (Chiam, 2005)

In the process of conducting this thesis, discussion was also made with various experts on the subject. Some have conducted proprietary small model-scale tests of subway carriages, on the order of 10% of full scale, resulting in heat release rates in the region of 5 MW. When scaled up, these tests would very likely result in HRRs in the order of those obtained by real-scale tests in the EUREKA experiments.

Research by Wilke (2002) yielded an HRR of 5.6 MW 30 minutes after the start of a fire for a U-Bahn train in Frankfurt. Derivation of this value comes from performing a series of fire tests and analysis of train carriage materials. (Chiam, 2005).

#### **4.2.3 Previously Proposed Design Fires**

The following chart shows the Frankfurt curve plus those used for design of subway stations in Vienna and Munich. (Haack, 2011). The curve in Vienna reaches 30 MW in 25 minutes, the one in Munich approximately 22 MW in 15 minutes.

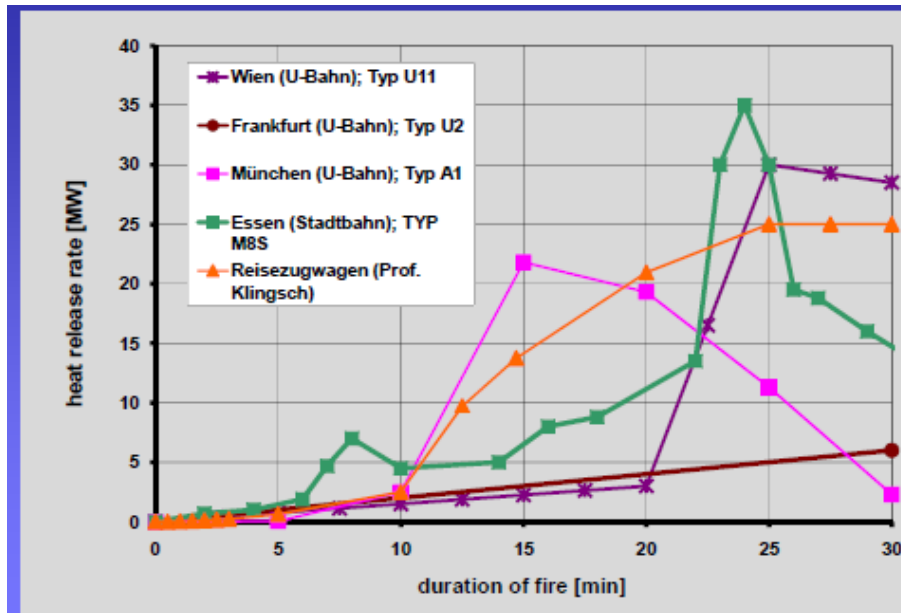


Figure 6 -Design Fires in Vienna, Munich, Frankfurt (Haack, 2011)

The following table, derived from Chiam (Chiam, 2005) provides an overview of HRRs used in subway systems for purpose of ventilation system design. This is followed by new data collected as part of the survey conducted under this project (see Appendix C).

Table 1 - Example Design Fires (Chiam, 2005)

Country	Subway Line	Peak HRR (MW)
Singapore	North South Line	24
Singapore	East West Line	24
Singapore	North East Line	15
Singapore	Circle Line	10
Australia	New South Link	10
Hong Kong	Lantau Airport Line	5
Hong Kong	Airport Express Line	10
Thailand	Chaloem Ratchamongkhon MRT line, Bangkok	7
Greece	Athens Subway	10
UK	St Paul's City Thameslink, London	16
USA	Mount Lebanon Tunnel light rail transit, Pittsburgh, PA	13.2
USA	Amtrak New York City Tunnels	31.1
USA	Ventilation system upgrade study for Washington DC(WMATA) system	18
USA	Ventilation system upgrade study for Washington DC (WMATA) system	23.1

Additional data collected under this project is presented in Table 2.

Table 2 - Additional Design Fires

Country	City	HRR (MW)	Comments
Australia	Sydney NSW	10	Recently designed station
Sweden	Stockholm Metro	15	New Citybanan Line. Reference to Eureka fire tests.
Portugal	Oporto Metro,	14	Eureka fire tests & review of vehicle material fire characteristics. New Subway System. Growth 3.4 w/m <sup>2</sup> . Total fire load fire load 79 MJ.
UK	London	8.8	From comprehensive research study & comparison of tests
UK	London Overground System	8	(Brown, 2011)
Denmark	Copenhagen	20 MW Car, 600 kW Platform	Metro new in 2002
Netherlands	Amsterdam	15 MW, fast, 9.5 min to peak	New Ceintuurbaan station. (Snel, 2008)
China	Not Specified	1.2-2	Car Materials assumed to be non-combustible.
Germany	Frankfurt	5.6	Peak in 30 minutes

One can easily see the large variation in chosen design fires in Tables 1 & 2. With a minimum of 5 and a maximum of 31.1, design fires are simply not consistent. But a valid question to ask is, should they be? For those referencing the real-scale Eureka fire tests, it appears they are referencing either the 13 MW German IC car, or the 16 MW British Rail 415 (see Figure 2). Both of these are rail cars, and the applicability to a subway system, depending upon construction, is questionable.

While the design values used above are not consistent, FIT also reached the conclusion that design fire selection should not necessarily be uniform:

*“The choice of design fires depends on the nature of the rolling stock which varies from country to country. When stringent fire resistance regulations have to be obeyed (e.g. DIN 5510, EN 45545, BS 6853) a less severe fire may be considered (pg 62 FIT General Report)... Without further knowledge and experimental evidence, when regarding a modern subway carriage fulfilling the EN 45545 or DIN 5510 a linear increase of the heat release rate to 6 MW after a fire duration of 30 minutes and a further increase to 15 MW after a fire duration of 60 minutes may be a practical choice. Especially older carriages with less fire resistance may burn more severely so that a steep increase to a maximum of about 25 MW within 12 to 15 minutes after beginning of the fire may be more appropriate.” (FIT)*

One might conclude from the above that newer carriages should contain materials tested in accordance with new standards, thus having a higher fire resistance and permitting a less severe design fire to be used. Old subway carriages, on the other hand, contain materials that are more combustible and adhere to less stringent requirements. Some recent research, such as that mentioned by Hughes Associates (Cutonilli, 2010), seems to claim the opposite. However the idea is also partially supported by newer real-scale tests in the METRO project. The newer carriage tested did not reach flashover until 110 minutes. After this, it had a comparable HRR to the old style carriage. This indicates that newer carriages

may be more resistant to small ignition sources, but could still flashover as a result of extreme scenarios, such as arson.

#### **4.2.4 Carry-on Luggage**

It is also important to note that only one of the above studies explicitly considers fuel loads brought onto a train, which may include combustibles such as luggage, strollers, bicycles, laptops, and pressurized cans. These items are transient and thus the available fuel load will constantly change as passengers enter and leave. During certain peak occupancy hours, it can be assured that the fuel load will contain additional carry-on items. In systems in mountain environments, such as the railway in Kaprun, Austria, items such as skis and snowboards are regularly present and will substantially increase the available fuel load. A field study conducted under the METRO project in the Stockholm metro showed that 82% passengers carried bags with them (Lonnermark, 2012). These items have the potential to considerably change the predicted fire growth rate and HRR, and should be considered when selecting a design fire.

As part of the METRO project, studies were conducted at SP in Sweden on hand luggage and miscellaneous items that could be brought onto subway carriages. One baby stroller was found to result in a peak HRR of 830 kW. A study of the Delhi subway system indicated that items carried onto the carriage may be approximately 50% of the total carriage fire load (METRO, 2011). Figure seven shows the heat release rates of the top five carry-on items, as tested in a cone calorimeter at SP (Kumm, 2010). One can easily see that if several items burn simultaneously, as will occur in near-flashover to flashover conditions, a cumulative HRR of carry-on luggage may reach 1 MW or even higher. If, for example, a design fire in a new station of 5 MW was selected (Lantau Airport Line, Hong Kong, Table 1), carry-on luggage of only 1 MW will represent a 20% increase in available fuel load. This is easily foreseen in an airport line with traveling passengers carrying plenty of luggage. If a much higher design fire is selected, say 24 MW (North South Line, Singapore, Table 1), a carry-on fuel load of 1 MW represents only a 4 to 5% error in design fire selection.

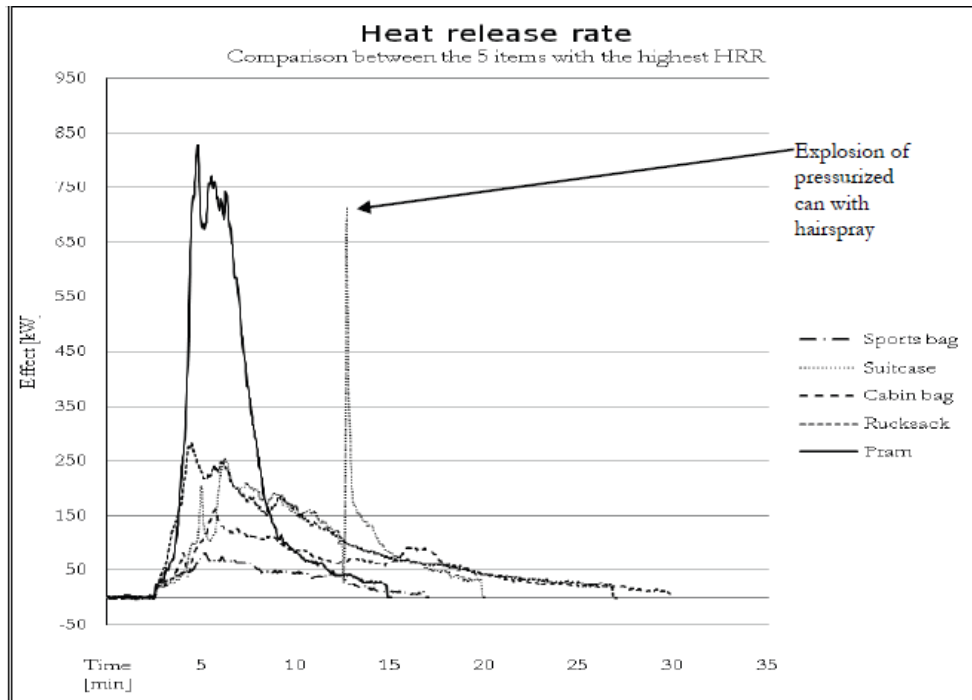


Figure 7 - HRR from carry on luggage. METRO Project (Kumm, 2010)

#### 4.2.5 Miscellaneous Issues Related to the HRR

The previous discussion all relates to design fires originating from a subway carriage. However, as in the design of any smoke control system, one must consider whether the system functions not only with large fires, but smaller ones as well. A probable fire in a subway station may start on the platform in a garbage can. In this case, the heat release rate is quite low in comparison to a carriage. However, a substantial amount of smoke may still be produced. With a lower HRR, the smoke generated may lose its buoyancy quicker when compared to a larger fire (due to differences in temperature and momentum). Such a scenario can present a safety hazard to platform occupants if the smoke forms a static layer within the station and fails to be vacated by the smoke control measures which were designed and implemented for much larger fires (which may rely heavily on strong smoke buoyancy). It can be seen from Table 1 that in the Copenhagen subway station, a 600 kW fire was considered, likely from an undercarriage or a platform trash can.

Finally, it is important to discuss ignition sources, which were briefly mentioned earlier in the report in connection with the Hughes Associates method (Cutonilli, 2010). Not all ignition sources will lead to flashover. Furthermore, different ignition sources lead to different fire growth rates. Typically, large ignition sources due to arson (for example, a large quantity of petrol), will lead to high growth rates and flashover will occur. Additional sources of arson, such as cigarettes, lighters, and newspapers, typically result in very slow growth. The carriage may not flashover (the HRR may in fact not be sufficient enough to induce fire spread). In this case, evacuation is possible and lives are not in jeopardy. This conclusion is also made clear in (Lautenberger, 2009). Here, an FDS model was used to predict fire development. A trash bag fire, at 290 kW, was deemed insufficient in the chosen carriage interior construction to cause fire spread. On the other hand, a 500 kW ignition source was deemed able to initiate fire spread. In



(Peacock R. A., 2004), full scale tests were conducted, and ignition sources between 25 kW and 200 kW were deemed necessary to promote significant fire spread. With a large trash bag, significant flame spread was observed. A risk assessment, based upon the carriage construction, should be conducted to evaluate necessary ignition sizes which may lead to flashover. If, due to the train construction, an extremely large ignition source is required for flashover, it may be possible to eliminate such a fire scenario. Such conclusions become vital to the design of ventilation systems in a station.

#### **4.2.6 Design Fire Proposal**

It is the position of the author that, when train construction characteristics are unknown, a conservative heat release rate should be used of at least 20 MW. For this project a HRR of 35 MW will be used with a growth rate of  $1.08 \text{ MW/min}^2$  (peaking HRR is at 341 seconds), as proposed by Ingason (Ingason H. , 2006). This conclusion is based on the following:

- a) Carry-on luggage must be considered and has been proven to contribute significantly to fire growth and fuel load.
- b) Current real-scale testing of subway carriages has resulted in HRRs of 35, 52, and 77 MW.
- c) Models in (Cutonilli, 2010) resulted in results with comparable HRRs to real-scale results.
- d) The fire performance of current materials based on bench-scale prescriptive codes may not necessarily be accurately extrapolated to real-scale performance.
- e) Small scale tests have resulted in heat release rates as high as 5 MW.

It should be noted that the data on the 52 and 77 MW fires were not made public until near the completion of this thesis, and therefore were not considered as design fires. They do however provide further substantiation for selecting a larger HRR than those presented in Tables 1 and 2.

#### **4.3 Risk Assessment Discussion**

An initial attempt was made at a risk assessment to consider the likelihood of a carriage on fire in a station. It was quickly realized that this undertaking was not feasible and outside the scope of the project. Some statistics were gathered over the course of the project regarding subway fires, and they are presented in [Appendix D](#).

## 5. Current Practices in Station Fire Safety

### 5.1 Results of Questionnaire

In order to fulfill the project's first objective and to obtain an idea of current approaches, globally, to fire safety in subway stations, a survey was posed to consultants. Ten replies were received, representing nine countries throughout Europe and Asia. One goal of the survey was to determine if the approach between different regions is homogenous, and if not, what the differences can be attributed to. The survey first aims to determine what kind of design fires (size and location) are used in smoke control design. Then the question is posed of whether trains are constructed in accordance with specific material standards. Finally, with the knowledge of these two, the next question is what types of smoke control are employed in stations, and if national standards exist for station design. The consultants were requested to fill out the survey by assessing one subway station in their subway system which they consider representative of the system as a whole. The questions are shown in [Appendix C](#) and some statistics and facts derived from the responses are presented below (in addition to the HRR information previously presented Table 2).

Replies came from the following cities: Sydney (Australia). London (UK). Stockholm (Sweden). Porto (Portugal). Paris (France). Shezhen City (China). Copenhagen (Denmark). Bangalore (India). Frankfurt (Germany).

- All replies except Paris and Bangalore state that a reasonable worst case interior fire is considered a design fire.
  - In both cases, subway carriages are constructed according to NFF16 101.
- 4 of 9 replies state that Arson is considered as a design fire.
- 4 of 9 state that they use longitudinal ventilation (Two of which are Paris and Bangalore)
- 4 of 9 state they use overpressurization as a method of smoke control.
- 8 of 9 state they use 'mechanical extraction'. Paris is the exception.
- Only 3 state they make use natural ventilation (1 of them states it is 'for concourse').
- Only one states they use 'transverse' ventilation. (Shezhen City)
- Only two state they use smoke screens or smoke barriers (Frankfurt & Bangalore).
- In Australia design fires are prescribed in published standards, however a performance based approach is allowed.
- France does not use design fires. Bangalore neither (based on fire classification in French norm)
- The station in Shezhen city did not consider a carriage on fire as a design fire. Trains are assumed to be non-combustible. The design fire is 1.2-2MW.
- The largest design fire used is 20 MW. The average of the seven specified design fires is 12.6 MW (not including the 1.2-2MW Shezhen city fire)

It is interesting to note that the majority of subway systems surveyed are using mechanical extraction to prevent smoke spread. Additionally, the average peak design fire size reported is substantially lower than all real-scale testing reported in Section 4.2.

## **5.2 Methods of Smoke Control**

### **5.2.1 Smoke Control Methods – Mechanical Ventilation**

Many possibilities exist for smoke control in subway stations. The primary purpose of the ventilation in any fire in a station is to maintain a smoke-free environment for station users, and in some cases to allow access for the fire fighters. The primary variable controlling the chosen method of control is the fire HRR and growth rate. Additional variables which may affect the necessary ventilation method are intended occupancy, station layout (exits, placement & orientation of obstacles, location below ground or to adjacent shops or buildings, etc.), and size and design of tunnels.

#### ***5.2.1.1 Longitudinal Ventilation***

Longitudinal ventilation refers to the control of smoke by use of air injection, often with jet fans placed throughout a tunnel, typically on the ceiling. Smoke is pushed in one direction, while the upwind direction remains smoke-free. Much research has been conducted in regards to effects of longitudinal ventilation on a tunnel fire. Carvel (Carvel) concluded it would be sensible to keep longitudinal ventilation velocities low in order to reduce the risk of fire spread (to carriages downstream). Furthermore, higher ventilation velocities will result in increased HRRs. To avoid this, Carvel recommends that in the initial stages of a fire, when the HRR is low, it is best to keep the longitudinal velocity low (1 m/s or less). As the HRR increases, the longitudinal ventilation will have less of an impact on fire growth, and it can be increased to prevent backlayering (Carvel). Jet fans must also be carefully designed so as to resist failure due to the high temperatures involved in a tunnel fire. Finally, some jet fans can be run in both a supply and exhaust mode. Fans used in this arrangement are often referred to as “push-pull”. If this is the case, one jet fan may be used to pull exhaust away from a location, while the other pushes the smoke towards the extraction fan (this is accomplished by drawing in a large quantity of air and expelling it at a high velocity, such that the imparted momentum prevents backlayering). The extraction is only possible where the fire incident occurs near the base of the fan shaft (Beard, 2005). When a jet fan is located at the entrance to a tunnel, with a fire occurring in a train within the station, the jet fan may assist in providing more tenable conditions by evacuating smoke from the station into the tunnel.

#### ***5.2.1.2 Transverse***

Transverse ventilation systems use both supply and extraction air ducts to uniformly distribute or remove air during normal operations. During a fire, they can serve as a mechanism for removing smoke. The ducts are served by fans. This scheme is shown in Figure 8.

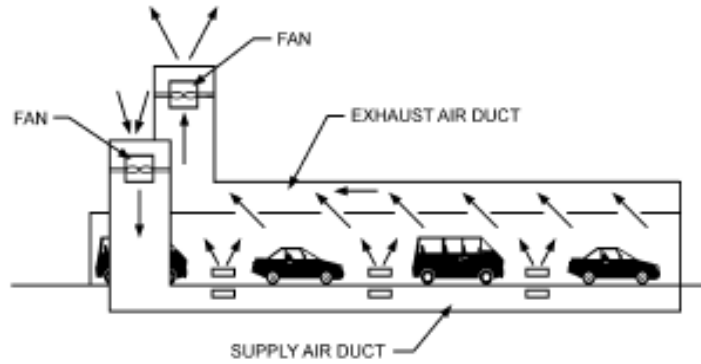


Figure 8 - Transverse Ventilation (ASHRAE, 2011)

### 5.2.1.3 Semi-Transverse

Semi-Transverse ventilation systems use either supply or extraction ducts, served by fans (ASHRAE, 2011). Extraction or supply is generally carried out at limited intervals. A combination of supply and exhaust semi-transverse systems is sometimes used in tunnels, in a zoned approach aiming to provide maximum extraction on only one side of the fire, with supply on the opposite (in contrast to fully transverse, the ducts run only a portion of the tunnel length, as in Figure 9). In addition to providing a high level of extraction and maintaining adequate operating conditions in supply mode, one benefit can include removal of substantial decision-making capabilities from the operator (Armstrong, 2001). The operator will only have to switch the system to “emergency” to turn on the exhaust mode. On the other hand, cost is high as fan plants must be constructed and a long ventilation duct must run the entire length of the tunnel. The ducts may take up a considerable amount of space, which should be factored into design considerations. In new tunnels/stations, this may affect the necessary excavation depth. In retrofit of existing tunnels/stations, space may be insufficient for duct placement. An important design option is using reversible fans. In supply mode (when installed in ceilings) they can supply fresh air to supplement normal operating conditions. In extraction mode they can exhaust smoke. Emergency fans are required to be reversible in some prescriptive codes (for example, NFPA 130).

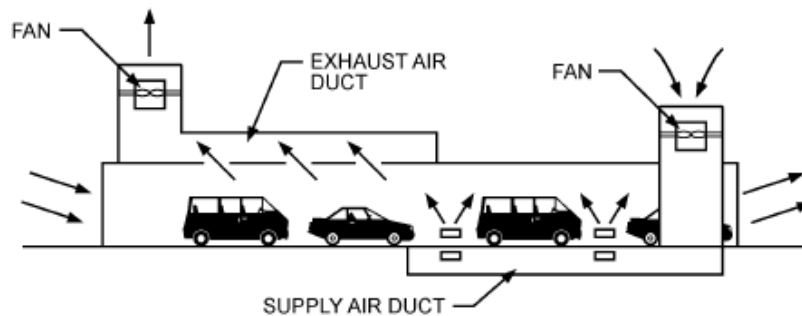


Figure 9 - Semi - Transverse Ventilation in a Tunnel, Supply and Exhaust (ASHRAE, 2011)

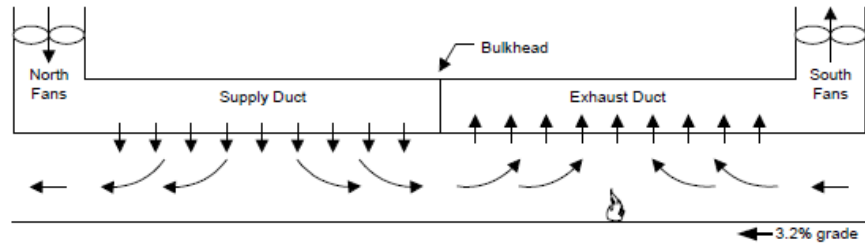


Figure 2: Two-Zone Partial Transverse Ventilation

Figure 10 - Zoned Semi Transverse Ventilation (Levy, 1999)

#### 5.2.1.4 Single Point Extraction

Single point extractions are typically additions to transverse ventilation systems. As the fan plant is usually located far from the duct inlets, single point extractions can be added as large openings within the duct, closer to the fire source. They can be operated during an emergency to extract large volumes of smoke (ASHRAE, 2011).

#### 5.2.1.5 Under Platform Exhaust (UPE)

UPE systems are located close to ground level in the guideways of the subway. The main function is to exhaust heat from the hot undercarriage of a train, most notably during braking when a train enters a station. Here, friction forces generate substantial amounts of heat, which may need to be removed to keep overall temperatures down in the station and system. UPE systems may contribute to smoke exhaust in the case of an undercarriage fire. In the event of a fire inside a carriage, the buoyancy of hot smoke will cause it to rise, reducing the effectiveness of UPEs, which are located below the carriage. One study, however, concluded that UPEs, when combined with tunnel ventilation fans, do provide additional smoke exhaust (Chen F. G.-C.-Y.-W., 2003). The study, however, did not analyze UPEs and tunnel ventilation fans separately for comparison. They found that the negative pressure created by the two caused replacement air to come in through the upper floors. The velocities were mentioned as high, but no numerical values were provided. This is an important consideration for egress, as high velocities may make occupants uncomfortable and thus affect evacuation behavior. Another study of the Calcutta subway system concluded that if operated in supply mode during a fire, and when combined with an over-track exhaust system (with appropriate extraction rates), smoke can be effectively managed (Gupta, 2011). A CFD analysis was conducted using FDS to verify smoke spread.

#### 5.2.1.6 Over-Track Exhaust (OTE)

An over-track exhaust system is typically used in normal operating conditions to allow for hot air from incoming trains to leave, lowering ambient temperatures, as well as mitigating the velocities induced due to train piston effect. However, such an exhaust system may also be used for smoke exhaust during a fire. The following figure displays a station with both OTE and UPE systems (Tabarra, 2004). An over-track exhaust system may be an efficient method of removing smoke, as it is located in close proximity to the fire source. This allows less air to be entrained and the volume of smoke to be extracted is less (when compared with extraction located at tunnel/station interfaces). Such systems, if designed for

both normal and emergency (fire) operations, should be capable of operating at high temperatures without diminished performance or failure.

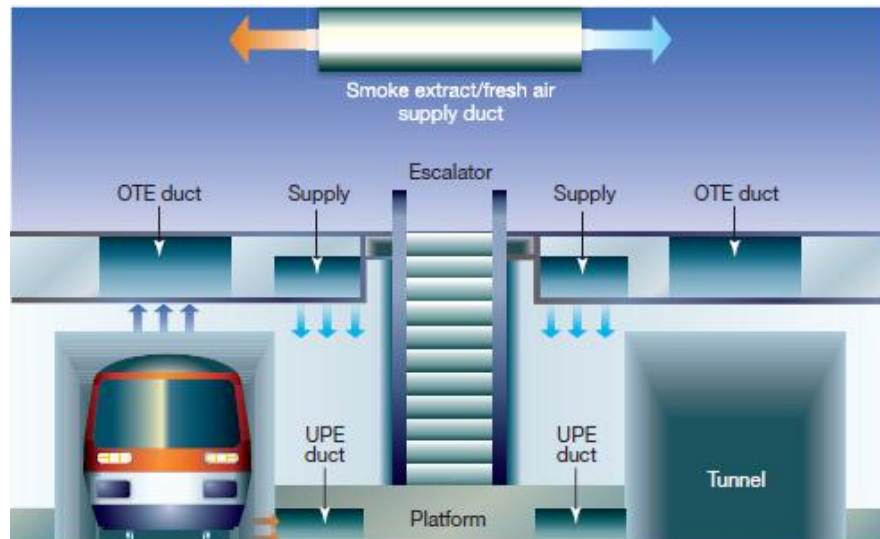


Figure 11 - OTE and UPE ventilation systems ( Tabarra, 2004)

### 5.2.2 Smoke Control Methods – Natural Ventilation

Natural ventilation relies on buoyancy to remove smoke from the system. This can be accomplished with or without vents. Without vents, reliance is placed on the lateral spread of the smoke once it hits the ceiling and stratifies, creating a thin smoke layer with a tenable environment below. In tunnels with grades, the longitudinal natural flow may be sufficient to accomplish this. With a 10% grade and a 1 km long tunnel, velocities of .5 to 1 m/s are possible (Beard, 2005). Natural ventilation may also be accomplished through a system of openings or shafts which vent the smoke to another location. Natural ventilation can be placed effectively in both stations and tunnels. The size and location of the shafts is a key factor in determining viability. Ambient conditions such as temperature and wind can also affect the performance of natural ventilation shafts. In addition, when used in tunnels, natural ventilation is most effective in short tunnels. In longer tunnels, as smoke spreads laterally, it will lose buoyancy as it mixes with cold air and loses heat to the surroundings, and depending upon the shaft locations, may no longer be buoyant enough to be exhausted. Short, as stated here, can be between 350 and 700 meters as defined in Germany and below 400 meters in the UK (Beard, 2005). In experiments conducted in a tunnel by Haerter, smoke stratification broke down at 400-600 meters away from the fire source (Beard, 2005). Generalizing this to stations, however, presents difficulties due to the large variations in station and system layout. Station width may change, and the presence of exits and leakage points will allow further vertical travel.

The piston effect of a train is often used as a means of everyday natural ventilation in stations and tunnels, to provide air flow in and out which both dilutes exhaust from trains and controls temperatures. In stations, the piston effect of the train can make waiting passengers uncomfortable. Thus, natural ventilation may be used to control this piston effect. Typically, shafts are placed at interfaces between tunnels and stations. As a carriage enters a station, the positive air pressure created

by the train pushing air in front of it can be relieved by what is referred to as a blast shaft. As the train departs the station and enters the next tunnel, the negative pressure it creates behind it can be utilized by what is referred to as a “relief shaft” (ASHRAE, 2011). Air enters through the relief shaft due to the negative pressure, bringing in fresh air. These shafts can have bypass and fan dampers installed. In emergency conditions, the fan damper can be opened and the bypass damper closed, allowing a reversible fan to either supply or exhaust air. Since these are typically located at tunnel/station interfaces, they can be considered when designing emergency ventilation not only in tunnels but stations. They could also potentially be combined with longitudinal ventilation (such as a jet fan) located in a station to push air toward the tunnel portals for extraction in the shafts.

Natural ventilation within the station confines may also be considered depending upon the layout. At a station in Xi’an, China, a three story underground station contained a large centrally-located atrium. A case study showed that using natural ventilation in the atrium, in combination with mechanical ventilation (which they have termed hybrid ventilation), was more effective than using only conventional mechanical ventilation (Gao, 2011).

### **5.2.3 Smoke Control Methods – Passive**

Alternative, non-mechanical ventilation methods should also be considered in station design. While not aimed at extracting smoke from the region, these methods may be effective in controlling, gathering, or channeling smoke away from evacuees in order to provide additional time to leave the station during an emergency.

#### ***5.2.3.1 Platform Screen Doors***

Platform screen doors (PSDs) are an increasingly popular feature in subway stations. As of 2009, platform screen doors were located in at least 44 subway systems around the world (Metrobits.org, 2009). Figure 12 shows a typical configuration of platform screen doors. PSDs form a wall (usually of a transparent material) which encloses the guideway, separating the train from the platform. They contain doors which are aligned with the train doors. In some cases, they may not rise to the full height of the ceiling; rather, they stop at an intermediate point, leaving a gap between the PSD and ceiling. When the train arrives, the platform screen doors open automatically in conjunction with train doors, and passengers pass through the PSDs into the train. PSDs are installed for a variety of reasons, from preventing passengers from falling into trainways, to providing for more passenger comfort by minimizing train piston effect as well as oncoming train noise. In warmer climates, PSDs are installed to work in conjunction with air conditioning systems to save energy and reduce costs. The PSDs separate the trainway from the platform, thus reducing the area necessary for air conditioning. Few studies have been conducted to determine the effect of PSDs on smoke spread. One notable study used CFD simulations to conclude that when used in conjunction with ventilation (an OTE system), PSDs are very effective (Roh, Ryou, Park, & Jang, 2009). The study failed to provide a detailed view of the geometry and design of the PSDs used in the simulation. Additional items of concern are at what temperature and in what manner the PSDs break when constructed of glass. Several disadvantages of PSDs may be initial cost as well as the cost and inconvenience resulting from break-down of the PSD operating systems.



Figure 12 - Platform screen doors in Dubai Metro (photo taken by author)

### ***5.2.3.2 Downstands & Smoke Screens***

A downstand is a physical obstruction originating from a ceiling and protruding downward. A beam which spans the length of a ceiling can be considered a downstand. Adding downstands is a common method to compartmentalize a space. This helps to both prevent smoke spread and to allow smoke to collect before being exhausted. Proper sizing and placement of downstands will help mechanical extraction systems perform more efficiently by preventing plugholing. Adding downstands may be difficult or impractical in tunnels but it more feasible in a station (Lord). Of course, this depends on station layout. A smoke screen differs from a downstand in that it is not fixed in place. When a fire is detected, a smoke screen can roll down into place to create a smoke barrier.

### ***5.2.3.3 Overpressurization***

Smoke moves from areas of high pressure to low pressure. Overpressurization can prevent smoke movement to particular areas by introducing a region of high pressure. Pressurization is possible in subway stations. However, it must be carefully designed due to the large space involved (Lord). Such large spaces may require a significant amount of equipment. Overpressurization in exits may be implemented in the exit if it is sufficiently enclosed to make pressurizing the space feasible. Such an illustration is shown below (Wahlström, 2011). In this scenario, overpressurization, PSDs, OPEs, and mechanical extraction are all utilized to provide an effective overall smoke management strategy.



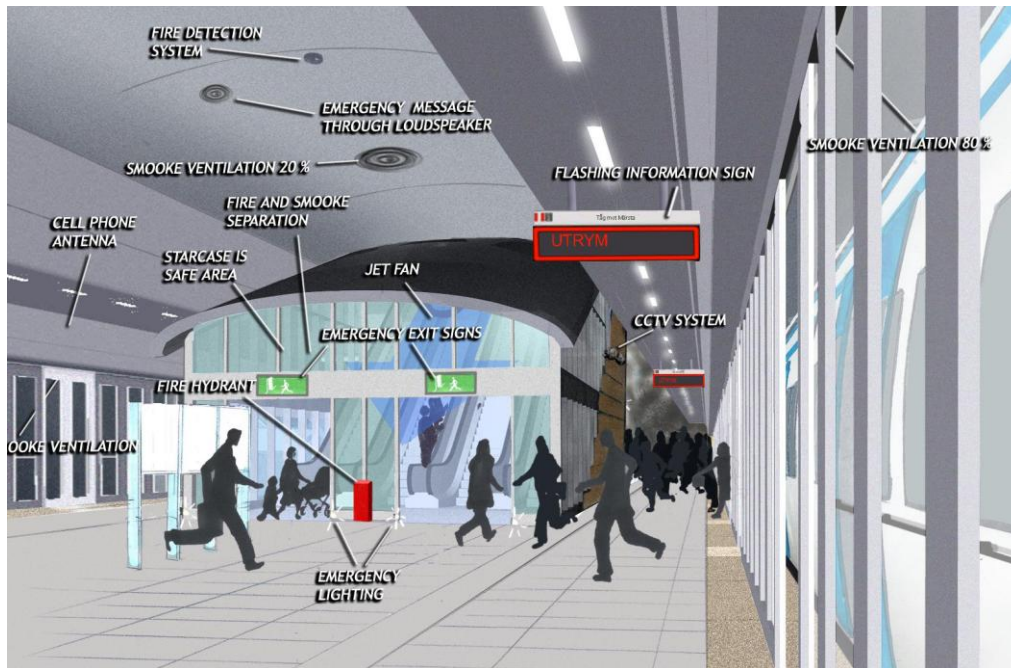


Figure 13 - Station Design with UPE, PSD, and Pressurized Stairwell (Wahlström, 2011)

## 6. Case Study Subway Station

### 6.1 Station & Tunnel Description

The layout of the case study station is seen in Figures 14 and 15. The station is a double platform style, separated by a central guideway in which trains run in both directions. It is a two level station consisting of a lower platform level and an upper concourse. Two escalators, two elevators, and four stairwells connect the platform with the concourse. The station is 100 meters long. The concourse contains one main exit to ground, comprised of two escalators and one stairwell. The two elevators which connect the platform to the concourse also connect the concourse to the ground level. There are electronic fare gates near the main exit for passengers to swipe their tickets in order to enter and exit the concourse. They are designed as chest-high doors which slide open upon acceptance of a ticket. There is an 18 meter long open space in the center of the station, taking the form of an atrium (it connects via open air both platform and concourse levels). Passengers on the concourse level thus may overlook a portion of the platform via a balcony. The concourse itself is only about half the length of the platform, or 45 meters. There is an area of approximately 37 meters long on the opposite side of the atrium at concourse level (but inaccessible to passengers), that is empty and has been reserved for future use. There are emergency exits at one end of the station at platform level (on *both* platforms). However, due to poor signage and obstructions, they are not likely to be used in an emergency.

The concourse level has an available floor area of approximately 680 m<sup>2</sup>. Each platform has an available floor area of approximately 375 m<sup>2</sup> (100 meters in length). Each floor is 3 meters in height. The station contains no grade. The occupant capacity of each platform is 400 people.

During a field study of the station, it was noted that the majority of the surfaces in the station were constructed of either brick or concrete. Exact specifications are unknown.

The tunnels are approximately 8 m wide x 6 m high. The construction style is unknown, however, it was assumed to be cut and cover, due to the difficulty in creating a bored tunnel with a rectilinear grid with the chosen CFD modeling approach.

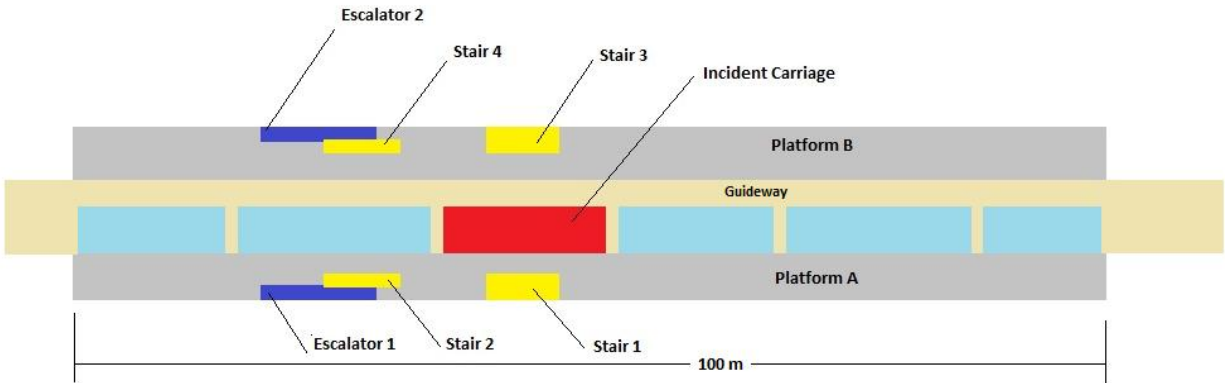


Figure 14 - Platform Level, Top View

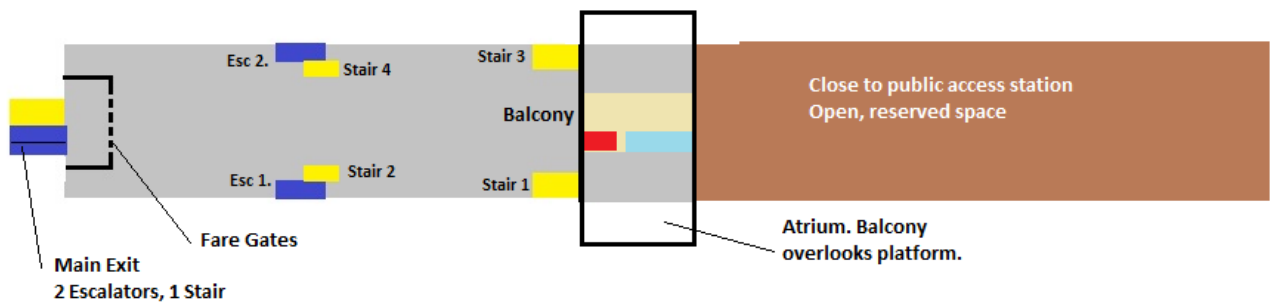


Figure 15 - Concourse Level, Top View

## 6.2 Train Geometry

Details of the train carriages are as follows:

Number of Carriages: 6

Carriage material: Aluminum

Number of doors per carriage: 3

Door width: 1.45 m

Carriage width/height: 2.7 m / 3.55 m

Total Length of 6 cars: 94 m

Specific window dimensions are unknown but were determined for CFD simulations based on field estimations. Interior furnishing material is unknown. The occupant capacity of each 6 car train is 800 people.

## 7. Evacuation Calculations

### 7.1 Prescriptive Approach

Prescriptive egress calculations were made on the station in accordance with NFPA 130 (NFPA, 2010). NFPA 130 has two primary egress requirements. First, the time to clear the platform during an emergency should be less than 4 minutes. Second, the platform occupant load should be able to be evacuated from the most remote point on the platform to a safe point within 6 minutes.

The results of the analysis indicate that at least two additional exits (of equal width to current exits) would be necessary to evacuate the platform within 4 minutes. This calculation assumes that the emergency exit, as described in Section 6, is not used. Improving signage and access to this exit would permit addition of only one new exit to meet the first prescriptive requirement. Though not necessarily a viable option, decreasing the station occupant capacity or increasing the width of existing exits would also assist in meeting these prescriptive requirements.

Assuming that the first requirement is met by providing enough additional platform-level exit capacity, the second requirement cannot be met without substantial design changes. This is due to both limited exit capacity as well as the presence of flow-restricting turnstiles. With the given occupant capacity, on the concourse level, it would take 11.5 minutes for everyone to evacuate through the main exit (consisting of two escalators and one stairwell, of which one is assumed to be blocked). To remedy this, more exit capacity is necessary.

Detailed calculations are presented in [Appendix A](#).

### 7.2 FDS+Evac Approach

A secondary egress analysis was conducted using the program FDS+Evac, to either validate or negate the results of the prescriptive process.

FDS+Evac is an agent-based egress program which is designed to operate on the existing platform of the FDS program (Korhonen T. H., 2011). Each human is driven by an equation of motion, moving in horizontal planes which represent floors in a building (Kuusinen, 2007). One distinct advantage of FDS+Evac is its ability to allow for coupling of fire and evacuation simulations. This is important as it has been shown that smoke and gas concentrations can affect evacuation of people.

In FDS+Evac, each agent has its own personal properties and escape strategies. Equations of motion are solved for each evacuee in a continuous two-dimensional space and time (Korhonen T. H., 2010). Sub-models are used for forces on agents (such as contact with walls, social forces with other agents, and contact with the fire). FDS+Evac can be run in a traditional manner (performing like programs such as Simulex and STEPS) without fire, in order to obtain an RSET. When coupled with the FDS fire model, gas concentrations are used to calculate FED (according to Pursers model), and smoke density affects agent walking speed and exit selection, allowing for more realistic evacuation representation.

FDS+Evac uses separate meshes than FDS to handle the movement of the agents. Finer meshes do not necessarily lead to more accurate flow fields to guide agents to exits (Korhonen T. H., 2010). Along with

mesh size, one variable item that may affect results is user-designated human properties, such as body size, mass, and various human related variables in the force models. However, the developers of FDS+Evac conducted thousands of studies to come up with recommended, pre-defined person types.

Finally, FDS+Evac is a stochastic model, meaning that simulations must be run multiple times and results compared (Korhonen T. H., 2010). Each simulation result may be slightly different.

With a constraint on the maximum occupant density of 4 persons/m<sup>2</sup>, FDS+Evac was not able to simulate the design load of 800 individuals spread over 5 cars, which approaches 4.6 persons/m<sup>2</sup>. Each car has an area of 35 m<sup>2</sup>. The number of agents thus was reduced so that the program was able to run properly.

FDS+Evac was initially used to simulate, without fire, the occupant load evacuating from a single platform and carriage. The results confirm that without additional exits, the platform is unable to be evacuated in less than 4 minutes. Furthermore, this simulation was conducted with only half of the intended evacuation occupant load as a result of the occupant density limitation (600 agents instead of 1200), no delay for pre-evacuation time, and wider platform-concourse stairwells than those which exist in reality (4.5 meters of total stairwell width between 3 exits was input, whereas approximately 3.6 meters exists as currently designed). As FDS+Evac is a stochastic model, 10 simulations were conducted. The average of these simulations showed that 322 seconds is necessary to evacuate the platform and 370 seconds for the entire station. Turnstiles were not simulated on the concourse level. The large queues at the platform stairwells which exist at four minutes are shown as follows:

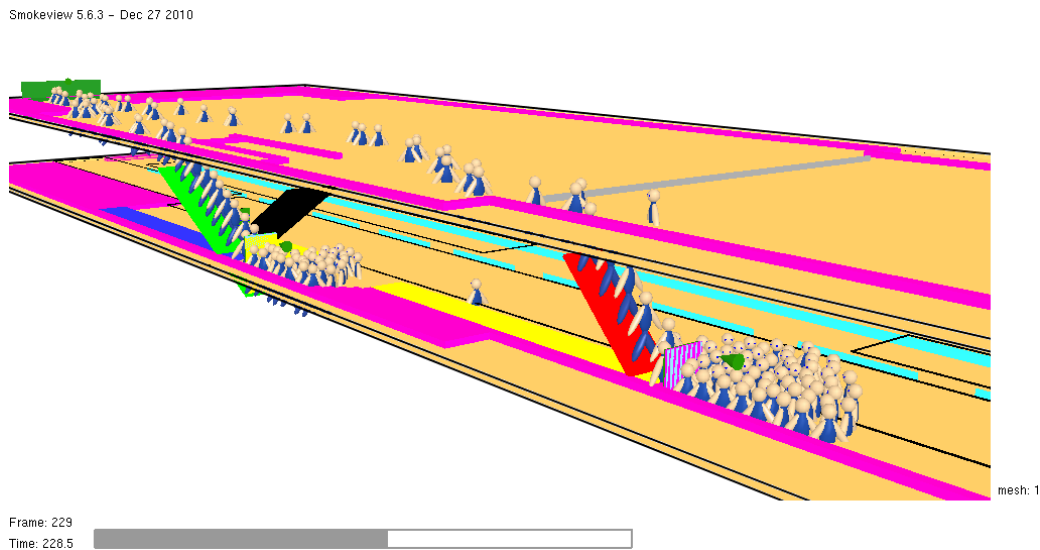


Figure 16 - Queuing at platform exits in FDS+Evac seen at 228 seconds.

## **8. CFD Simulations**

### **8.1. Choice of FDS**

CFD modeling was chosen over other available options, such as two-zone models and hand calculations, due to the complexity of the metro station geometry. FDS 5 was chosen as the CFD software for this project, in part due to its open-source availability and extensive use within the fire safety community.

FDS uses a LES (Large Eddy Simulation) approach to modeling the thermally-driven flows. It is best suited for relatively low speed flow (such as in a fire). The LES approach assumes that large-scale eddies dominate turbulent flow and contain the majority of the energy within the system. Based on the chosen grid size, FDS attempts to directly resolve the large scale whirls and fluctuations, and approximates the sub-scale turbulence. The sub-scale model used is called the Smagorinsky model, based on the eddy viscosity assumption. The approach assumes that small scales are in equilibrium, and thus, energy production and dissipation are in balance (Kim, 2008).

FDS has also been validated for use in long and narrow geometries. Simulations were conducted with FDS V2.0 to attempt to validate results from the Memorial Fire Test #321A (conducted in the Memorial road tunnel in USA). The fuel was a 40 MW pool fire and a single point ceiling ventilation supply was present. The equations were solved over 480,000 cells, and results gave good predictions of overall phenomenon, on par with other engineering programs. The recommendation was made, however, to use a finer grid to more accurately predict temperatures (Beard, 2005).

### **8.2 Organization of Simulations**

The simulations were organized progressively in order of expected benefit and complexity of protective measures. First, methods of only passive fire protection were considered. Then, only mechanical ventilation was considered. Finally, a combination of the two methods (termed hybrid) was looked at. The trials are below. It should be noted that the base case was altered slightly from the as-received station. An open balcony on the concourse overlooking the platform was mentioned in Section 6.1. It was decided that in order to avoid immediate smoke filling of the concourse, that this balcony must be enclosed. Thus, this case was taken as the starting point and assumed for all simulations.

- I. Passive Smoke Control
  - a. Base case
  - b. Base case + smoke screens
  - c. Base case + stairwells enclosed
  - d. Base case + stairwells enclosed + platform screen doors
  - e. Case d., with the platform screen doors revised.
  - f. Base case + longitudinal smoke screens + stairwells enclosed
  - g. Base case + multiple smoke screens + stairwells enclosed
- II. Mechanical Smoke Control
  - a. Longitudinal Ventilation
    - i. Push Only
    - ii. Push-Pull

- iii. Pull Only
    - iv. Pull-Pull
  - b. Transverse Ventilation (extraction)
    - i. Extraction via the atrium ceiling
    - ii. Extraction to reserved space via platform ceiling (termed ceiling exh hereafter)
    - iii. Extraction to reserved space via side of atrium (termed side exh. hereafter)
- III. Hybrid (Passive + Mechanical) Smoke Control
  - a. Stairwell Pressurization
  - b. Push + Stairwell Pressurization
  - c. Push + Ceiling Exhaust + Stairs Enclosed
  - d. Push + Ceiling Exhaust+ Stair Enclosed + Revised PSD
  - e. Push + Side Exhaust + Stairs Enclosed + Revised PSD
  - f. Side Exhaust + Stairs Enclosed + Revised PSD
  - g. Ceiling Exhaust + Stairs Enclosed + Revised PSD
  - h. Pull + Stairs Enclosed
  - i. Pull + Stairs Enclosed + Smoke Screens
  - j. Pull-Pull + Revised PSD
  - k. Push-Push + Side Extraction + Stairs Enclosed

## 8.3 Input Parameters

### 8.3.1 Geometry

The design fire was placed in a carriage located close to the middle of the station, offset toward the station side containing the main exit. This position was deemed as most severe as it represents the shortest distance in which smoke would have to travel to reach the stairwells. The exact location is shown in Figures 14 & 15.

Figures 17 and 18 show a front and isometric view of the station construction:



Figure 17 - Front station view, XZ plane, cut at Y=45, platform level

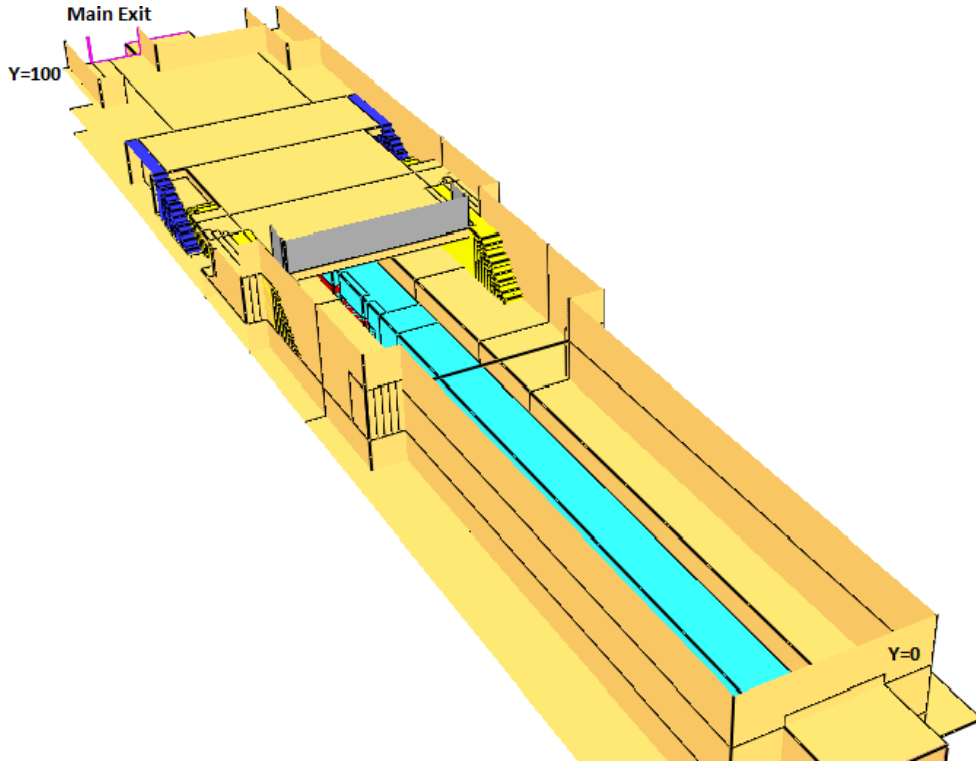


Figure 18 - Isometric station view (concourse ceiling clipped for clarity)

### 8.3.2 Material Selection

The solid surfaces of the station apart from the carriages were designated as inert. FDS treats this as a non-reacting isothermal surface. That is, the temperature is fixed (it is a user-specified temperature, ambient in this case) (McGrattan). Heat loss from the system does occur at these surfaces, but the surfaces are maintained at ambient temperature. Heat transfer is based on conduction, convection, and radiation. In this case, heat transfer due to conduction is negligible as smoke is a moving fluid, and heat transfer within the solid surfaces is not considered.

$$Q_{wall} = Q_{cond} + Q_{conv} + Q_{rad} = h(T_{gas} - T_{wall}) + Q_{rad,in} - \varepsilon T_{wall}^4$$

Both convection and radiation depend upon the temperature differences between the surface and gas. FDS internally calculates the convective heat transfer coefficient to determine the convective loss (McGrattan), based on the gas temperature computed near the wall. Radiative transfer occurs from the wall to the system and from the system to the wall. The loss from the wall to the system is constant, as the wall temperature is held at ambient. FDS uses a radiative transport model to calculate  $Q_{rad,in}$ . Emissivity is assumed to be an independent material property. (Mcgrattan)

An additional simulation was conducted to determine the sensitivity of this input parameter. The simulation specified a combination of brick and concrete as the surfaces of the stations, as noted during the field study. The brick and concrete properties are as follows. Results are contained in Section 9.

Table 3 - Thermal Properties, Brick/Concrete (Karlsson, 2000)

Brick	
Specific Heat	.84 kJ/kg-K
Conductivity	.69 W/m-K
Density	1600 kg/m <sup>3</sup>
Concrete	
Specific Heat	.8 kJ/kg-K
Conductivity	1.2 W/m-K
Density	2100 kg/m <sup>3</sup>

To represent heat transfer to and through the carriage walls, they were defined as aluminum, for all simulations. Material properties are isotropic. The specific heat was taken as a constant .9 kJ/kg-K (Metals - Specific Heats). The conductivity varies and thus was specified via a ramp function as follows:

Table 4 - Temperature vs Conductivity for Aluminum (efunda)

Temperature (°C)	Conductivity (W/m-K)
25	237.0
75	240
125	240
225	236
325	231
525	218

### 8.3.3 Window Properties

Window failure may occur in an enclosure fire due to the high temperatures. If a window breaks, it may drastically affect the course of a fire due to an inflow of oxygen or an outflow of pyrolysis gases or smoke. Predicting glass breakage thus is very important in simulating a fire, and may substantially influence performance criteria from visibility to temperature. However, uncertainties in such predictions pose a problem. As a result of research conducted during this project, a value of 600 degrees Celsius was determined to be the temperature at which windows would fail. Each window in the carriage containing the fire is divided into an upper and lower zone in FDS. A detector is placed on each zone, and when the specified temperature is reached, that pane of the window will fall out. The detectors are modeled as sprinklers with an RTI of 100 and an activation temperature of 600 C. Four windows were modeled, containing 8 panes.

A detailed literature review of previous testing and research on the subject is presented in [Appendix F](#).

### 8.3.4 Soot Production

A critical component that must accompany the HRR in any simulation is the smoke production. The volume of smoke produced can greatly affect the size of necessary extraction. The toxicity of the smoke can have a substantial effect on the ASET, even in the presence of reasonable smoke extraction systems.

Butler and Mulholland (Butler, 2004) discuss that smoke yield varies greatly between well-ventilated and under-ventilated fires. It can be expected that a subway carriage fire will be initially well-ventilated. As



the fire grows and consumes more of the surrounding oxygen, the fire will transition to an under-ventilated fire. Ventilation conditions may then change based on the amount of doors that are open and whether windows break. Based on such a discussion, it seems appropriate that the soot yield should change over the course of the fire. The following table summarizes smoke yields, as originally determined by Tewarson.

**TABLE 1**  
**Smoke Yields for Flaming Combustion in Air from Tewarson**

Material	Smoke Yield ( $g_{\text{smoke}}/g_{\text{fuel}}$ )	Comments
Solids (Polymers)		
Teflon (PTFE)	0.003	C—F halogenated linear structure
Wood (red oak)	0.015	C—H—O structure
Polymethylmethacrylate (PMMA)	0.022	C—H—O structure
Polypropylene (PP)	0.059	C—H branched structure
Polyethylene (PE)	0.060	C—H linear structure
Nylon	0.075	C—H—O—N linear structure
Polyester (PET)	0.089–0.091	C—H—O aromatic structure
Polycarbonate (PC)	0.112	C—H—O aromatic structure
Rigid polyurethane (PU) foam	0.104–0.130	C—H—O—N aromatic structure
Flexible polyurethane (PU) foam	0.131–0.227	C—H—O—N aromatic structure
Polystyrene (PS)	0.164	C—H aromatic structure
Polyvinylchloride (PVC)	0.172	C—H—Cl halogenated linear structure

Figure 19 - Soot Yields of various materials (Tewarson A. )

Chiam (Chiam, 2005) also conducted simulations of a subway carriage fire in FDS. Using the known material distribution in carriages in Singapore’s Circle Line, FRP polyester was determined to be the material of the highest quantity and thus its properties were used in simulations. The reaction parameters for FRP polyester used by Chiam are shown below. The chemical formula is that of FRP polyester. The fraction of soot used was 6.2%.

S/no	Parameter	Value	Remark
1	Chemical formula	$C_{5.77}H_{6.25}O_{1.63}$	
2	Energy per unit mass $O_2$ (kJ/kg $O_2$ )	11900	
3	Fraction of CO from fuel (kg/kg)	0.0705	
4	Fraction of soot from fuel (kg/kg)	0.062	
5	Radiative fraction	0.35	
6	Molecular Weight of fuel	101.6	Calculated
7	Stoichiometry coefficient for $CO_2$	5.77	Calculated
8	Stoichiometry coefficient for $H_2O$	3.125	Calculated
9	Stoichiometry coefficient for $O_2$	6.5175	Calculated

Figure 20 - FRP Polyester properties (Chiam, 2005)

The default value in FDS for propane is  $.01 g_{\text{smoke}}/g_{\text{fuel}}$ . Anywhere from .06 to .1 may have a large effect on the final simulation results and must be included. Following the work of Roh, Ryou, Park, and Jang

(Roh J. R., 2008), it is assumed that a subway carriage is composed of a mixture of materials including polyethylene, polypropylene, nylon, polyester, and polyurethane. An averaged value of these materials of  $.09 \frac{g_{\text{smoke}}}{g_{\text{fuel}}}$  will be used in the FDS simulation (Tewarson's values for polyurethane, as shown in Figure 19, have been averaged to 16.5%). Smoke yields in under-ventilated fires were found to have approximately 2.8 times the smoke yield (Tewarson A. J., 1993). To the knowledge of the author, it is not possible in FDS to manually designate soot yield as a function of ventilation conditions. Therefore,  $.09 \frac{g_{\text{smoke}}}{g_{\text{fuel}}}$  was used as a constant value for all simulations.

### 8.3.5 Heat Release Rate & Combustion Parameters

The HRR is represented by a rectangular burner in FDS, 14 meters in length by 2.5 meters wide. The fire grows to 35 MW in 341 seconds (Ingason H. , 2006). It is assumed that only one carriage is on fire, and that the fire covers the entire interior from the onset (flame spread is not modeled). The burner height is set at an approximate seat level of 80 cm above the floor. The HRRPUA method was used to define the HRR of the fire. In this method, pyrolysis and heat feedback to the burning surface are not modeled. Instead, a gas burner with a specified fuel flow rate is created (McGrattan).

Figure 21 displays a 2-D view of the subway carriage on fire, located in the guideway. The burner is in red, with only the top surface set as the burner surface.

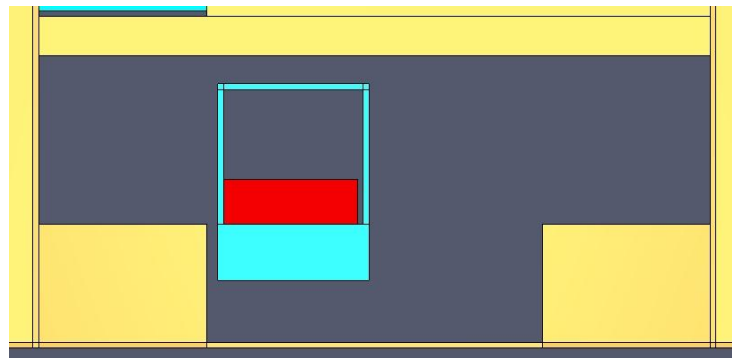


Figure 21 - Front view of carriage and burner

The mixture fraction approach was employed in FDS to model combustion. The mixture fraction model assumes that fuel and oxygen mix and react quickly and completely (in FDS Versions 2 through 4 this was assumed to be instantaneous). The user defines the fuel chemical formula and soot yields, which FDS uses to compute the burning rate and amount of combustion products formed (McGrattan) The chemical formula shown in Figure 20 was used as input to FDS.

### 8.3.6 Boundary Conditions

The station studied contains tunnels on either side linking it to additional stations. These stations are also underground and connect to further stations. There is a tunnel grade between stations on either side, which is not constant throughout the tunnel section, and ranges from 0% to 3.5%. The grade on both sides is in the same direction. The tunnel lengths to the adjacent stations are 496 m and 395 m, respectively, representing elevation changes of 9.2 and 5.6 meters. The station itself contains no known natural or mechanical ventilation. Only one known shaft is present in one of the tunnels. However, its

construction was unable to be determined. Due to the above uncertainty, the small elevation changes, and the short tunnel distances it was chosen to make the boundary conditions between the tunnels and station as “OPEN”. It is realized that this choice can have a large effect in reality and should be chosen with more precision when studied on a system level. However, this was an important simplification of the problem. The main exit on the concourse level was also set as an “OPEN” boundary. An open boundary is considered a passive opening to the outside. FDS assumes ambient conditions are assumed beyond the vent (McGrattan). This allows flow both in and out of the boundary, depending upon conditions inside the station. The domain of the CFD analysis included the entire station plus a five meter length extending into each tunnel. Later in the project these boundary conditions were verified. Several cases were conducted with dynamic pressure boundaries based on calculations seen [Appendix H](#). The results are discussed in Section 9.

No slip boundary conditions exist at the walls. This implies the continuum tangential gas velocity at a surface is zero (McGrattan). As grid size is not fine enough to resolve the boundary layer, a wall model is employed in FDS approximate the velocity gradient.

In cases with longitudinal ventilation, the boundary conditions at the tunnel portals were changed from “OPEN” to a constant inlet or outlet velocity over the entire portal boundary. This is another important simplification that can not necessarily be applied in practice, but was considered acceptable for the intent of the thesis.

### **8.3.7 Radiation Model**

The default gray-gas radiation transport model in FDS was used. An alternative wide-band radiation model is recommended for low-soot fuels due to the high computational cost (McGrattan). As a high soot production rate is specified here ( $.09 \text{ g}_{\text{smoke}}/\text{g}_{\text{fuel}}$ , vs.  $0.01 \text{ g}_{\text{smoke}}/\text{g}_{\text{fuel}}$  as default), this model was not considered.

Additionally, the fraction of energy released from the fire as thermal radiation must be considered. The FDS default radiative fraction of .35 was used, indicating that 35% of the heat released is in the form of radiation. The default choice is due again in part to the input specification of a sooty fuel. The soot production rate is nine times the default rate, which is most applicable to fuels with low soot production (for example, methanol). The default choice is also due to the dependence on the solver to accurately resolve the flame sheet to predict the radiative fraction. It is stated that with mesh cells on the order of one centimeter or larger, the temperature near the flame surface cannot be relied upon to accurately compute the source term in the radiation transport model (McGrattan). Given that the mesh cells are on the order of 20 centimeters and larger, it was decided not to rely on this calculation and instead use the default value of .35.

## **8.4 Tenability Criteria**

Very often, the first design criterion to be exceeded during a fire is visibility. When people cannot see, walking speed decreases. This results in an increased evacuation time and a potential increase in inhalation of toxic gases (Milke, 2002). Jin developed a relation between visibility and smoke obscuration. The relation is as follows:

$$S = \frac{K}{\alpha}$$

S represents visibility (in meters), the distance at which an object can just be seen.  $\alpha$  represents the “extinction coefficient” (in  $\text{m}^{-1}$ ). FDS calculates the extinction coefficient as a product of the density of smoke particulate, and a mass specific extinction coefficient which is fuel dependent (McGrattan). The default FDS value for mass specific extinction coefficient is  $8700 \text{ m}^2/\text{kg}$ , suggested for general flaming combustion of plastics and wood. K is a constant as defined by the work conducted by Jin, dependent upon factors such as color of smoke, object illumination, intensity of background illumination, and visual acuity of observer. (Milke, 2002). FDS assumes this value to be equal to 3.

Thus, with  $K$  constant, and the mass specific extinction coefficient constant, the visibility in FDS is calculated primarily based on the changing density of smoke particulate at each grid location. This, in turn, is dependent upon the soot yield and the tracking of its density within space in FDS.

Typically, a value of 10 meters is taken as the limit under which conditions are untenable. This is specified as a requirement in NFPA 130.

Visibility was tracked in FDS using slice files and beam detectors. Beam detectors were placed at strategic points within the station. The output quantity of these beam detectors is percent obscuration. Percent obscuration is taken over a designated distance, based upon the soot density. This value can be converted into visibility. Calculations are shown in [Appendix E](#).

In addition to visibility,  $60 \text{ }^\circ\text{C}$  is taken as the tenability criteria for temperature and  $2.5 \text{ kW}/\text{m}^2$  as the tenability criteria for radiant heat flux (NFPA, 2010).

## 9. Results

### 9.1 Grid sensitivity

A grid sensitivity study was conducted to determine grid independence. A simulation becomes grid independent when further refinement of the grid has no additional effect on the results. The non-dimensional parameter  $D^*/dx$  is recommended as a measure of how well the flow field is resolved (McGrattan).  $D^*$  represents the characteristic fire diameter.

$$D^* = \left( \frac{\dot{Q}}{\rho_{\infty} c_p T_{\infty} \sqrt{g}} \right)^{\frac{2}{3}}$$

It is important to note that this non-dimensional value is intrinsically tied to the chosen HRR. With smaller HRR's, smaller length scales are present, and thus smaller cells (and thus more total cells) will be necessary to obtain an equivalent resolution. Thus, any grid sensitivity study should be conducted with one specific reference HRR value. It was decided to use the peak HRR value, 35 MW, to calculate  $D^*$ . This enables the space to be properly resolved once the fire reaches its peak HRR. If a lower HRR is chosen (representing an instant during the growth phase), and when combined with the large domain, the quantity of cells becomes very large and thus simulations become constrained by computational power. With a peak HRR of 35,000 kW, the characteristic fire diameter is 3.96. In order to ensure that the flow is properly resolved, FDS developers have recommended as a starting point  $D^*/dx > 10$  (Groups, 2008), in which  $dx$  is the cell size. This produces a recommended starting cell size of 39 cm. Stated otherwise, with 39 cm cells, the burner will have 10 cells spanning its length. For sake of comparison, if 17,500 kW is chosen, 30 cm cells would be the suggested starting point with  $D^*/dx$  still equal to 10. The following table summarizes the chosen meshes, based on a HRR of 35 MW.

Another important aspect of grid resolution is the comparison of the chosen grid size with the size of the obstructions. A 39 cm cell will not accurately place a 10 cm thick obstruction. In all simulations, the thinnest obstructions chosen were 10 cm, representing glass enclosures of stairs, platform screen doors, and carriage walls (the heat transfer computation in the carriage is not bounded by the grid size, as the layer thickness is specified in FDS). However, using cells of 10 cm would result in simulations with at least 10 million cells (considering that the solver in FDS is optimized when cells are equal in XYZ directions). This is simply not practical in terms of simulation size and a compromise must be made. The final meshes used for the study are as follows:

Mesh Size	Mesh #	Number of Cells	Total Number of Cells	XYZ size (cm)	$D^*/dx$
Coarse		222,480	222,480	50x50x30	7.92
Medium		979,000	979,000	25x25x30	15.84
	Mesh 1	540,000		20x29x20	
Fine	Mesh 2 -Fire Zone	450,000	1,701,000	20x20x20	19.8

	Mesh 3	675,000		20x30x20	
	Mesh 4 - Tunnel	18,000		20x25x20	
	Mesh 5 - Tunnel	18,000		20x25x20	
	Mesh 1	1,080,000		20x19x15	
	Mesh 2 -Fire Zone	600,000	3,078,000	20x20x15	19.8
<b>Very Fine</b>	Mesh 3	1,350,000		20x20x15	
	Mesh 4 - Tunnel	24,000		20x25x15	
	Mesh 5 - Tunnel	24,000		20x25x15	

Figure 22 - Mesh Specifications

Figure 23 presents temperature vs. height in the subway station, for each of the four grids described above. Each data point represents an averaged value of temperature at a different height over 30 seconds. Simulation time was 420 seconds, thus the temperatures were averaged from 390 seconds to 420 seconds, appreciably far enough from the time at which the HRR stops growing and becomes constant, 341 seconds. The values are also taken along the longitudinal centerline of the station, and at a distance 14 m downstream of the nearest fire source edge, so as to avoid contact with the temperature fluctuations in the flaming region. Results show that the very fine mesh begins to converge with the fine mesh. The y-axis in Figure 23 below is clipped to start at 2 m height, as the temperatures near the bottom of the guideway shows no variation between grids. There are two distinct regions in the chart, one above 6 meters, and one up to just over 5 meters. This is due to the fact that there is a floor slab which has a user specified height from 5.2 to 5.9 meters. The actual position of the floor slab varies based on grid size, and this explains why for some grids temperatures higher than ambient are seen over 5.2 meters. Based on the results of this sensitivity study, the fine mesh was chosen for further simulations. While not entirely grid independent, the grid was selected as it offered a compromise between computational time and accuracy.

An additional grid sensitivity study could not be completed on a case including ventilation due to the long processing times. However, all cases with ventilation were also conducted with the *fine* mesh.

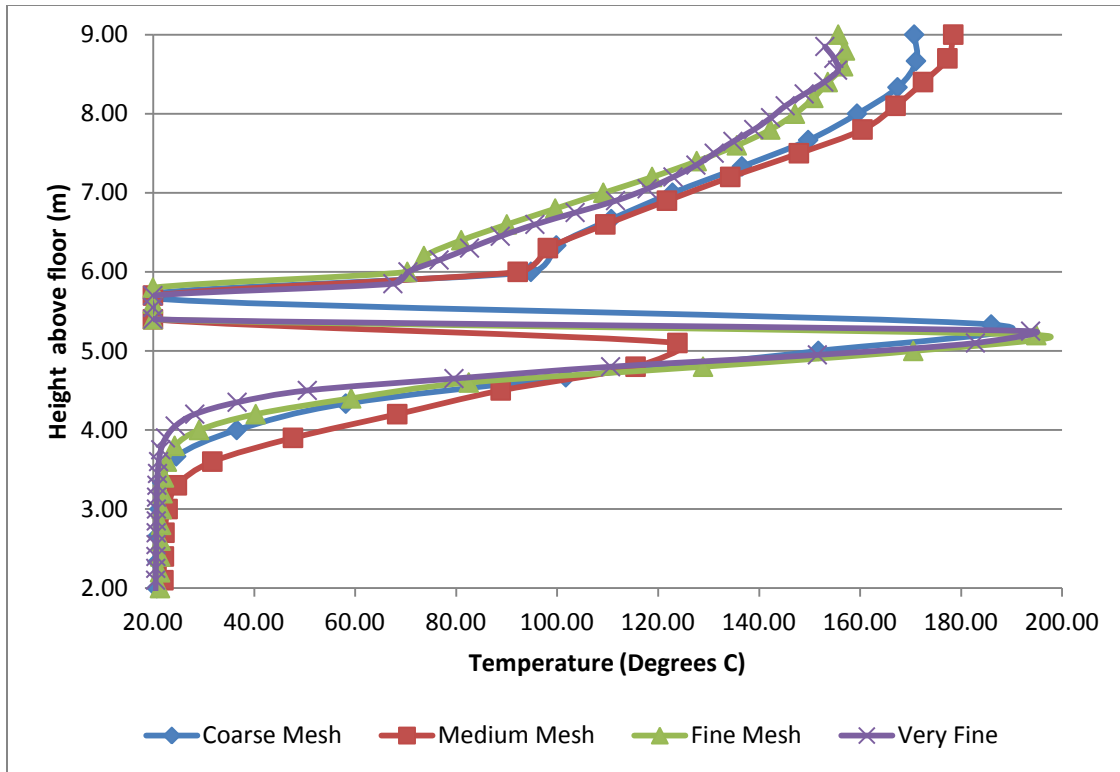


Figure 23 - Grid Sensitivity, All Meshes, Temperature vs. Station Height. Location 14 meters from fire source along station centerline. Averaged over 30 seconds from 390 to 420 seconds. Very fine and fine meshes converge.

## 9.2 Material sensitivity

It was expected that additional computational time would be required if conduction heat transfer through all surfaces of the station was simulated, due to the very large surface area of the station. Therefore, a study was conducted to determine if the selection of inert for the station material properties had a substantial effect on simulation results. Table 3 highlights the properties used for brick and concrete. Figure 24 shows the results from the additional simulation when compared to the base case with a fine grid. The curve represents temperature vs. height, at a distance of 15 meters from the end of the carriage, along the centerline of the station. Each point represents an averaged value over 30 seconds, beginning 50 seconds after the design fire has reached steady state (as with the grid study). The horizontal lines represent the floor between the platform and concourse levels. The temperatures at platform level are nearly identical, whereas a difference of approximately 10% is seen at the ceiling of the concourse level. The effect of this difference is that when brick and concrete are simulated as properties of the surfaces, less heat transfer occurs to these objects, and therefore temperatures in the station are slightly higher. Applying inert to these surfaces, therefore, results in slightly lower temperatures. Lower temperatures lead to less buoyant smoke, which results in the smoke layer descending quicker. Therefore, it was decided to select inert for all simulations, as it also allows for quicker computational times and provides more conservative results (it is expected visibility tenability conditions will be exceeded faster if the smoke layer descends quicker). It can also be said that higher temperatures which develop due to simulating material properties may cause temperature tenability criteria to be exceeded quicker, however, it is anticipated that this difference will be negligible.

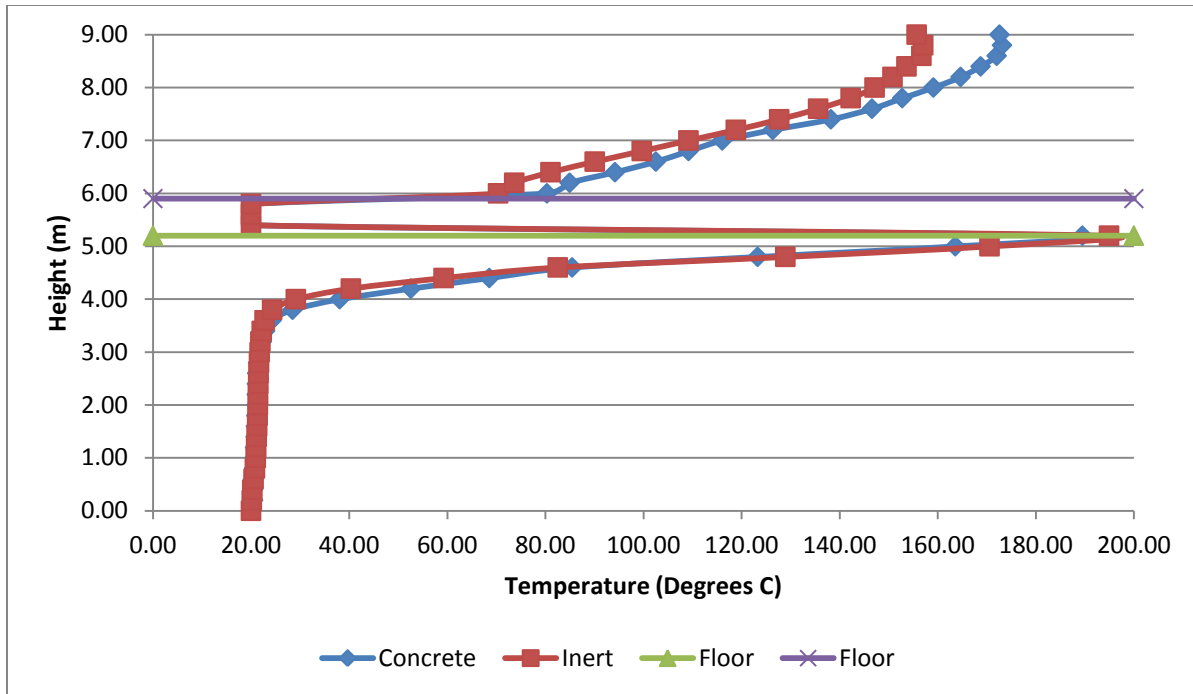


Figure 24 - Temperature vs. Height. Concrete and Brick vs inert station material properties.

### 9.3 Boundary Condition Sensitivity

As previously mentioned, “OPEN” boundary conditions were used for the majority of the simulations. This was done primarily due to the uncertainty in the behavior of the subway system as a whole. As a check, pressure loss calculations were made, assuming that each adjacent station is at ambient pressure (due to the possibility of larger stations, openings, or ventilation). The drop in pressure was used as a dynamic pressure boundary condition in FDS. As one tunnel length is longer than the other, this resulted in different dynamic pressure boundaries for each portal.

FDS assumes that the fluid flow is inviscid, steady, and incompressible. Therefore, Bernoulli’s principle holds true. The basic form of the Bernoulli equation is reduced by neglecting hydrostatic pressure head, and executed in FDS as follows, from (McGrattan):

$$\mathcal{H} = \text{DYNAMIC\_PRESSURE}/\rho_{\infty} + |\mathbf{u}|^2/2 \quad (\text{outgoing})$$

$$\mathcal{H} = \text{DYNAMIC\_PRESSURE}/\rho_{\infty} \quad (\text{incoming})$$

In practice, at an otherwise quiescent boundary, specifying a positive dynamic pressure will result in inflow to the station, and a negative, outflow. Due to the assumption that the adjacent stations are maintained at atmospheric pressure and that pressure loss occurs in the tunnels, dynamic pressures of -2.82 Pa and -3.56 Pa are specified (see [appendix H](#) for detailed calculations). This should result in outflow. As there is a slight pressure difference between portals, flow can be expected to move toward the region of lower pressure. The base case with dynamic pressure boundaries was compared to that with “OPEN” boundaries. It is seen in Figure 26 that this results in tenable conditions at V1 for 12 more seconds, and 77 more seconds at V3 (refer to Section 9.5 for location details). Flow is seen to be



preferentially drawn toward the right portal, which has the lowest pressure. The pressure on the concourse is seen to be slightly higher than the platform, also leading to tenable conditions for longer on the concourse. Velocities through the main exit with the dynamic pressure BCs were in the range of 1.5-2 m/s, whereas with “OPEN” BCs, this phenomenon does not occur. A comparison of the two showing dynamic pressure at the station centerline, averaged from 70 to 100 seconds over the station height, is shown in Figure 25 (taken at Y=80, 20 meters from portal). Since the majority of the cases were initially conducted with “OPEN” boundaries, the results were taken with caution and several additional cases conducted with dynamic pressure boundary conditions. “OPEN” boundary conditions were generally expected to be more severe in terms of preventing smoke spread, as smoke is not preferentially drawn to one portal due to the pre-existing pressure difference. It is also noted that the pressure differences due to buoyancy of hot gases from the fire play a larger role in driving smoke flow in the station, when compared to the natural flow (in the absence of fire) generated in the station due to the pressure difference between portals.

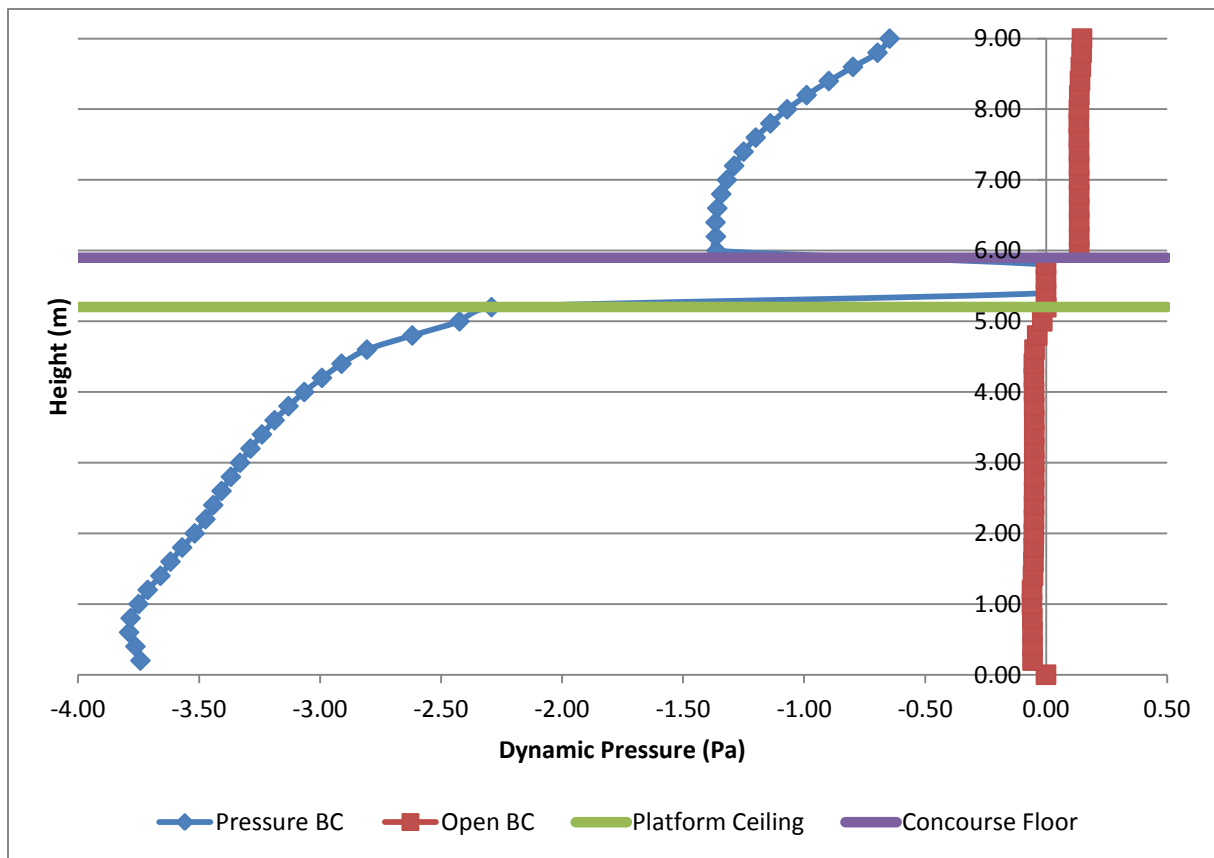


Figure 25 - Dynamic Pressure vs. Height for OPEN and Dynamic Pressure BCs Taken 20 meters from tunnel portal and averaged over 30 seconds from 70 to 100 seconds

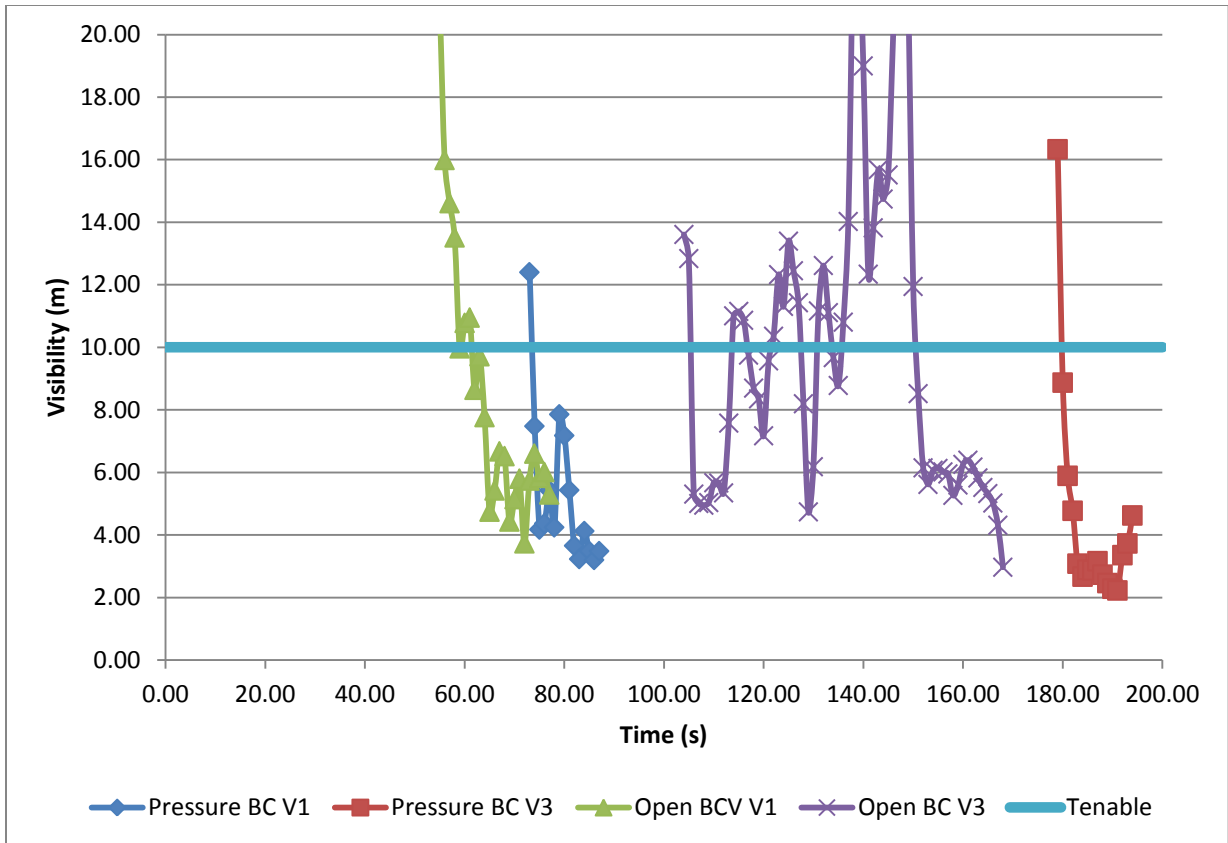


Figure 26 - Visibility at V1 & V3, Open vs. dynamic pressure BCs. 10 meter tenability criteria. See Figure 32/33 for location.

### 9.4 Resulting HRR

The following chart shows the resulting HRR from the FDS simulations, for the base case with a fine mesh. In blue is the theoretical HRR curve, which was used as input to the simulation. The red curve shows the resulting HRR where no window breakage is simulated. The green curve compares the resulting HRR when window breakage is simulated. The yellow curve follows the right hand y-axis and shows the mass burning rate, which is identical for cases in which window breakage was simulated and not simulated. This is important as it confirms that the quantity of soot injected into the system is identical in both cases. The HRR curve was also compared with that of the very fine mesh and results were similar.

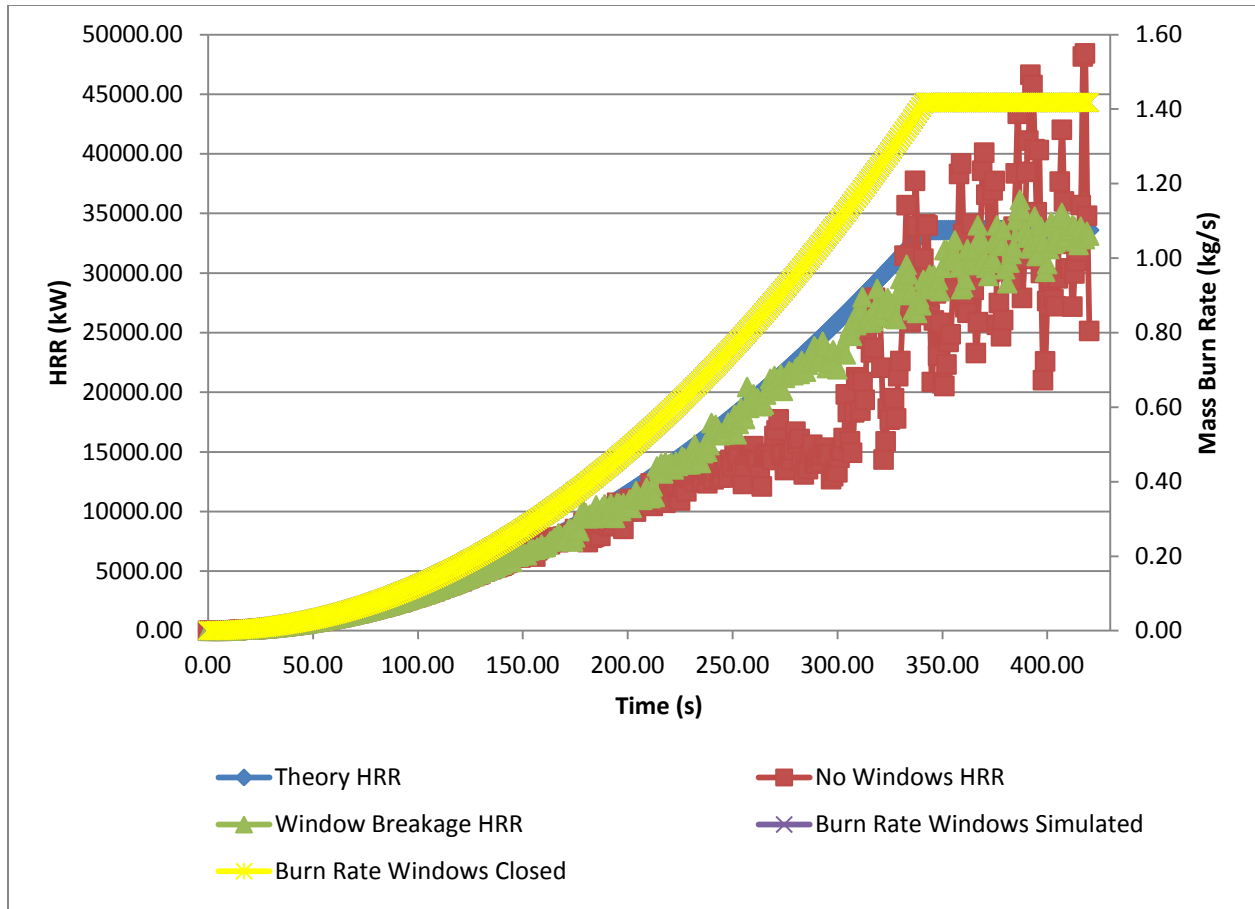


Figure 27 – Resulting HRR & Burn Rate verse time. Burn rate windows simulated not seen as it is identical and thus overlapped by the yellow curve. Yellow curve follows right Y-axis. Green curve (windows breaking), follows theoretical HRR curve most closely/

It can be seen that around 200 seconds, the red HRR curve begins to diverge from the input (in blue). This is due to the oxygen concentration in the station decreasing and not mixing with the pyrolysis gases in sufficient concentration and time. At this point, flames are leaving the carriage which is on fire and consuming oxygen in the surrounding region. Large fluctuations in HRR are seen starting at 300 seconds. Here, flames are seen outside the carriage. As flames leave the carriage and consume all of the available oxygen in the vicinity, energy is released and the HRR increases. After mixing and combustion occurs, the HRR decreases due to lack of oxygen. Once more fresh air comes in, the HRR spikes then decreases, and the fluctuations continue as such. After 341 seconds, the FDS input reaches its maximum burning rate. It can be seen after this time on the chart that while there are still large HRR fluctuations due to oxygen availability, the average HRR appears to be at the input value of 35 MW.

The green curve, however, follows the theoretical curve better. This is due to the windows breaking, the first of which occurs at around 175 seconds and the last at around 260 seconds (see Figure 28). As pyrolysis gases exit the carriage in new locations, mixing with oxygen in the station is enhanced, leading to more combustion.

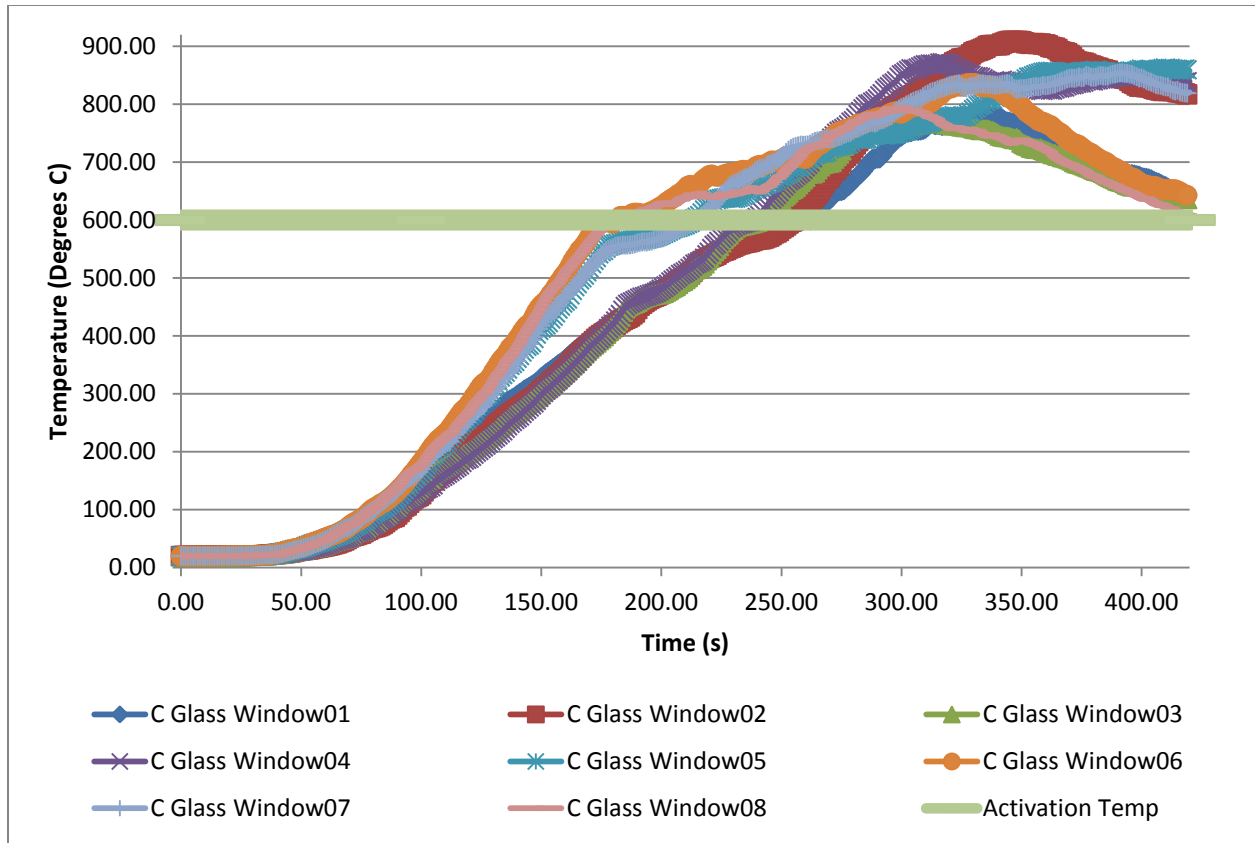


Figure 28 - Glass temperature vs Time, base case, fine mesh. 8 thermocouples representing 8 window panes. Fallout at 600 Celsius.

The majority of simulations were conducted before the results of windows breaking were discovered. Therefore, some results are presented where glass breakage has not been simulated, and are indicated as such. The final simulations for case ranking were all verified for performance in case of glass breakage. As a check, the red and blue curves in Figure 29 show that over time (for the base case), the temperature of the smoke over the height of the station can vary up to approximately 35% near the platform ceiling, and 20-25% just above the concourse floor. These temperatures are averaged over 30 seconds (from 390 to 420 seconds), 15 meters downstream from the carriage on fire, along the station centerline. It should be noted these conditions represent the worst case, as the HRR is at steady state (35 MW), and after 390 seconds, even by prescriptive methods, the station should no longer contain people. The green and purple curves show a much smaller difference in temperature, of maximum 16 %, but for the most part less than 10 %. These curves represent the temperatures at the same location, however, averaged over 30 seconds during the *growth* stage of the fire, from 200-230 seconds. This is a more realistic time interval when considering egress. Four of the windows were broken by the end of this duration.

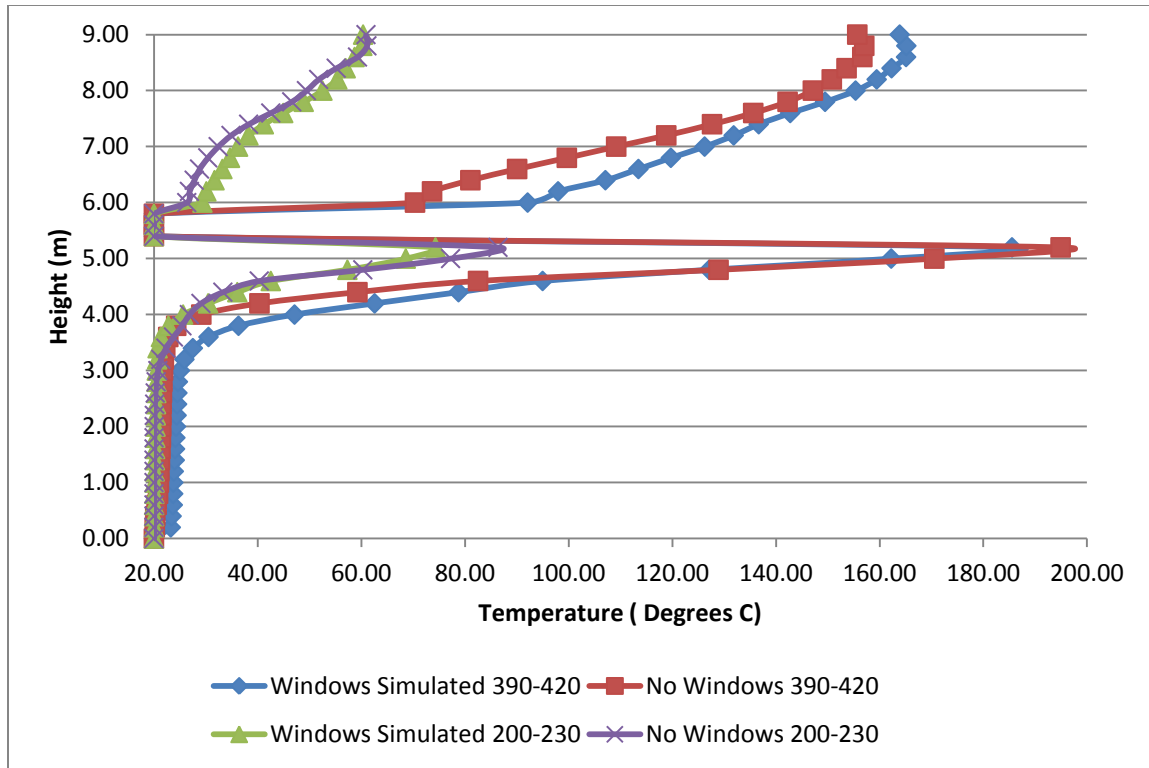


Figure 29 - Temperature vs Height, Window breakage vs. no window breakage. 15 meters from fire source. Averaged over 30 seconds from 200-230 and 390-420.

To verify why the red and green HRR curves in Figure 27 deviate from the input HRR, the oxygen concentration outside the carriage was studied. Figures 30 and 31 shows the oxygen mass fraction at individual points just outside of the fire region, along the length of the carriage, averaged over 5 second intervals for 5 continuous intervals (total 25 seconds), during two different stages of the fire growth. It can be seen that there are three spikes in each of the five intervals, attributed to the three doors of the carriage in which pyrolysis gases leave, mix with air, combust, and thus lower oxygen concentration. The decrease in oxygen concentration is seen in Figure 30 to be small from 90 seconds to 115 seconds, where the HRR is low and the curve follows closely the theoretical curve in Figure 27. The station is still well ventilated at this point. Between 305 seconds and 330 seconds, the oxygen concentration drops dramatically, corresponding to the large fluctuations seen in Figure 31. Each of the 5 vertical boxes in Figures 30 and 31 can be thought to represent the carriage length containing the design fire, arranged in increasing averaged times from left to right. One way of viewing the chart is to look at the progression of the first, second or third spike in each of the 5 vertical divisions. In this manner the fluctuations in oxygen concentration outside the carriage with time can be seen, explaining the fluctuations in HRR.

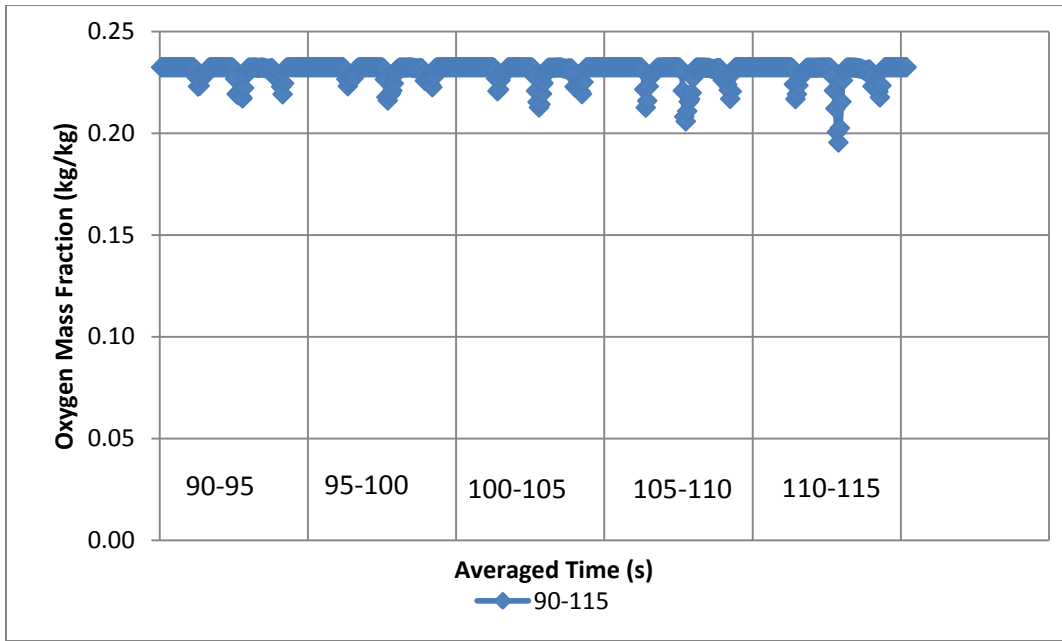


Figure 30- Oxygen Mass Fraction vs. Time. Data points along the length of the carriage, just outside. Each vertical section represents the length of the carriage on fire, proceeding in averaged time from left to right. First vertical box is averaged from 90-95, second from 95-100, and so on. Spikes represent the three doors of the car. The change in the first spike in each subsequent vertical section represents fluctuations in oxygen mass fraction just outside the carriage, as flames leave and then return to the carriage via one door. Only small fluctuations are seen during this time interval as station is well ventilated and fire is small.

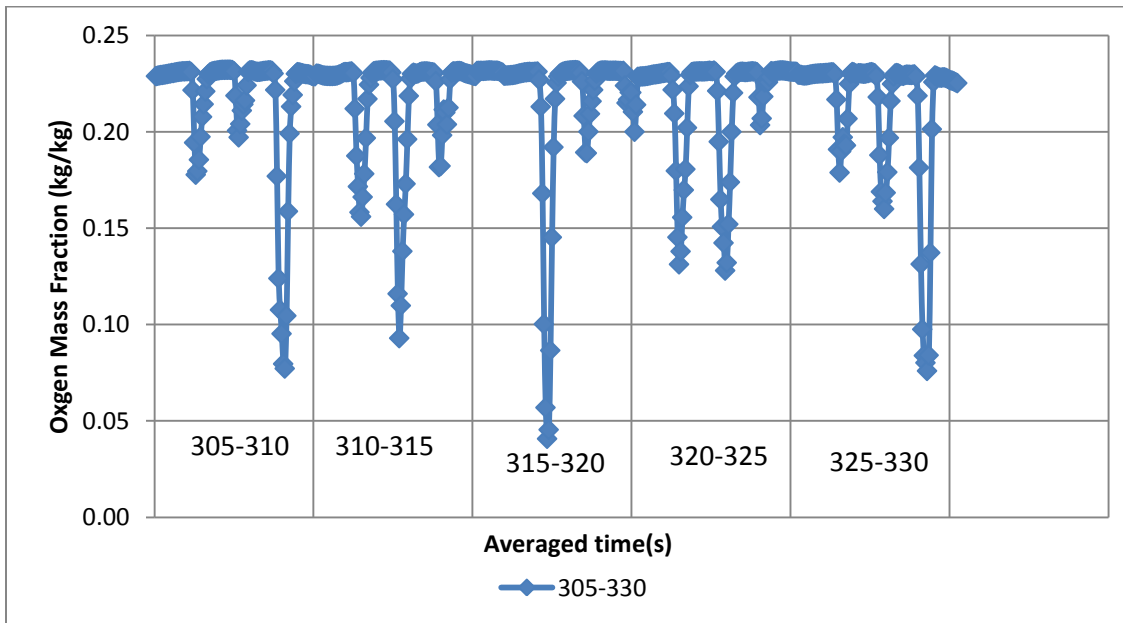


Figure 31 - Oxygen Mass Fraction vs. Time. Data points along the length of the carriage, just outside. Each vertical section represents the length of the carriage on fire, proceeding in averaged time from left to right. First vertical box is averaged from 300-305, second from 305-310, and so on. Spikes represent the three doors of the car. The change in the first spike in each subsequent vertical section represents fluctuations in oxygen mass fraction just outside the carriage, as flames leave and then return to the carriage, of one door. Large fluctuations are seen in this chart as the fire is large and station less well ventilated.

## 9.5 Simulation Results – Concourse Level Visibility

Visibility was the main tenability criteria tracked using FDS. Temperature is considered in Section 9.7. Figures 32 and 33 show the locations chosen to track tenability criteria, representing critical points between platform and concourse level. All detectors are placed two meters above floor level, and the point-to-receptor distance of the beam detectors is 1.4 meters. All points are located on the concourse due to the fact that once tenable conditions are exceeded at these points, no additional passengers can be expected to escape the station through the main exits. Platform visibility is considered in Section 9.6.

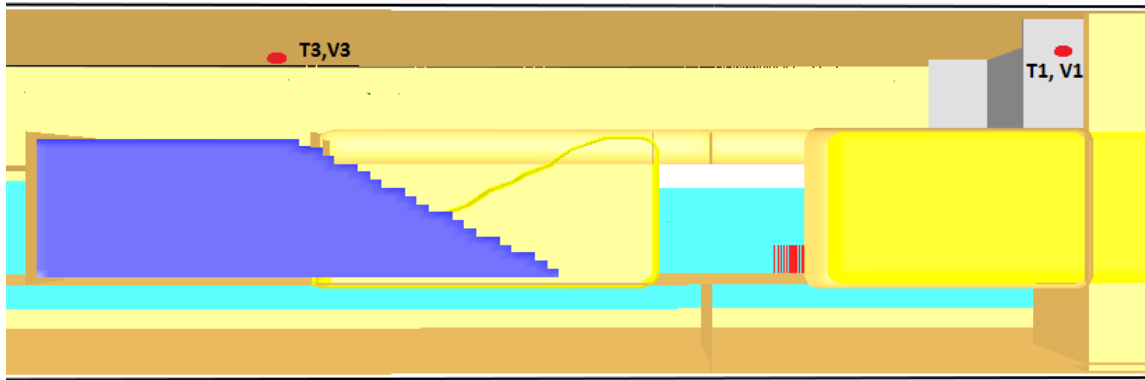


Figure 32 - Locations of visibility and temperature detectors in FDS, Side View

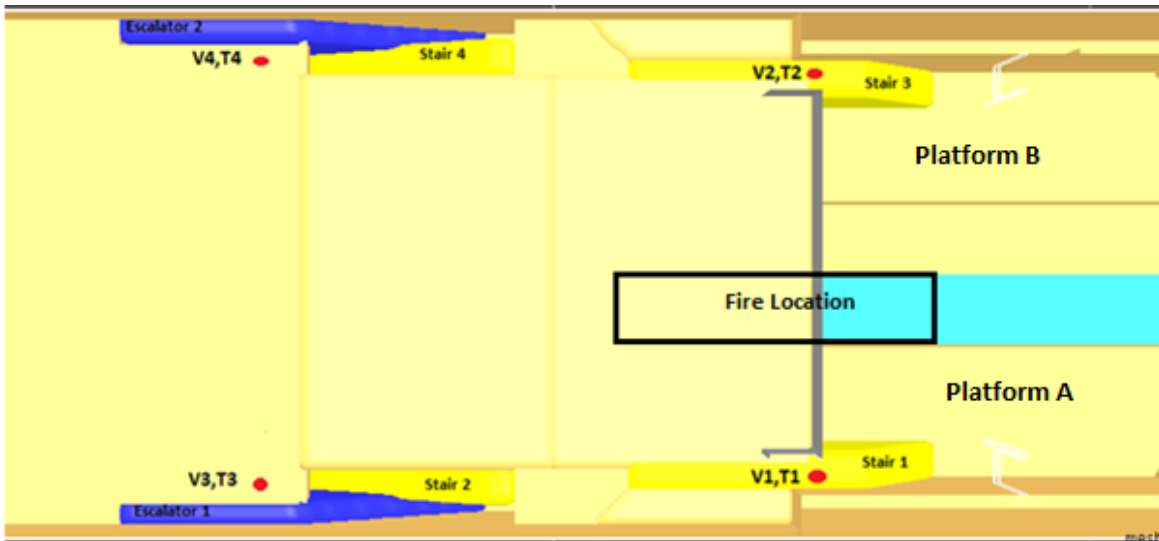


Figure 33 - Location of visibility and temperature detectors in FDS, Top View, Concourse Level

The following table shows the results of all simulations. The time at which visibility tenability criteria is exceeded is displayed for V1 and V3.

Table 5 - Results of all simulations, Time to exceed visibility shown at V1 and V3 (Refer to Figure 32/33 for locations)

	Case	BCs	Window Breakage Simulated	V1	V3
Passive Protection	Base Case (BC)	Open	N	62	106
	Base Case (BC)	Pressure	N	74	180
	BC + Smoke Screens	Open	Y	79	118
	BC + Stairs Enclosed(1)	Open	N	140	211
	BC + Stairs Enclosed (2)	Open	Y	140	224
	BC + Stairs Enclosed + PSD	Open	N	124	215
	BC + Stairs Enclosed + Revised PSD (1)	Open	N	185	289
	BC + Stairs Enclosed + Revised PSD (2)	Open	Y	188	288
	BC + Stairs Enclosed + Smoke Screens	Open	Y	160	198
	BC + Multiple Smoke Screens + Stairs Encl.	Open	Y	166	163
Longitudinal Ventilation Only	Push Only	Open	N	48	125
	Push-Pull	Open	N	46	120
	Pull Only	Open	N	107	205
	Pull-Pull (1)	Open	N	156	238
	Pull-Pull (2)	Open	Y	176	246
Transverse Ventilation Only	Atrium Vents	Open	N	49	186
	Side of Reservoir Extraction (80 m <sup>2</sup> /s)	Open	N	51	158
	Side of Reservoir Extraction (120 m <sup>3</sup> /s)	Open	N	49	100
	Ceiling Exhaust (1)	Open	N	55	87
	Ceiling Exhaust (2)	Pressure	N	55	179
Hybrid Smoke Control	Stairwell Pressurization	Open	N	197	247
	Push + Stairwell Pressurization	Open	N	162	135
	Push + Ceiling Exhaust + Stairs Enc.	Open	N	116	256
	Push + Ceiling Ex. + Stairs Enc + Revised PSD	Open	Y	250	388
	Push + Side Ex. + Stairs Enc + Revised PSD	Open	Y	192	143
	Side Ex. + Stairs Encl + Revised PSD	Open	Y	356	413
	Ceiling Ex + Stairs Enc+ Revised PSD	Open	Y	363	365
	Pull + Stairs Enclosed	Open	N	384	359
	Pull + Stairs Enclosed + Smoke Screens	Open	Y	>420	397
	Pull-Pull + Revised PSD + Stairs Enc.	Open	Y	>420	>420
Push-Push + Side Extract + Stairs Enc.	Open	Y	89	100	



### 9.5.1 Passive Smoke Control

The results show that passive smoke control methods are not effective in providing sufficient evacuation time before tenability limits are exceeded.

*Base Case:* The base case was first simulated in order to draw comparisons to further simulations. The balcony was enclosed to prevent immediate smoke spread to the concourse, as shown by the white barrier seen in Figure 34.

*Smoke Screens:* The smoke screens were modeled as .70 meter deep obstructions originating from the ceiling, 1 meter outside the carriage guideway, running the longitudinal length of the station. In the atrium, they were extended to the ceiling. The results show they are only a slight improvement over no smoke control. It was seen in the FDS simulation that as the fire grew, the smoke layer in the carriage descended. This caused smoke to spill out of the doors at a lower height, assisting the smoke in bypassing the smoke screens. Furthermore, the smoke layer depth under the ceiling quickly exceeded the depth of the smoke screens. This indicates the depth of the smoke screens is an important variable controlling screen effectiveness, which is limited by the station design. Deeper smoke screens were not possible in this scenario due to the low ceiling height (as exiting passengers could come into contact with them at head level). Smoke screens are colored red in Figure 34.

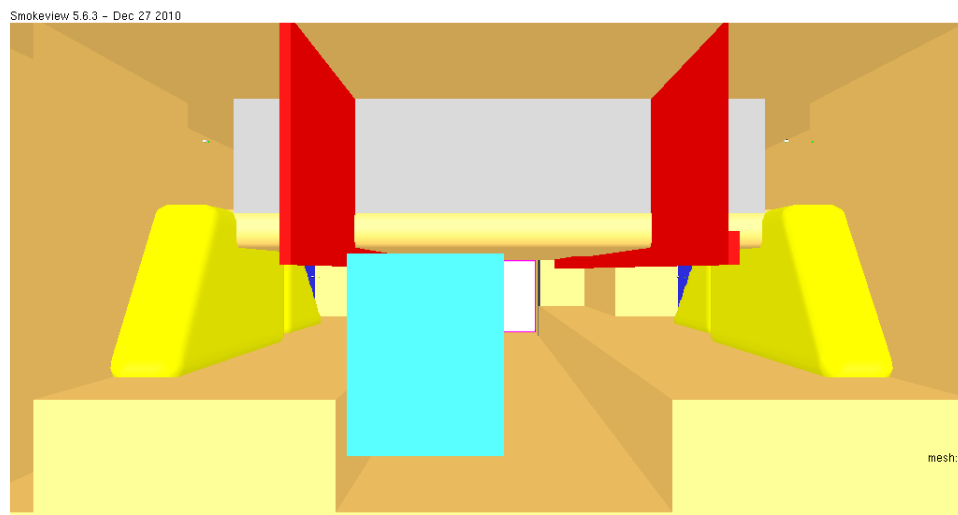


Figure 34- Smoke Screens as seen in Smokeview

*Stairs Enclosed:* The stairs were enclosed to attempt to limit smoke spread to the concourse. Access to stairway exits 1 & 3 is provided via doorways, 2.2 meters in height, shown in Figure 35. Stairwells 2 and 4, and escalators 1 and 2 (refer to Figures 13 & 14) were more difficult to enclose in the same manner due to the unique design, however, attempts were made to do such via walls and strategically placed screens as shown in Figure 36. This case was simulated with and without window breakage. Conditions at V1 remain unchanged as windows do not break before tenability is lost here. However, tenable conditions exist longer at V3 as the broken windows disperse more smoke away from this stairwell.

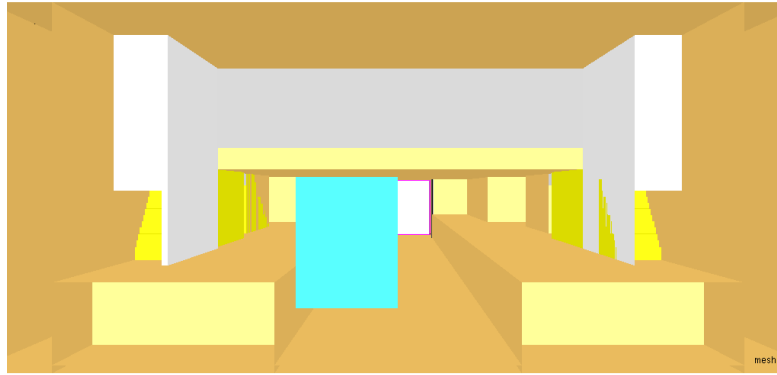


Figure 35 - Stairs 1 & 3 Enclosed

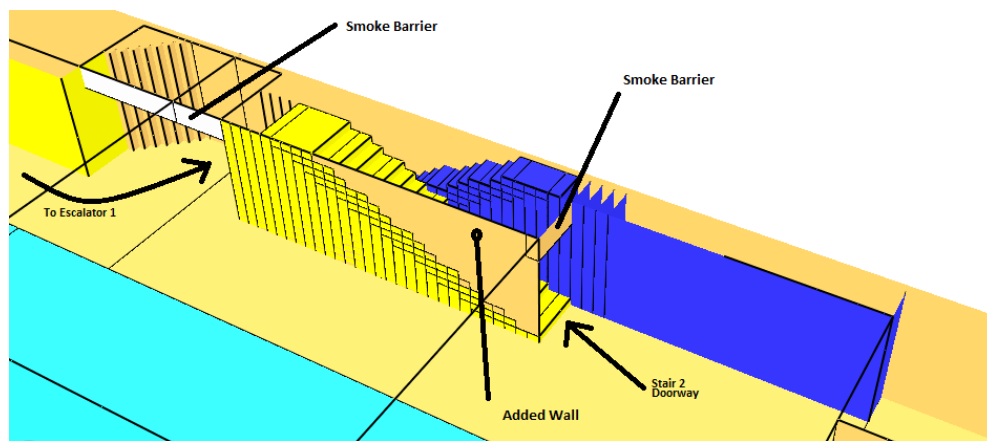


Figure 36 - Stairs 2/4 & Escalators 1/2 enclosed (concourse not shown)

When compared to the base case and smoke screens, enclosing the stairs proved to be more effective in increasing the time at which tenable conditions exist at concourse level.

*Platform Screen Doors + Stairs Enclosed* : The platform screen doors were modeled with all doors continuously open on platform A, due to the expectation that passengers will be escaping from all carriages. On platform B, they were closed. The closed doors proved effective in eliminating any platform level smoke movement to platform B. This would allow for any waiting passengers on platform B to escape in the absence of smoke. This assumes the glass used for the platform screen doors do not break due to elevated temperatures and that the doors are well sealed to prevent leakage.

Platform screen doors were simulated in two configurations. In the first case they were placed at the edges of the platforms, as appears to be the current practice in PSD design. In the second case, they were moved farther away from the platform, to determine if the buoyancy of the hot smoke could be used to more effectively capture escaping smoke. The design is shown in [Appendix G](#). With the revised platform screen doors, the visibility criterion is exceeded at 185 seconds at V1, and 290 seconds at

V3. Figure 37 shows how the platform screen doors limit smoke spread to platform B. This case was simulated with and without window breakage as seen in Figure 39/40, and minimal difference in performance was seen.

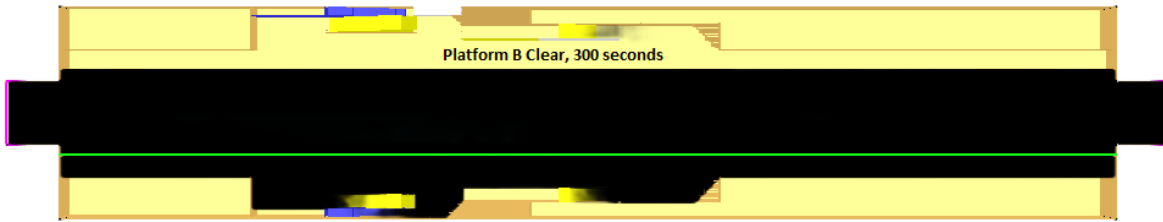


Figure 37 - Top view of platform level with platform screen doors (seen in green). Platform B clear after 300 seconds.

*Smoke Screens + Stairs Enclosed:* Both of these methods were combined, to study the cumulative effect. The result is that at V1, the sum is better than each protective measure individually. However, at V3 tenability is actually maintained for 20-25 seconds less when compared to simply enclosing stairs. There was no discernible reason for this behavior.

*Multiple Smoke Screens + Stairs Enclosed:* More smoke screens were added, perpendicular to the longitudinal ones, to attempt to compartmentalize the station. At V3, performance decreased. The screens compartmentalized the smoke more effectively, keeping smoke closer to the centrally located stairwells, and inhibiting spread further down platform to tunnels. On the contrary, these screens did aid in improving tenability at the far reaches of the platform level. The screens are seen in Figure 38.

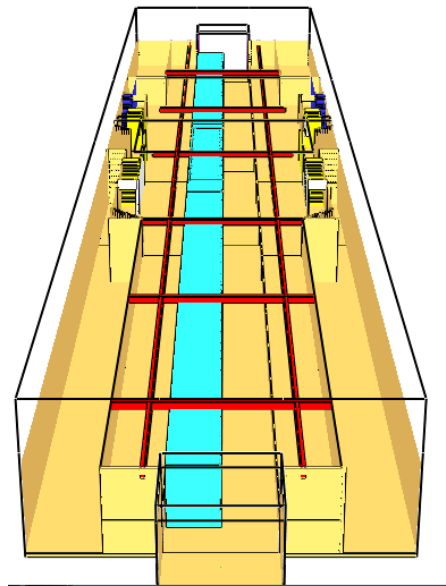


Figure 38 - Multiple smoke screen design. Additional screens bisect longitudinal screens.

The revised platform screen doors are the best performing passive smoke control method. Figures 39 & 40 display the visibility results of all passive methods, at points V1 and V3. Window breakage is noted where simulated.

The downside of the revised PSDs is that the available platform width for passengers is reduced, possibly making large numbers of passengers uncomfortable or reducing capacity. The difference in this case was a minimum platform width of 2.8 m in the first case, and only 2 m with the revised doors. [Appendix G](#) contains a visual comparison of how the smoke buoyancy aids containment within the revised platform screen doors. .

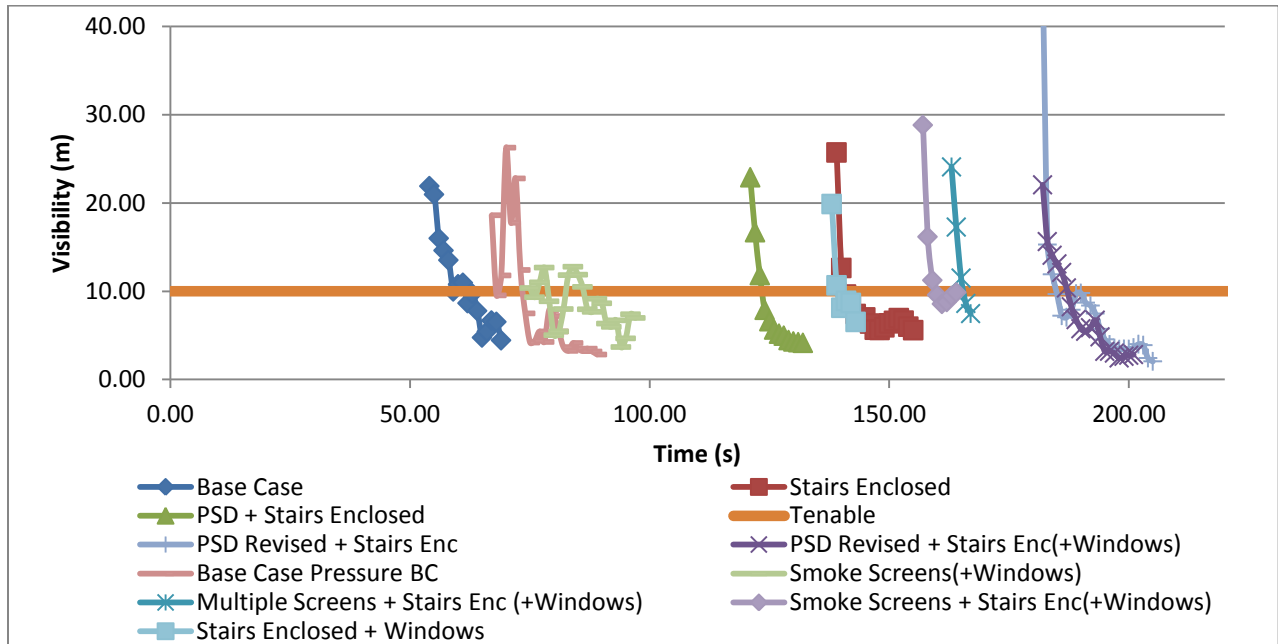


Figure 39 - Visibility at point V1 (see figure 32/33 for location) .Tenability exceeded under 10 meters.

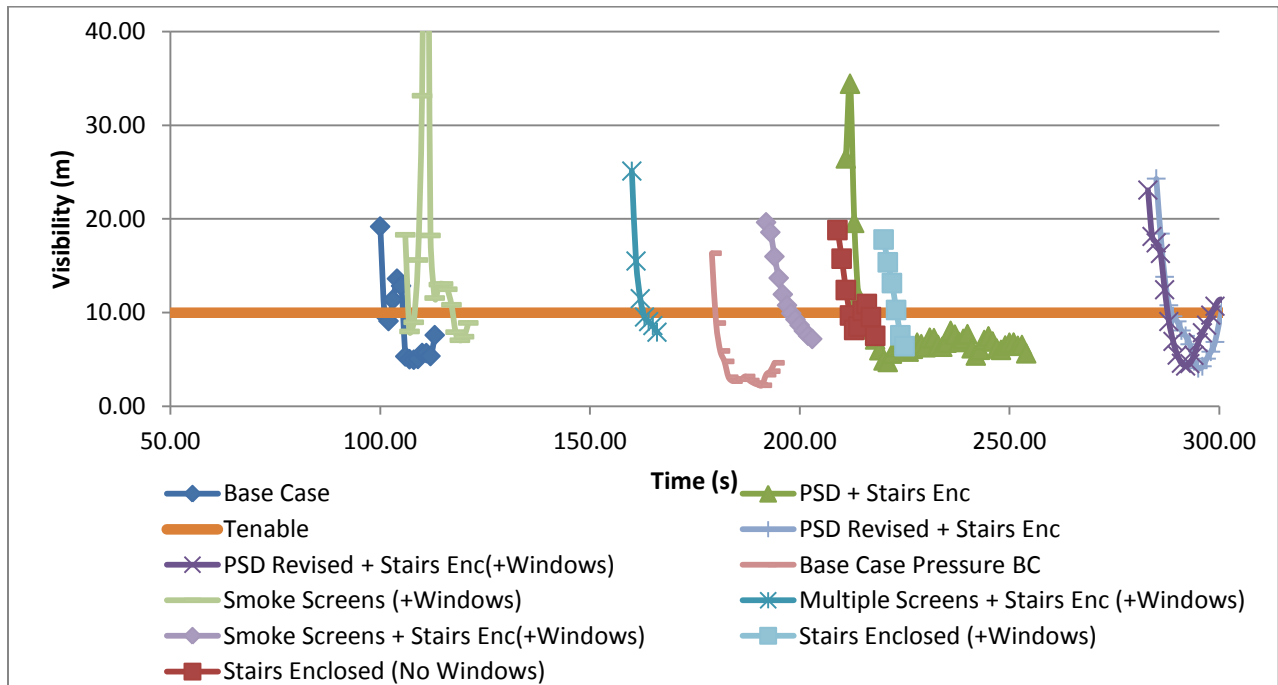


Figure 40 - Visibility at V3 (see figure 32/33 for location). Tenability exceeded under 10 meters

## 9.5.2 Mechanical Smoke Control

Appendix B shows initial calculations used in order to approximate the necessary extraction rate and critical velocity to prevent backlayering. As a starting point,  $80 \text{ m}^3/\text{s}$  ( $288,000 \text{ m}^3/\text{hr}$ ) was used for the extraction rate, and  $3 \text{ m/s}$  was used as the critical velocity. When applied to the tunnel portal, a velocity of  $3 \text{ m/s}$  is equivalent to a volumetric flow of  $144 \text{ m}^3/\text{s}$  (without adjustment based on grid spacing in FDS)

### 9.5.2.1 Longitudinal Ventilation

Figures 45 & 46 show the resulting visibility as a function of time at points V1 and V3.

*Push Only:* A  $3 \text{ m/s}$  “push” (inlet) boundary condition was applied to the left tunnel in order to prevent backlayering. As expected, backlayering was prevented on this side of the tunnel. However, with no means of extraction and air being primarily supplied at platform level, the remainder of the station was filled quickly. Visibility was exceeded at approximately 50 seconds at V1 and 120 seconds at V3. Smoke still spreads to the concourse through all stairwells.

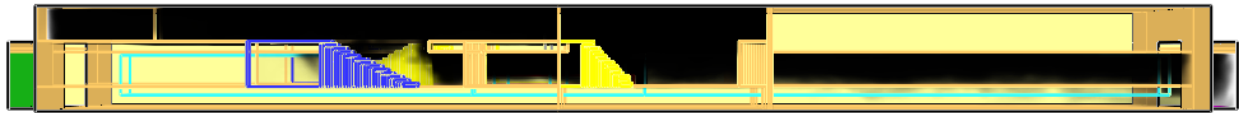


Figure 41 - Push Only, Smoke spread at 180 seconds

*Push Pull:* A  $3 \text{ m/s}$  “push” (inlet) boundary condition was applied to one tunnel in order to prevent backlayering, and a  $3 \text{ m/s}$  “pull” (outlet) boundary condition was applied to the opposing portal to remove smoke. In this configuration, the “push” again prevents smoke from backlayering to this side of the tunnel for over 3 minutes. However, it still works to supply air from the bottom level of the station, allowing smoke to flow freely to the concourse. The outlet velocity on the platform serves to pull some smoke out in comparison to the case with “pull only”, but this is not sufficient. Results are nearly identical to the “push only”. Tenability is lost at V1 after approximately 50 seconds, and 120 seconds at V3.

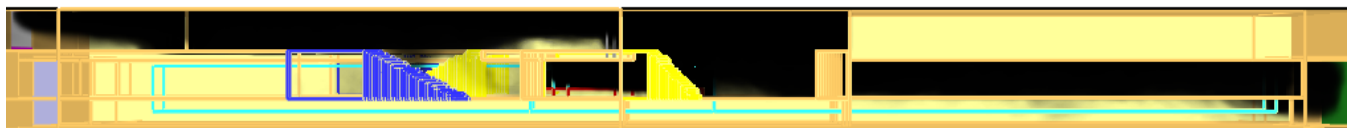


Figure 42 - Pull Pull, Smoke spread at 180 seconds.

*Pull Only:* This case was identical to “push only”. However, the direction of the boundary condition was reversed. A large improvement in tenability was seen on the concourse. This is due to the fact that removing air at platform level causes make-up air to be supplied from the main exit at concourse level. The benefit of this is it provides resistance to hot smoke attempting to migrate upwards. Tenability is lost at V1 just after 100 seconds, and just after 200 seconds at V3. The right hand side of the station is kept clear. While pulling at  $3 \text{ m/s}$ , the make-up air that is supplied at concourse level through the main exit comes in at between  $2$  to  $3 \text{ m/s}$ , with occasional fluctuations seen between  $3$  and  $4 \text{ m/s}$ .

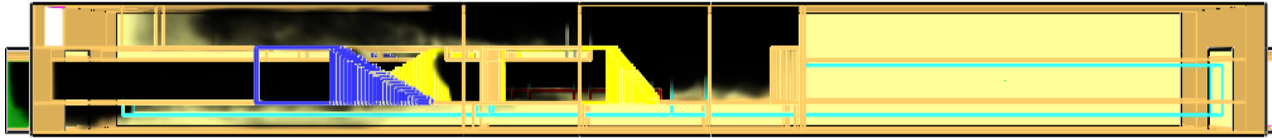


Figure 43 – Pull Only, Smoke spread at 180 seconds

*Pull-Pull:* A two m/s “pull” was initially applied to both tunnel portals. 2 m/s was chosen instead of 3 m/s because it was expected that make up air would enter the concourse through the main exit at high velocities, making egress uncomfortable. This was confirmed, and although tenable conditions were maintained for longer, velocities of 10 m/s were still seen at concourse level. Therefore, an additional case was conducted, with the boundary velocity change to .75 m/s (resulting in unadjusted volumetric flows of 36 m<sup>3</sup>/s at each portal). In this configuration visibility at V1 is lost at 170 seconds and at V3, 245 seconds. Although the concourse is kept clear for longer, the pulling of air at both portals causes the entire platform to fill with smoke (see Figure 41 at 180 seconds). This case was also simulated with window failure, and this resulted in tenable conditions at V1 & V3 for a slightly longer period of time.

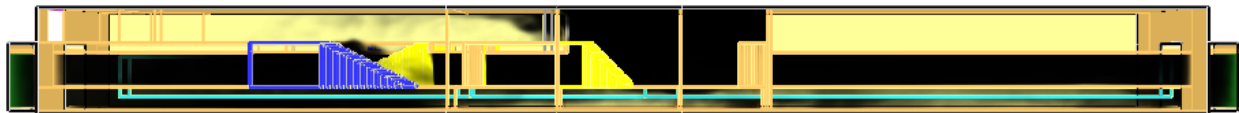


Figure 44 – Pull-Pull, 180 seconds

In terms of concourse visibility, the pull-pull configuration maintains tenable conditions for the longest duration. At the platform level, the push only configuration, push-pull, and the pull only configuration each maintain visibility on one half of the station. This is offset by a quicker loss in visibility at concourse level. Overall, none of these solutions provides tenable conditions for long enough, when compared to both the 4 minute NFPA 130 requirement, or the 322 second FDS+Evac derived RSET.

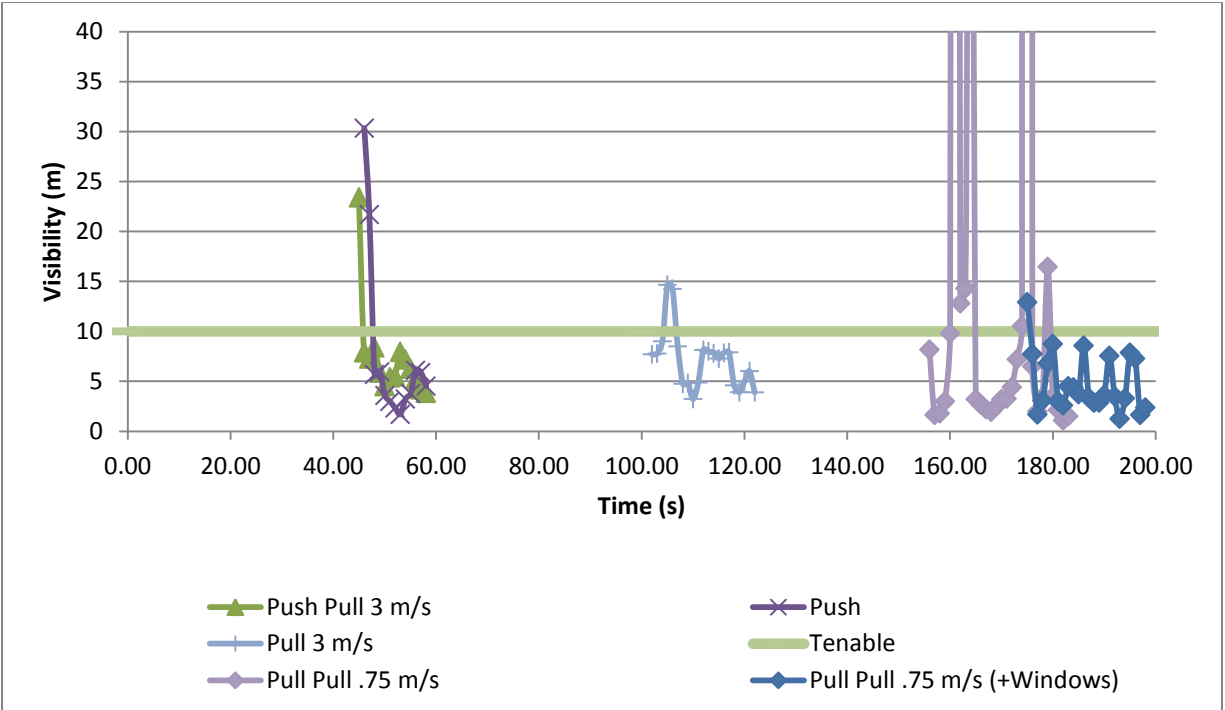


Figure 45 – Visibility at V1 (refer to Figure 32/33 for location). All cases longitudinal ventilation only.

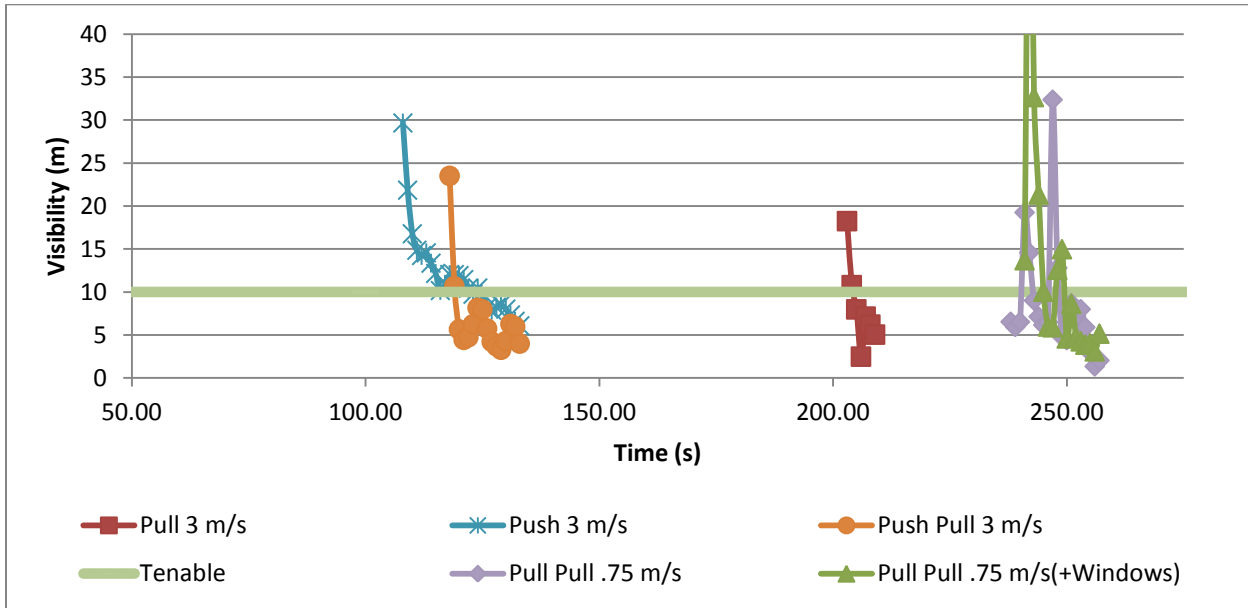


Figure 46 – Visibility at V3 (refer to Figure 32/33 for location). All cases longitudinal ventilation only.

### 9.5.2.2 Mechanical Extraction

The station contains a large, enclosed, empty space at concourse level. This space is inaccessible to the public and was reserved for future use. In attempting to extract smoke from the station, this space was utilized. Several locations for extraction points were considered. Visibility at points V1 and V3 is shown

in Figures 51 & 52. In all cases, no additional measures of passive protection are considered when compared to the base case. Window breakage was not simulated.

*Atrium Vents:* Two vents were placed in the atrium ceiling, each with an area of  $13.5 \text{ m}^2$  and extraction rates of  $40 \text{ m}^3/\text{s}$ . Vents were approximately 3.7 times longer in the X direction than the Y direction to prevent plugholing, and spaced 6 meters apart to maximize the efficiency of each vent. This was the best of the three arrangements, as it provided the most direct extraction path and utilized the smoke's buoyancy most effectively due to the placement of extraction locations placed on the station ceiling. Visibility was exceeded at V1 after 53 seconds and at V3 at approximately 185 seconds. Once the plume impinges on the station ceiling, a jet is created in which part of it spreads to the vents and part of it spreads immediately to the concourse. The extraction from the atrium is not enough to compensate. Enclosing the stairs would prevent immediate spread to the concourse. Make-up air is supplied primarily through the tunnel portals. This allows the platform to remain clear for a longer duration, as seen in Figure 47. The right hand side of the platform is clear and the left hand side is partially clear due to incoming air which opposes smoke flow.

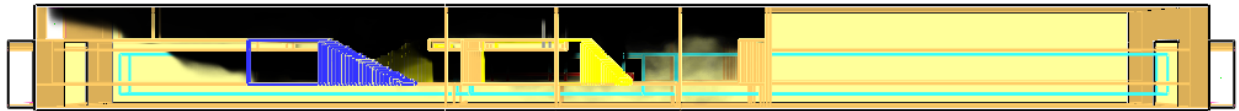


Figure 47 - Atrium Vents, 240 Seconds

*Ceiling Vents:* Ten square exhaust ports, each with an extraction rate of  $8 \text{ m}^3/\text{s}$  and an area of  $.50 \text{ m}^2$  were placed along the centerline of the station at the platform ceiling. Each port is separated by 3.1 meters to maximize efficiency. The smoke is extracted from the station into the reserved space. Exhaust ports are shown in green in Figure 48. This is the worst performing of the three arrangements, primarily due to the fact that the ports do not use the smoke's buoyancy very well. The atrium fills first, and once smoke spreads underneath the ceiling and ports, extraction begins. Also, the ports are located further from the fire source, so some ports are never utilized for extraction, as seen in Figure 49.

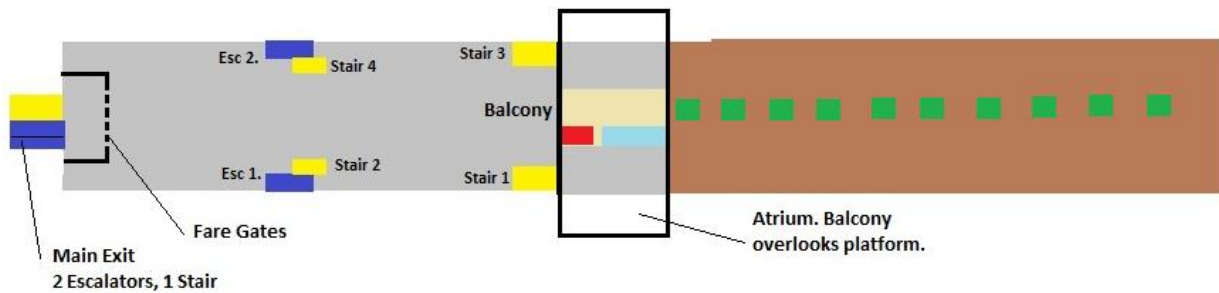


Figure 48 - Exhaust ports for ceiling vents



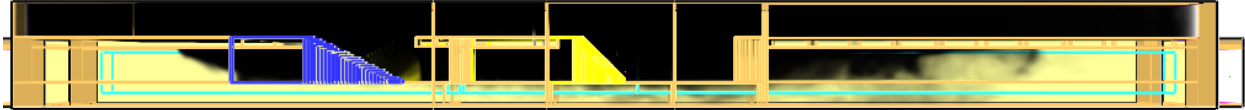


Figure 49 -10 exhaust ports (some exhaust ports seen not extracting), 240 seconds

Figures 51 and 52 also show visibility with this method as seen when boundary conditions are “OPEN” and with dynamic pressure BCs. The difference is negligible at V1; however at V3 tenable conditions exist for longer due to the pressure difference between portals, which directs flow away from V3. With these boundary conditions, more of the 10 vents are utilized for extraction than seen in Figure 49.

*Side Extraction:* This again uses the reserved space for smoke extraction, but places the extraction location at the vertical interface between the reserved space and the atrium. The idea is to utilize the smoke buoyancy, while still making use of the reserved space. As expected, at V3 the performance is better than the ceiling vents, but worse than the atrium vents. This case was conducted with extraction rates of both 80 m<sup>3</sup>/s and 120 m<sup>3</sup>/s. The larger extraction rate was seen to decrease the time at which tenability is exceeded.

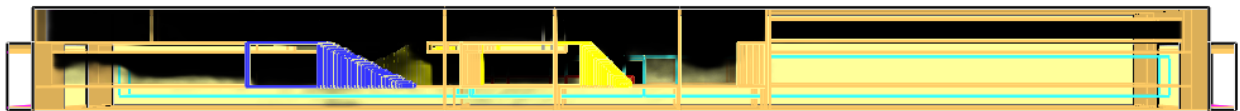


Figure 50 - Side Extraction, 240 seconds

In all cases, tenability is exceeded on the concourse before the 4 minute NFPA 130 requirement for clearing the platform (indicating that with a smoke-filled concourse, the only egress option would be to evacuate through the tunnels or platform emergency exits if conditions allow). Tenability is maintained to various degrees spatially and temporally on the platform level in all cases. Therefore, to maximize the duration and extent in which tenable conditions exist in the station, these methods should be combined with either a passive method of smoke control, longitudinal ventilation, or overpressurization, as seen in the following section.

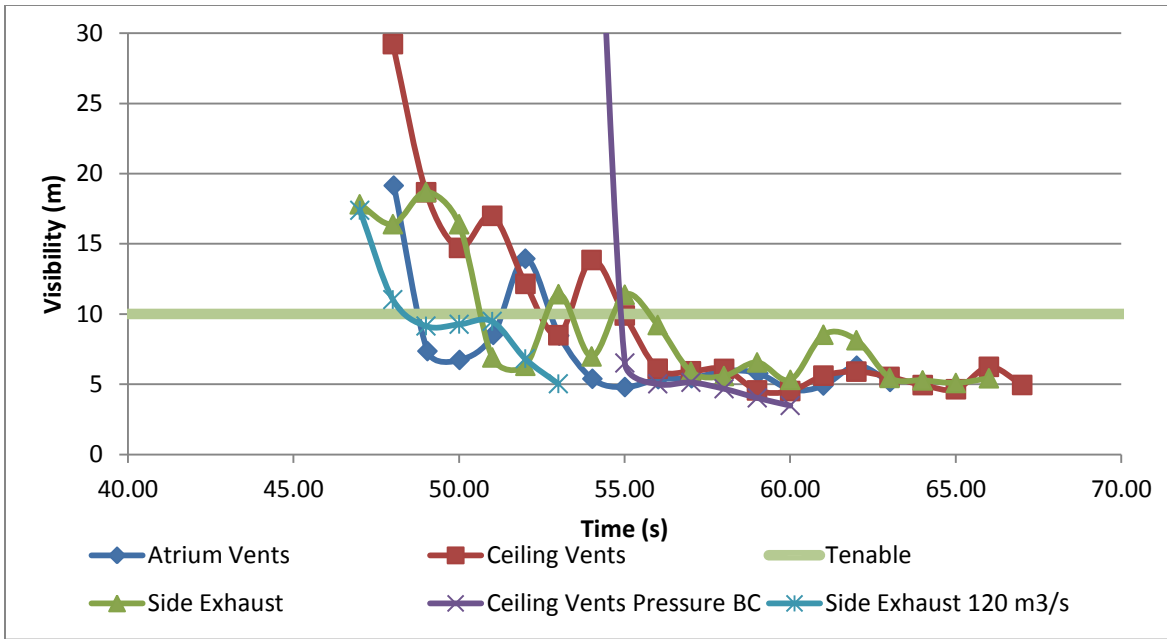


Figure 51 - Visibility at V1 (refer to Figure 32/33 for location), all mechanical extraction methods

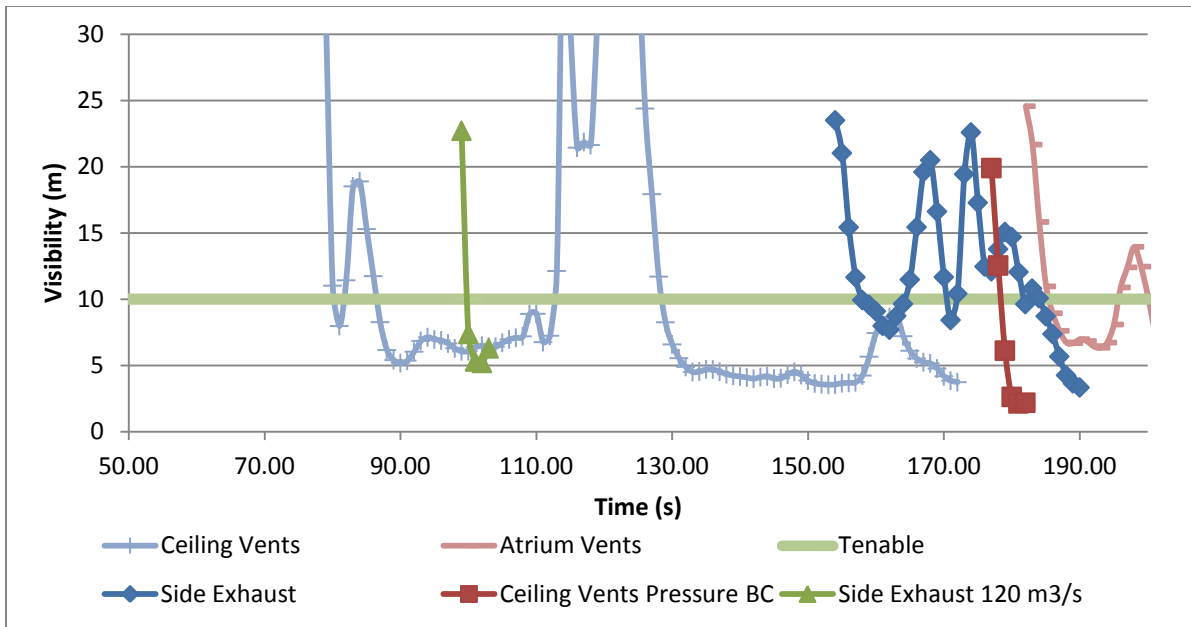


Figure 52 - Visibility at V3 (refer to Figure 32/33 for location), all mechanical extraction methods

### 9.5.2.2 Hybrid Methods of Smoke Control

**Stairwell Pressurization:** An attempt was made to pressurize the stairwells to prevent smoke spread to the concourse. Due to the difficulty in enclosing stairwells two/four and escalators one/two, only stairwells one and three were pressurized (see Figure 14 and 15). This prevented smoke from entering the concourse through these stairwells. However, smoke still was easily spread through the remaining stairs and escalators. Visibility tenability is exceeded at V1 in 197 seconds and in 247 seconds at V3.

*Push + Stairwell Pressurization:* As seen in Table 5, tenability is lost quicker on the concourse when a push boundary condition is applied in addition to stairwell pressurization. This is due to the fact that the smoke which previously spread to the tunnel actually is forced up to the concourse. As a benefit, the left side of the platform is kept clear. [Appendix I](#) compares the two cases by showing visibility at X=2.6 m (slice through the stairwells), at 180 seconds. A higher critical velocity might prevent backlayering to a greater degree such that less smoke would spread to the concourse (indicating also that the formulas used for critical velocity may not be on the safe side). Visibility at V1 is exceeded in 162 seconds and in 135 at V3.

*Push + Ceiling Exhaust + Stairs Enclosed:* This combination is seen to be more effective in maintaining the visibility criteria at both V1 and V3, when compared to push only or ceiling exhaust only. V1 is exceeded at 116 seconds, and V3 is exceeded at 256 seconds.

*Push + Ceiling Exhaust + Stairs Enclosed + Revised PSD:* When platform screen doors are added, more smoke is contained within the boundaries of the PSDs at platform level. Thus, the concourse remains clearer for longer. V1 is exceeded at 250 seconds and V3 is exceeded at 388 seconds.

*Push + Side Exhaust + Stairs Enclosed + Revised PSD:* The previous case was changed to see the effect in altering the exhaust location from platform ceiling to the side of the reserved space. In this arrangement concourse tenability was exceeded much faster. This appears to be due to the fact that the ceiling exhaust creates a greater pressure difference along the length of platform A (due to the 10 distribution points), causing the smoke to flow away from points V1 and V3. The tradeoff is that point V7 (discussed in Section 9.6), loses tenability much faster on the platform level. [Appendix J](#) shows figures of the pressure distribution in the station. [Appendix J](#) also shows velocity vectors in stairwell two, providing further rationale as to why less smoke spreads to the concourse with the ceiling exhaust.

*Side Exhaust + Stairs Enclosed + Revised PSD:* The push was removed from the previous case to view the difference. Tenability at V1 is exceeded at 353 seconds and at V3 at 413 seconds. Without a 'push' to prevent backlayering, smoke is allowed to fill the platform and also leave through the tunnels. Make-up air is also supplied through the stairwells, from the concourse to the platform. Thus, tenability improves at platform level.

*Ceiling Exhaust + Stairs Enclosed + Revised PSD:* The location of extraction was again switched to study the effect. The performance at V1 is only slightly improved, whereas at V3 it decreases by about 50 seconds to 365 seconds. Still, tenability is maintained for 6 minutes at both locations.

*Pull + Stairs Enclosed:* The stairs were enclosed in addition to the 'pull' only case, to improve tenability at the concourse level. V1 was exceeded in 384 seconds, and V3 in 359. The platform level is filled with smoke quickly.

*Pull + Stairs Enclosed + Smoke Screens:* Smoke screens were added to the previous case, as in Figure 34. V1 was not exceeded in 420 seconds, and V3 was exceeded in 397 seconds.

*Pull-Pull + Revised PSD + Stairs Enclosed:* .75 m/s outlet velocity boundaries were applied to each portal. Both V1 and V3 were not exceeded after 420 seconds, demonstrating that enclosing the stairs and adding revised PSDs to the 'pull-pull' configuration substantially improves tenability at a concourse level.

*Push-Push + Side Exhaust + Stairs Enclosed:* It was attempted to prevent backlayering from both sides of the fire, to confine the smoke and then extract it from a central location. This strategy did not work, as visibility at V1 and V3 are exceeded in only 89 and 100 seconds, respectively. A higher extraction rate or extracting through the ceiling of the atrium (possibly coupled with slightly higher ventilation rates) could make this situation more viable for concourse level smoke control.

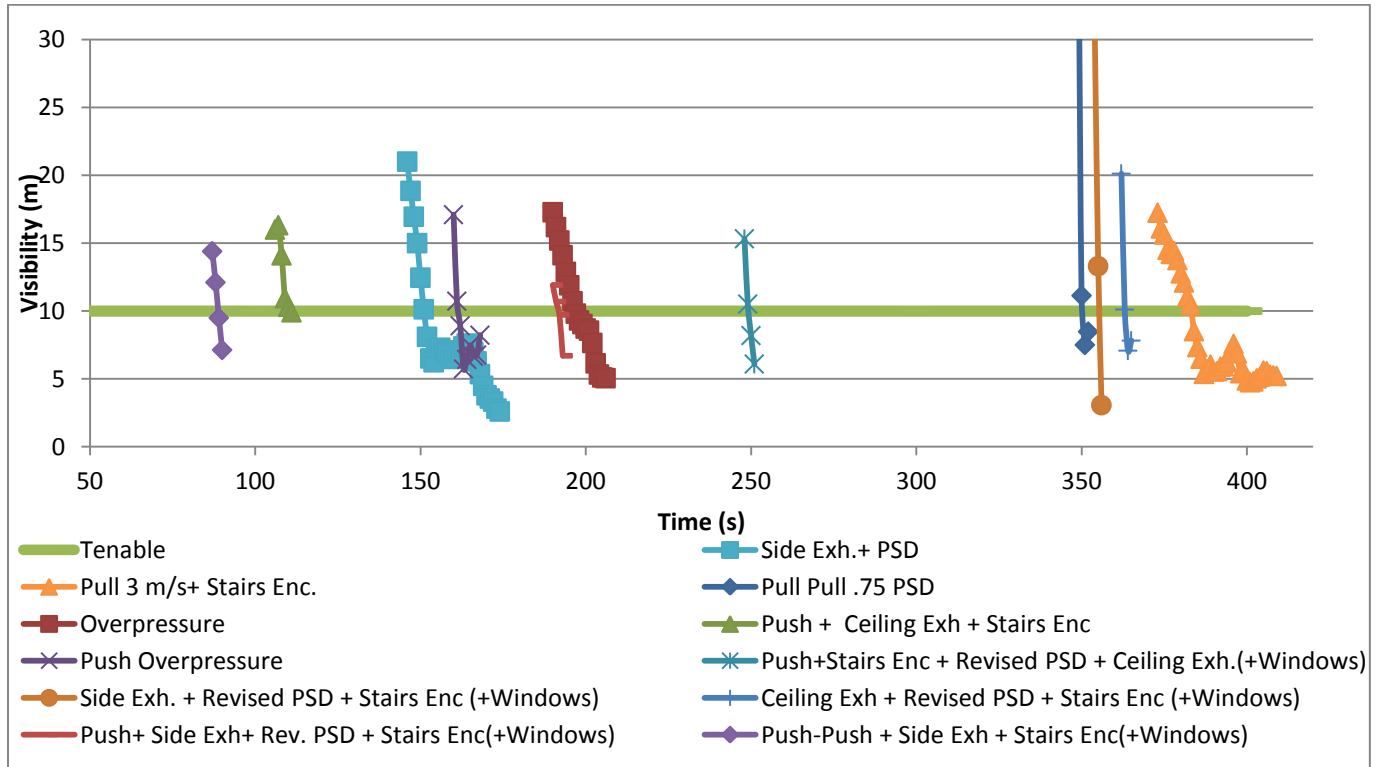


Figure 53 - Visibility at V1 (refer to Figures 32/33 for location). All hybrid methods of smoke control. Pull-Pull with revised PSD+ Windows not shown as tenability not exceeded in 420 seconds.

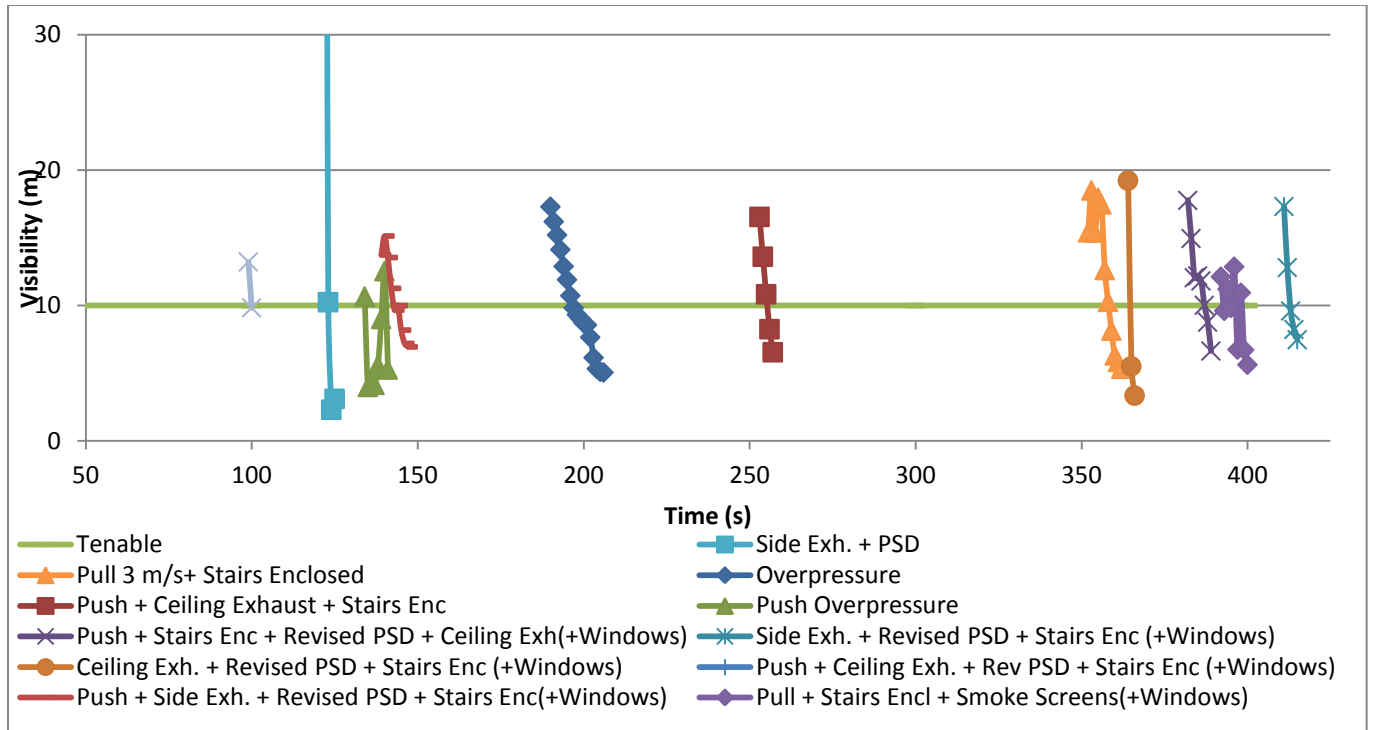


Figure 54 - Visibility at V3. (refer to Figures 32/33 for location). All hybrid methods of smoke control. Pull-Pull with revised PSD+ Windows not shown as tenability not exceeded in 420 seconds.

### 9.6 Simulation Results – Platform Level Visibility

A limited number of the above cases were conducted in which visibility was tracked at platform level. Four beam detectors were placed at the locations shown in Figure 55, placed 2 meters above the floor. Detectors V4 and V5 span 1.4 meters, detectors V6 and V7 span 2 meters (point to receptor). T5 represents a temperature detector at platform level.

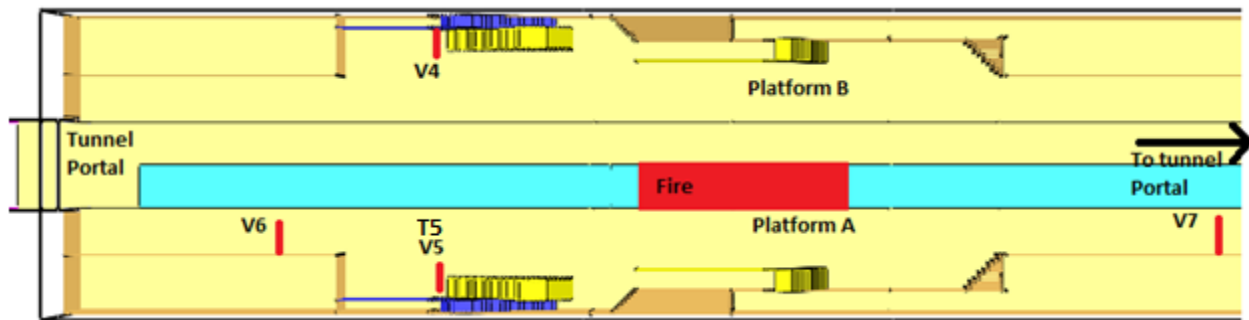


Figure 55 - Placement of beam detectors V4, V5, V6, and V7. Top view. Platform level.

The cases were primarily hybrid methods of smoke control, with a few cases of passive methods only for comparison’s sake. Figures 56-59 show the resulting visibility plots at V4, V5, V6 and V7, with comments contained in the captions.

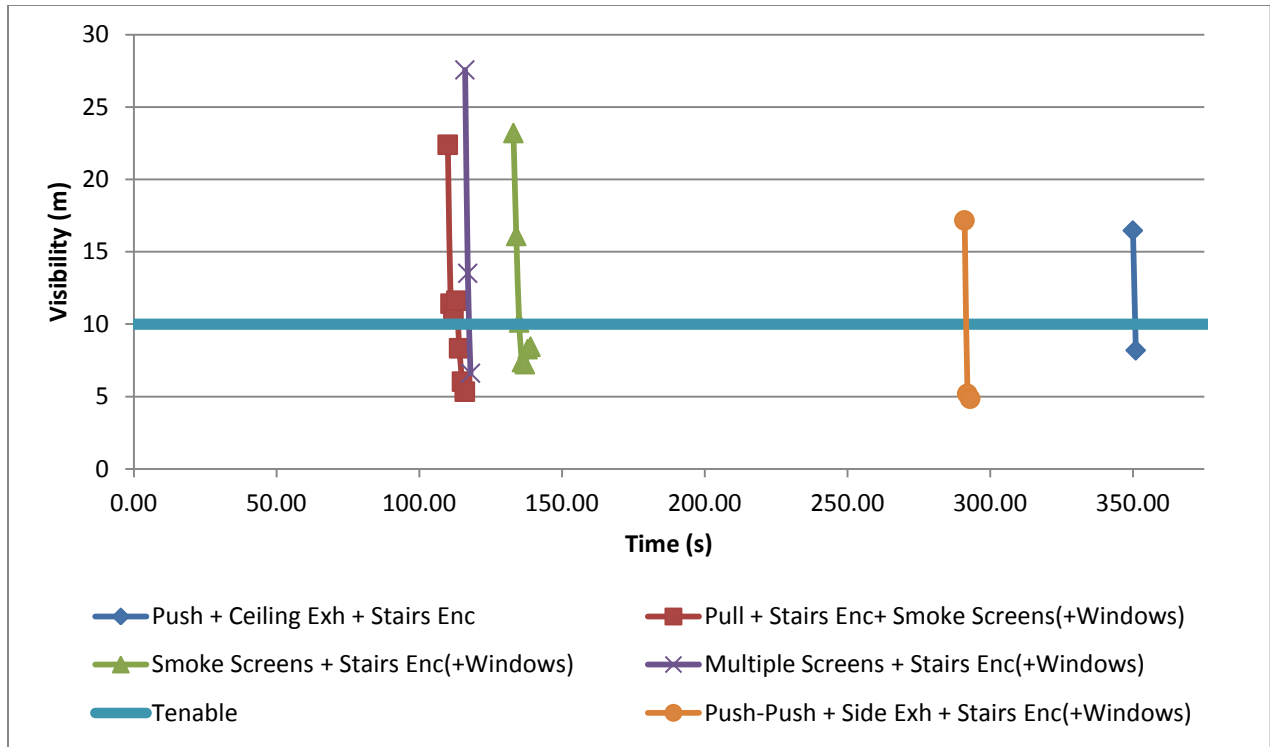


Figure 56 - Visibility at V4. No cases with platform screen doors are shown as smoke does not spread to platform B. The best case is where smoke is pushed and exhausted, mitigating backlayering and thus spread to Y=75.

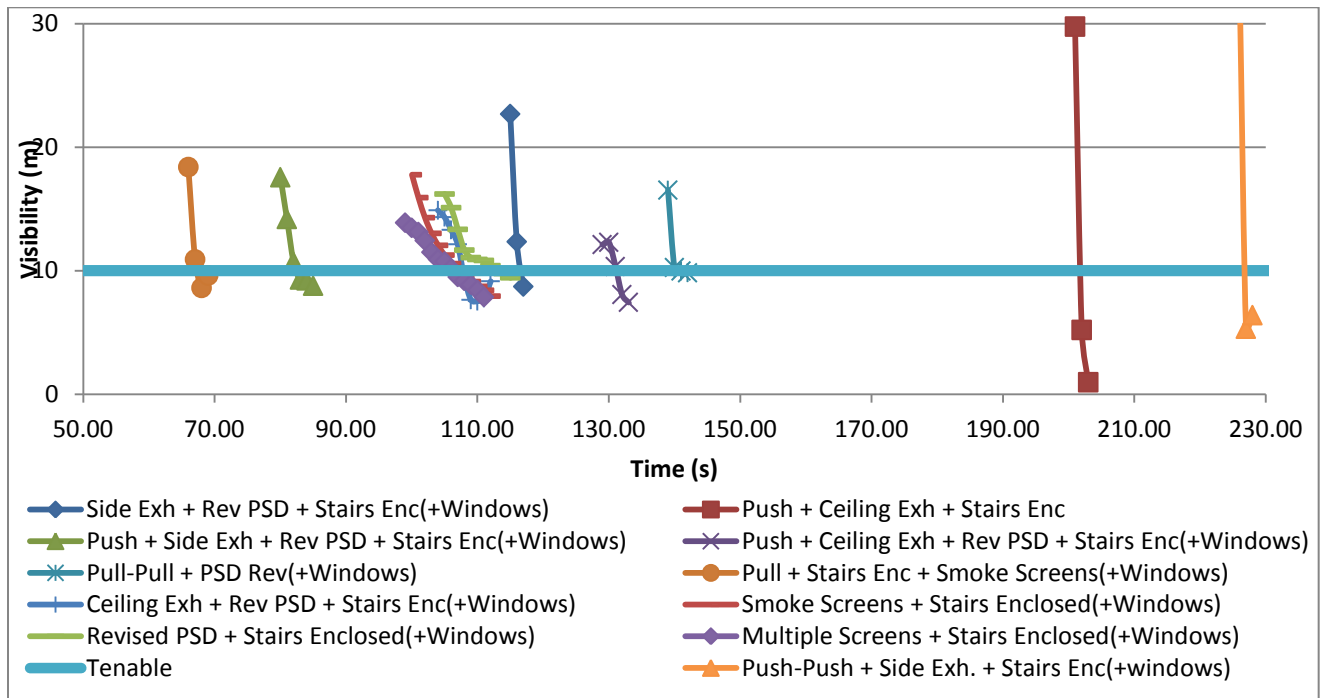


Figure 57 - Visibility at V5. Cases with "Push" and with the revised platform screen doors perform well. When 'Push' is combined with platform screen doors, the 'push' only prevents smoke from backlayering within the PSDs. Smoke that is not caught by the PSDs is free to spread on the platform and therefore tenability at V5 is lost quicker with PSDs.

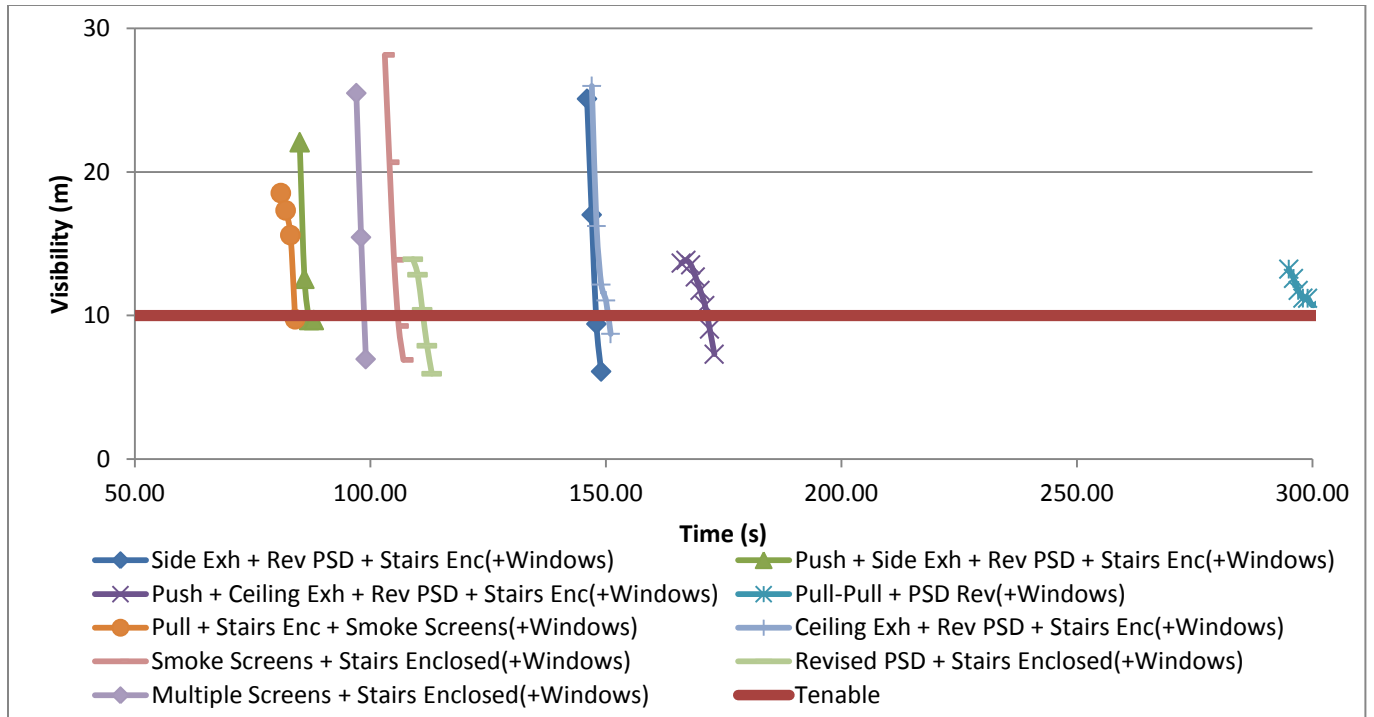


Figure 58 - Visibility at V6. Pull-Pull with PSDs is seen as the best case scenario. This is due to a higher pressure region which prevents flow to this area of the platform. Instead, smoke which has previously entered the platform is actually pulled back into the guideway through the open doors in the PSDs. [Appendix J](#) details this phenomenon. Push-Push configuration not shown at tenability is maintained for longer than 420 seconds.

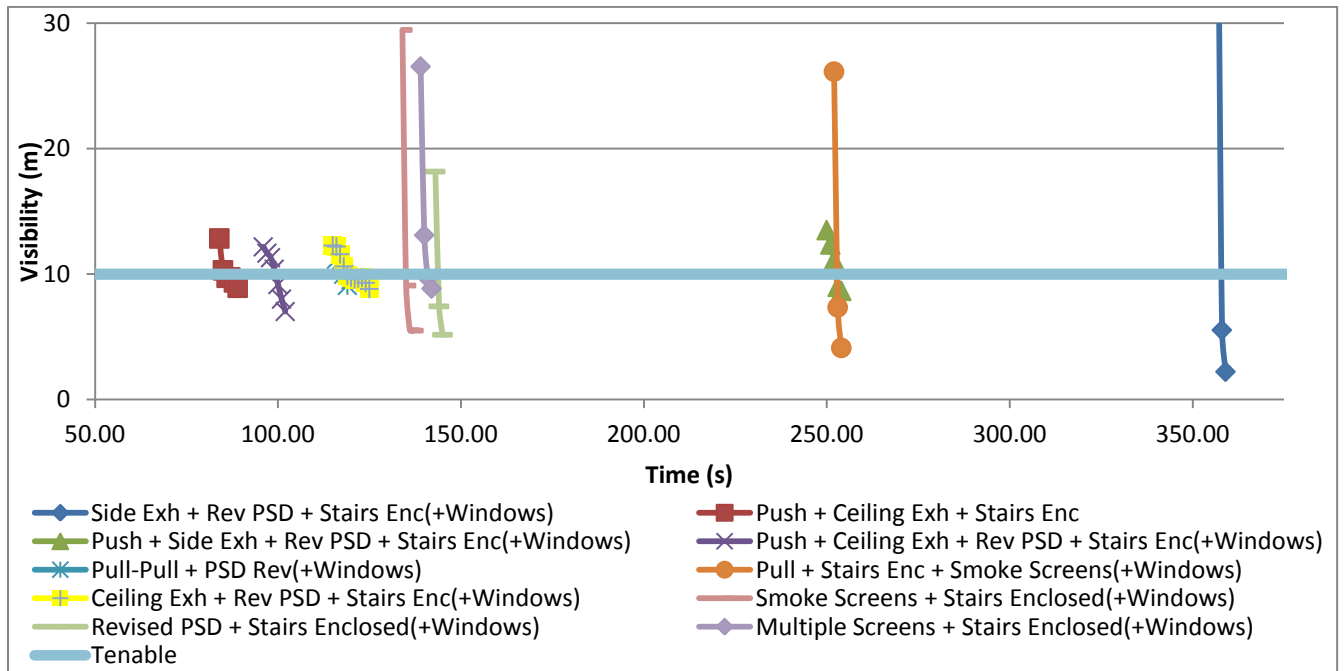


Figure 59 - Visibility at V7. All hybrid methods of smoke control. Two of the three best cases use platform screen doors. The other of the top three pulls from the portal opposite V7, permitting V7 to maintain tenable conditions for longer.

## 9.7 Simulation Results - Temperature

Visibility was the primary variable looked at in the above analysis, as it was generally the first criteria to be exceeded. As time marches, the fire grows, and higher temperatures result. For cases where smoke is controlled for longer durations, higher temperatures become a problem. In some cases, temperature criteria may be exceeded before visibility. Temperature was tracked at several points. At point T3 on the concourse level (see Figures 32/33), tenability is exceeded in only one case. At T5 on platform level, all cases except one maintain tenability for at least 4 minutes. Table 6 presents the times at which the 60 degree tenability criterion is exceeded. [Appendix K](#) plots the temperature-time evolution of each case at T3 and T5.

Table 6 - Time at which temperature tenability criteria is exceeded. \* indicates passive only protection

Case	Description	Time to 60 Celsius	
		T3	T5
V	Pull-Pull + PSD Revised + Stairs Enc.	420	420
II	Side Exh + Rev. PSD + Stairs Enc	420	368
III	Push + Ceiling Exh. + Rev PSD + Stairs Enc	420	366
IV	Ceiling Exhaust + Rev PSD + Stairs Enc	420	348
I	Push-Push+Side Exh + Stairs Enc	420	306
VII*	Revised PSD + Stairs Enc	365	341
VIII	Push + Ceiling Exh. + Stairs Enc	420	420
IX	Pull + Stairs Enc + Smoke Screens	420	369
VI	Push + Side Exh+ Revised PSD + Stairs	420	420
XI*	Smoke Screens + Stairs Enc	420	420
X*	Multiple Smoke Screens + Stairs Enc	420	420

## 9.8 Simulation Results – Small Fire

To study the effectiveness of one of the better performing smoke control systems when a small fire occurs (resulting in less buoyant smoke), case II was simulated for a second time. The design fire chosen was 500 kW, reaching this peak value in 30 seconds, and modeled as a burner the size of a garbage can. The fire was placed on the platform adjacent to stairwell 2/escalator 1. In this case, V5 and V6, located in close proximity to the fire, only maintained visibility criteria for 9 and 37 seconds, respectively. However, tenability was maintained at all other points which were tracked on the platform and concourse. The smoke did not have enough buoyancy to rise to the concourse in large quantities. Additionally, some smoke entered the guideway through open platform screen doors and was evacuated by the exhaust system. Figure 76 and 77 in [Appendix K](#) show several shots from Smokeview.

## 9.9 Ranking of Methods.

The 11 cases in Section 9.6 were ranked at each location at which visibility was tracked (V1, V3, V4, V5, V6, and V7). Points were assigned based on best to worst performing. A one was assigned to the case maintaining tenability for the longest amount of time, a two for the second longest, and so on. Cases which attained equivalent times of tenability were assigned the same score, and cases maintaining



visibility for 420 seconds were all assigned ones. For each case, the respective scores at each of the six tenability points were summed, resulting in a total score. The case with the lowest total score represents that which maintains tenability best overall within the station. It does not represent the case which performs the best in all locations; however, this approach allows for an overall picture to be seen. The smoke control of the best performing cases can then be studied for possibilities to further enhance performance, or can be used in conjunction with an appropriate evacuation plan.

**Table 7 - Ranking of cases, sorted from lowest score to highest. Case Descriptions in Table 6. Time in seconds is shown under the “VX” columns. V1/V3 are on concourse level. V4/V5/V6/V7 are distributed at various points at platform level. \* Indicates passive only protection**

Case	Windows	V1	Rank	V3	Rank	V4	Rank	V5	Rank	V6	Rank	V7	Rank	Sum
V	Y	420	1	420	1	420	1	148	3	308	2	118	8	16
II	Y	356	3	413	2	420	1	101	8	148	5	358	2	21
III	Y	250	4	388	4	420	1	132	4	172	3	100	9	25
IV	Y	363	2	365	5	420	1	108	6	151	4	119	7	25
I	Y	89	10	100	11	292	3	227	1	420	1	420	1	27
VII*	Y	188	6	288	6	420	1	114	5	112	6	144	4	28
VIII	N	116	9	256	7	351	2	202	2	420	1	86	10	31
IX	Y	420	1	397	3	114	6	68	10	84	10	253	3	33
VI	Y	192	5	143	10	420	1	83	9	87	9	253	3	37
XI*	Y	160	8	198	8	136	4	107	7	106	7	135	6	40
X*	Y	166	7	163	9	118	5	107	7	99	8	141	5	41

## 9.10 Simulation and Ranking Comments

The top four configurations shown in Table seven all contain platform screen doors with the revised design, indicating that this can be a strong consideration within an overall smoke control strategy. Problems with PSDs as designed here may include the temperature rating of the glass, temperature sensitivity of cables and equipment within the tunnels, smoke spread to adjacent stations, difficult access via tunnels for firefighters due to smoke channeling, and limited platform space. [Appendix L](#) shows shots of the two best performing cases.

The two configurations with the worst overall performance use only smoke screens and stairwell enclosures, and are not sufficient in controlling smoke spread. When combined with the revised platform screen doors (case VII), they do perform better overall than several other strategies which incorporate ventilation.

When “pulling” through one portal, case IX maintains tenability very well at concourse level. However, platform visibility is lost very quickly as only smoke screens and stair enclosures are present. Adding the revised platform screen doors improves the situation greatly. Case V, the best overall performing case, pulls through both portals and contains the revised platform screen doors instead of smoke screens. Thus, “pulling” cases maintain tenability most effectively at concourse level but must rely on additional measures to improve platform level visibility.

Visibility at point V5 on the concourse is the most difficult location to control. This is primarily due to its close proximity to the design fire. Smoke does not have to travel far to reach V5. The two best performing cases at this point do not have platform screen doors. Due to the fact that this point is in the center of the station, once visibility is lost, no passengers can escape from the right half of the station. If emergency exits were placed at platform ends, this exit could be less heavily relied upon for egress.

Only one case does a good job of controlling smoke through all platform level locations. This is case I (Push-Push Side Exhaust Stairs Enclosed). The platform ends are kept clear, and if coupled with emergency exits at both ends, could provide for smoke free escape routes. The problem with this case is that it has the worst performance of all cases at concourse level. This case could be investigated further. A shot from Smokeview at four minutes is included in [Appendix K](#).

Tenability is exceeded in 118 seconds or less, in all cases, at at least one point within the station. This indicates that controlling smoke spread throughout the majority of the station is a very difficult task. Focusing on several parts of the station and coupling it with appropriate exit design and an evacuation plan is a more viable option. It is possible that tweaks to the critical velocity, extraction rate, or extraction size and locations could be made, however, it is not certain that such changes would be substantial enough to change the results of this study drastically.

It is not explicitly clear whether side exhaust is more effective than ceiling exhaust, when considering the overall ranking. Cases III/VI and II/IV are identical with exception to extraction location. In the first set (III/VI) ceiling exhaust performs better, while in the second set (II/IV) side exhaust performs better.

Exhaust through the atrium was not considered in any hybrid cases. This is due to the fact that with the existing station it would require substantial construction work. Figures 47,51, and 52 show however that when used alone it is more effective than both extracting through the side of the reservoir and through the ceiling ports

In all cases, visibility is exceeded at some point on the platform (V4-V7) before temperature at T5 is exceeded. This confirms the primary importance of the visibility criteria.

## 10. Conclusions

FDS V5.0 was used to conduct CFD simulations of an existing underground subway station. Various methods of smoke control were employed in an attempt to maintain tenable conditions to support safe egress. The main conclusions and findings from this research are:

- No method of smoke control studied is successfully able to maintain tenable conditions on both the platform and concourse. Typically, a trade-off is seen between maintaining good conditions on either the platform or the concourse. Hybrid methods of smoke control perform best.
- Smoke spread from the carriage to the platform is most effectively minimized through platform screen doors.
- Platform screen door design can very important if used for fire safety purposes. Traditional platform screen doors are ineffective in limiting smoke spread. If widened they can more effectively prevent smoke spread by using the hot smoke's buoyancy.
- Smoke spread (backlayering) at platform level is most easily prevented by longitudinal ventilation. The benefits are primarily seen at the station extremities. The extent of the benefit depends on the critical velocity and the interaction with mechanical extraction and passive methods. Station emergency exits can be placed with this principle in mind.
- Not all formulas for critical velocity are on the safe side.
- 'Pulling' through tunnel portals tends to prevent smoke spread to the concourse, keeping the main exit free of smoke.
- Enclosing the stairwells is an effective method of preventing smoke spread to the concourse.
- In this station, more exit capacity is necessary in combination with smoke control methods to ensure safe egress of all occupants.
- Smoke screens were ineffective. Smoke screen depth is important but is limited by the height of the station. Lateral smoke screens compartmentalized the smoke more, preventing spread to the station extremities, but caused the center of the station and concourse to fill quicker.
- Platform screen doors are effective in containing additional smoke when windows break. This assumes that windows do not shatter explosively and damage the screens.
- Smoke control should be taken in the context of the station layout. Exit location in relation to the overall smoke control strategy is of utmost importance.
- Applying extraction rates from standardized methods of smoke control does not necessarily lead to a good design. In order to obtain an appropriate design, CFD should be considered a design tool, not a validation tool.

A lot of additional data was generated under this project which has not been presented. The author was unable to process such a large volume of data, and it is possible that additional findings or trends were missed. The best cases here could be used as a starting point to arrive at a safe plan for this station.

Critical velocity and extraction rates and locations were not substantially varied and could be optimized. Not all possible methods of smoke control have been considered (even some methods presented in Section 5.2 could not be included in this project). The conclusions drawn are meant to be general, and it is possible that each item could be investigated in more detail.

## 11. Acknowledgements

I would like to thank the following for providing support during my thesis:

My mom and dad for their support and proofreading a technical thesis which is a far cry from either of their professions!

Aunt Kath, Peter, and Katie for visiting me during my time here and providing some home away from home.

Xavier Deckers (from Fire Engineered Solutions) for his supervision and guidance, and the late nights spent at his office looking over things.

Guillermo Rein for his responsiveness and for supplying a wealth of contacts over the last 2 years. Also for his quick replies, positive reinforcement, and genuine interest in my success and success of the IMFSE students.

Chris Lautenberger for meeting with me while I was home and providing his insight, which helped me get off to a good start in completing my thesis.

The consultants in many countries which have taken their time in providing me with invaluable thoughts and data for my survey.

Dennis, Mark, Netsanet, Hernan, Setareh, Andrej, Claudia, Brecht, Karliss, and the rest of the IMFSE gang for making my time in Europe full and memorable, and for providing academic support in addition to friendship and adventures. And to the many people met along the way that made it such a journey.... there are too many to mention.

Eduardo Bogado and his family in Asunción. If it wasn't for all those lazy days at your house studying Spanish and drinking mate cocido, I probably would not have made it here.

## 12. References

(n.d.). Retrieved 03 22, 2012, from efunda:

[http://www.efunda.com/materials/elements/TC\\_Table.cfm?Element\\_ID=Al](http://www.efunda.com/materials/elements/TC_Table.cfm?Element_ID=Al)

*Metals - Specific Heats*. (n.d.). Retrieved 03 01, 2011, from The Engineering Tool Box:

[http://www.engineeringtoolbox.com/specific-heat-metals-d\\_152.html](http://www.engineeringtoolbox.com/specific-heat-metals-d_152.html)

(2009, June 8). Retrieved April 3, 2012, from Metrobits.org: <http://mic-ro.com/metro/platform-screen-doors.html>

Agency, E. R. (2010). *2010 Railway Safety Performance in the European Union*.

Ahres, M. (2010). *U.S. Vehicle Fire Trends and Patterns*. NFPA.

Armstrong, J. P. (2001). Hong Kong: Fire Strategy, Life Safety, and Ventilation in Road Tunnels. *Rapid Excavation & Tunneling*, (pp. 435-452).

ASHRAE. (2011). *ASHRAE Handbook - HVAC Applications. Chapter 15. Enclosed Vehicular Facilities*.

Beard, A. C. (2005). *The Handbook of Tunnel Fire Safety - First Edition*. Thomas Telford Publishing.

Beyler, C. L. Heat Release Rates of Fully-developed Fires in Railcars. *Fire Safety Science - Proceedings of the Eighth International Symposium*, (pp. 1169-1180).

Brabrauskas, V. *Glass Breakage in Fires*. Fire Science and Technology.

Brown, M. (2011, September 13-14). Transport for London. *METRO Project Seminar*. Avrika, Sweden.

Butler, K. M. (2004). Generation and Transport of Smoke Components. *Fire Technology, Issue 40*, pp. 149-176.

Carvel, R. (n.d.). Retrieved from Tunnel Ventilation and its Influence on Fire Behaviour.:

[http://www.see.ed.ac.uk/~rcarvel/tunnel\\_ventilation.html](http://www.see.ed.ac.uk/~rcarvel/tunnel_ventilation.html)

Chen, F. C. (2003). Stack Effects on Smoke Propagation in Subway Stations. *Continuum Mech. Thermodynamics*, 425-440.

Chen, F. G.-C.-Y.-W. (2003). Smoke Control of Fires in Subway Stations. *Theoretical Computational Fluid Dynamics*, (pp. 349-368).

Chiam, B. H. (2005). *Numerical Simulation of a Metro Train Fire*. Department of Civil Engineering, University of Canterbury.

Colella, F. (2010). *Multiscale Modelling of Tunnel Ventilation Flows and Fires, Doctorate Thesis*.

Cutonilli, J. B. (2010). Predictions of Rail Car Heat Release Rates. *March 17-19, Fourth International Symposium on Tunnel Safety and Security*. Frankfurt, Germany.

Everts, B. (2012, January 11). Email Correspondence - NFPA. (N. Bartlett, Interviewer)

FIRESTARR. (2001). *Contract SMT4-CT 97 -2164, Final Report*. FIRESTARR Project.

FIT. *General Report. FIT - Fire in Tunnels*.

Gao, R. L. (2011). Fire-induced smoke control via hybrid ventilation in a huge transit terminal subway station. *Energy and Buildings Issue 45* , pp. 281-289.

Groups, F. G. (2008, Jan 11). *Grid Sensitivity Analysis*. Retrieved March 14, 2012, from FDS & Smokeview Discussions. Google Group.: [http://groups.google.com/group/fds-smv/browse\\_thread/thread/6a7804115cdadef1/e323d6f2bd646d9a?Ink=gst&q=d\\*#e323d6f2bd646d9a](http://groups.google.com/group/fds-smv/browse_thread/thread/6a7804115cdadef1/e323d6f2bd646d9a?Ink=gst&q=d*#e323d6f2bd646d9a)

Gupta, S. (2011, August 15-16). Design of Smoke Ventilation System for Kolkata Metro. *Fire and Evacuation Modeling Technical Conference* . Baltimore, Maryland.

Haack, A. (2011). Real Fires and Design Fires. *Fire in Tunnels. Technical University of Barcelona, Catalunya*.

Hadjisophocleous, G. H. (2012). Full-scale Experiments for Heat Release Rate Measurements of Railcar Fires. *Symposium on Tunnel Safety and Security*, (pp. 457-466). New York.

Hall, J. (2011). *Requested Input to ASTM E2061 X8 Statistics on Fires in Rail Transportation*. NFPA.

Ingason, H. (2006). Design Fires in Tunnels. *Second International Symposium: Safe & Reliable Tunnels. Innovative European Achievements*. Lausanne.

Ingason, H. (2005). *Model Scale Railcar Fire Tests. SP Report 2005:48*. SP Fire Technology.

Karlsson, B. Q. (2000). *Enclosure Fire Dynamics*. Boca Raton: CRC Press.

Kim, E. W. (2008). Fire Dynamics Simulator (Version 4.0) Simulation for Tunnel Fire Scenarios with Forced, Transient, Longitudinal VentilationFlows. *Fire Technology* , 137-166.

Korhonen, T. H. (2011). FDS+Evac: Herding Behavior and Exit Selection. *International Association of Fire Safety Science* .

Korhonen, T. H. (2010). *Fire Dynamics Simulator with Evacuation: FDS+Evac. Technical Reference and User's Guide. FDS 5.5.0 Evac 2.2.1*. VTT Technical Research Center of Finland.

Kumm, M. (2010). Carried Fire Load in Mass Transport Systems. *A study of occurrence, allocation, and fire behaviour of bags and luggage in metro and commuter trains in Stockholm* . Mälardalen University.

Kuusinen, J.-M. (2007). *Group Behavior in FDS+Evac Evacuation*. Helsinki University of Technology.

Lautenberger, C. C. (2009). Using Computer Fire Modeling to Reproduce and Predict FRP Composite Fire Performance. *Composites & Polycon 2009. American Composites Manufacturers Association.*

Levy, S. S. (1999). FD Model for Transverse Ventilation Systems. *The First International Conference on Tunnel Fires*, (pp. 223-233). Lyon.

Li, Y. I. (2010). Study of Critical Velocity and backlayering length in longitudinally ventilated tunnel fires. *Fire Safety Journal* , 361-370.

Lonnermark, A. L. (2012). Large-scale Commuter Train Fire Tests - Results from the METRO Proejct. *International Symposium on Tunnel Safety and Security*, (pp. 447-455). New York.

Lord, J. M. *Smoke Management 101 for Tunnels & Stations.*

Marlair, G. L. (2008). *UPTUN Work Package 2 Fire Development and mitigation measures D211. Fire scenarios and accidents in the past.*

McGrattan, K. H. *Fire Dynamics Simulator (Version 5) Technical Reference Guide, NIST Publication 1018-5.*

McGrattan, K. M. *Fire Dynamics Simulator (Version 5) Users Guide. Publication 1019-5. NIST. .*

METRO. (2011, September 13-14). *Presentations at the METRO Seminar. Carried Fire Load in Underground Mass Transport Systems.* Arvika, Sweden.

Milke, J. K. (2002). *Principles of Smoke Management.*

Montecinos, C. W. (2010). Equivalent Roughness for pressure drop calculations in mine ventilation. *13th US/North American Mine Ventilation Symposium*, (pp. 225-230).

NFPA, 2. (2010). NFPA 130. *Standard for Fixed Guideway Transit and Passenger Rail Systems .*

Peacock, R. A. (2004). *Fire Safety of Passenger Trains; Phase III: Evaluation of Fire Hazard Analysis Using Full Scale Passenger Rail Car Tests. NIST Report, NISTIR 6563.*

Peacock, R. B. (2001). Development of a Fire Hazard Assessment Method to Evaluate the Fire Safety of Passenger Trains. *Fire and Materials. 7th International Conference and Exhibition* (pp. 67-78). San Antonio: Interscience Communications Limited.

Peacock, R. B. (1999). Evaluation of Train Car Materials in the Cone Calorimeter. *Fire & Materials Issue 23* , pp. 53-62.

Peacock, R. B. (1999). Evaluation of Train Car Materials in the Cone Calorimeter. *Fire & Materials, Issue No. 23* , pp. 53-62.

Roh, J. R. (2008). CFD Simulation and assessment of life safety in a subway train fire. *Tunnel and Underground Space Technology Journal .*



- Roh, J., Ryou, H., Park, W., & Jang, Y. (2009). CFD Simulation and assessment of life safety in a subway train fire. *Tunnelling and Underground Space Technology, Volume 24, Issue 4* , pp. 447-453.
- Shields, T. S. (1998). Behaviour of Glazing in a Large Simulated Office Block in a Multi-Storey Building. *Journal of Applied Fire Science* , pp. 333-352.
- Shields, T. S. (1997/1998). The Behaviour of Double Glazing in an Enclosure Fire. *Applied Fire Science* , pp. 267-286.
- Snel, A. (2008). Fire Safety Engineering for Deep Underground Metrosystem. *Underground Space Challenges in Urban Development*.
- Strege, S. L. (2003). Fire Induced Failure of Polycarbonate Windows in Railcars. *Fire & Materials* , pp. 269-278.
- Tabarra, M. A.-Z. (2004, November). Design of a modern subway ventilation system. *Tunnels & Tunneling International* .
- Tewarson, A. Generation of Heat and Chemical Compounds in Fires. In *SFPE Handbook of Fire Protection Engineering*.
- Tewarson, A. J. (1993). Ventilation-Controlled Combustion of Polymers. *Combustion and Flame, Vol. 95* , 151-169.
- UL, N. (2008, November). Recommended Fire Safety Practices for Rail Transit Materials Selection. *Project No. DC-26-5243-00* . National Association of State Fire Marshals.
- USFA. (2002). *Rail Terminal Fires*. US Fire Administration. Topical Research Series Volume 2. Issue 13.
- Wahlström, B. (2011, September 14). Fire safety design for tunnels and stations. *METRO Seminar* . Arvika, Sweden.
- White, N. D. (2005). Full-scale Fire Experiment on a Typical Passenger Train. *Fire Safety Science- Proceedings of the Eighth International Symposium*, (pp. 1157-1168).
- Yoon, S.-W. C. (2009, May 13-16). Development of Quantitative Risk Analysis Tool for the Fire Safety in Railway Tunnel. *International Forum on Engineering Decision Making* . Hakone, Japan.

## Appendix A: NFPA 130 Calculations

Evacuation calculations conducted in accordance with NFPA 130.

### *Design values*

Platform Load: 800 people (400 per platform)

Train Load: 1600 people (800 per train)

3 platform-concourse exits per platform:

2 stairwells: 1400 mm wide each (total 2800)

1 escalator: 900 mm wide

0 emergency exits

6 ticket entry/exit stalls at concourse level, 3600 mm width

1 handicap/service exit ticket stall, 800 mm width

3 platform-street level exits:

1 stairwell: 1400 mm wide

2 escalators: 900 mm wide each

1 Elevator from platform-street level

### Requirements:

Time to clear platform < 4 minutes

Evacuate platform occupant load from most remote point on platform to safe point < 6min

### Assumptions

Specific flow through stairs/escalators = .0516 persons/mm-min

### Calculations (Using Given Number of Exits):

Platform Exit Capacity= .516 persons/mm-min\*(2800mm+900mm)=190.92 persons/min

a) Time to clear platform  $1 = F_p = \frac{\text{Platform occupant load}}{\text{Platform Exit Capacity}} = \frac{1200 \text{ persons}}{190.92 \text{ persons/min}} = 6.28 \text{ min} > 4 \text{ min}$

b) Evacuate platform load to most remote point

a.  $W_p = \text{Waiting time at platform egress element} = F_p - T_1 = 6.28 - 1.19 = 5.09 \text{ min}$

- b. Where  $T_1$  is longest walking time on platform to stairs/escalator. In this case 45 meters at 37.7 m/min
- c. Concourse Load = Platform Load  $-(F_p * \text{emergency stair capacity})$ 
  - No emergency stairs, therefore  $W_p=1200-6.28*0=1200$  persons
- d. For both platforms egressing, total concourse load =2400 persons
- e.  $W_{fb}$  =Waiting time at fare barriers on concourse =  $F_{fb} - F_p = 6.66-5.09 = 1.57$  min
- f.  $F_{fb}$ =Flow through fare barriers =  $\frac{\text{Concourse Load}}{\text{Fare egress capacity}} = \frac{2400 \text{ persons}}{360 \text{ p/min}} = 6.66$  min
- g.  $W_c$  =Waiting time at concourse egress =  $F_c - \max(F_{fb} \text{ or } F_p) = 20.2-6.66=13.54$  min
- h.  $F_c$ =concourse flow time =  $\frac{\text{Concourse Load}}{\text{concourse egress capacity}} = \frac{2400 \text{ persons}}{118 \text{ p/min}} = 20.2 \text{ min}$
- i. Total Egress Time, Platform 1 = Walking time + Waiting time =  $3.69+5.09+1.57+13.54 = 23.9$  minutes
- j. Total Egress Time, Platform 2 = **23.94 minutes > 6 min**

Calculations (1 Emergency Exit):

$$\text{Time to clear platform 1} = F_p = \frac{\text{Platform occupant load}}{\text{Platform Exit Capacity}} = \frac{1200 \text{ persons}}{263.16 \text{ p/min}} = 4.55 \text{ min} > 4 \text{ min}$$

Evacuate platform load to most remote point

- a.  $W_{p1}$  =Waiting time at platform egress element =  $F_p - T_{1(1)} = 4.55 - .66 = 3.89$  min
- b.  $W_{p2}$  =Waiting time at platform egress element =  $F_p - T_{1(2)} = 4.55 - .69 = 3.86$  min
- c. Where  $T_1$  is longest walking time on platform to stairs/escalator. In this case 25 meters at 37.7 m/min
- d. Concourse Load = Platform Load  $-(F_p * \text{emergency stair capacity})$ 
  - $W_p=1200-4.55*72.4=871$  persons
- e. For both platforms egressing, total concourse load =1742 persons
- f.  $W_{fb}$  =Waiting time at fare barriers on concourse =  $F_{fb} - F_p = 4.80-4.55 = .25$  min
- g.  $F_{fb}$ =Flow through fare barriers =  $\frac{\text{Concourse Load}}{\text{Fare egress capacity}} = \frac{1742 \text{ persons}}{360 \text{ p/min}} = 4.80$  min
- h.  $W_c$  =Waiting time at concourse egress =  $F_c - \max(F_{fb} \text{ or } F_p) = 14.67-4.6=9.87$  min
- i.  $F_c$ =concourse flow time =  $\frac{\text{Concourse Load}}{\text{concourse egress capacity}} = \frac{1742 \text{ persons}}{118 \text{ p/min}} = 14.67$  min
- j. Total Egress Time, Platform 1 = Walking time + Waiting time =  $3.15+3.89+.25+9.87= 17.16$  minutes
- k. Total Egress Time, Platform 2 =  $W_{p1}$  =Waiting time at platform egress element =  $F_p - T_1 = 4.55 - 1.19 = 5.09$  min

Calculations (2 Emergency Exits):

$$\text{Time to clear platform 1} = F_p = \frac{\text{Platform occupant load}}{\text{Platform Exit Capacity}} = \frac{1200 \text{ persons}}{335.4 \text{ p/min}} = \mathbf{3.57 \text{ min} < 4 \text{ min}}$$

Evacuate platform load to most remote point

- l.  $W_{p1}$  = Waiting time at platform egress element =  $F_p - T_{1(1)} = 3.57 - .66 = 2.92 \text{ min}$
- m.  $W_{p2}$  = Waiting time at platform egress element =  $F_p - T_{1(2)} = 3.57 - .69 = 2.89 \text{ min}$
  
- n. Where  $T_1$  is longest walking time on platform to stairs/escalator. In this case 25 meters at 37.7 m/min
- o. Concourse Load = Platform Load - ( $F_p * \text{emergency stair capacity}$ )
  - $W_p = 1200 - 3.57 * 2 * 72.4 = 683 \text{ persons}$
- p. For both platforms egressing, total concourse load = 1366 persons
- q.  $W_{fb}$  = Waiting time at fare barriers on concourse =  $F_{fb} - F_p = 3.79 - 3.57 = .22 \text{ min}$
- r.  $F_{fb}$  = Flow through fare barriers =  $\frac{\text{Concourse Load}}{\text{Fare egress capacity}} = \frac{1366 \text{ persons}}{360 \text{ p/min}} = 3.79 \text{ min}$
- s.  $W_c$  = Waiting time at concourse egress =  $F_c - \max(F_{fb} \text{ or } F_p) = 11.5 - 3.79 = 7.72 \text{ min}$
- t.  $F_c$  = concourse flow time =  $\frac{\text{Concourse Load}}{\text{concourse egress capacity}} = \frac{1366 \text{ persons}}{118 \text{ p/min}} = 11.5 \text{ min}$
- u. Total Egress Time, Platform 1 = Walking time + Waiting time = 3.15 + 2.92 + .22 + 7.72 = **14 minutes**

***Waiting time at concourse must be reduced by adding additional exits to increase capacity. Travel time & distance could be reduced by adding another exit location to the concourse. The only other option is reducing the occupant capacity (this could be verified by conducting a field study to determine if the design capacity is realistic)***

## Appendix B: Ventilation Calculations

### Mechanical Ventilation Estimates

The fire source is assumed to be an entire carriage, at seat-height, with an area of 14m in length by 2.5 m width (for 35 m<sup>2</sup> total area).

#### Plume mass flow rate

The height of the carriage is very short, so the plume will impinge quickly, create a ceiling jet, and go out the doors, entraining more air as a spill plume. An axial plume is probably not really developed due to the low ceiling height and width of the door spill edge. Furthermore, as the HRR increases, the flames will impinge on the ceiling and all equations will be invalid. The following is an attempt to get a first idea of what the possible mass plume flow rate could be.

Using the Thomas model (Which is also CR 12101-5)

$$\dot{m}_p = .188Pz^{\frac{3}{2}}$$

$$\dot{m}_p = .188(2.5 + 2.5 + 14 + 14)1.6^{\frac{3}{2}} = 12.56 \frac{kg}{s}$$

Using Line plume equation from enclosure fire dynamics (Karlsson, 2000):

$$\dot{m}_p = .21 \left( \frac{\dot{Q}}{B} \right)^{\frac{3}{2}}$$

Assuming Q=35 MW, B=14, then m=61kg/s

However, this equation is only valid for  $L < z < 5B$  (where L is flame height).

$$L = .035 \left( \frac{\dot{Q}}{B} \right)^{\frac{2}{3}} = 6.44 \text{ m}$$

If z is taken as 1.6 m, using a spreadsheet, the equation breaks down when Q=4248 kW (at this point L is 1.58 m so z at 1.6 m become sin the range. for  $L < z < 5B$ ). At this value m=15.2 kg/s This still does not take into account entrainment due to spill out of the carriage and travelling up to ceiling.

Therefore, doubling is assumed to take into account these uncertainties, and **30 kg/s** is taken as a starting point for smoke control. This is a first estimate and the extraction rate which is based upon this value may end up needing to be altered.

## Vent flow rates for extraction

From NBN S21-208-1

$$\dot{V} = \frac{m_p}{\rho_a} * \frac{T_s}{T_a}$$

$$T_s = T_a + \theta$$

$$\theta = \frac{Q_c}{m_p} = \frac{35000 * .7}{30 \frac{kg}{s} * \frac{1kJ}{kg - K}} = 816 K$$

$$T_s = 20 + 816 = 836 K$$

$$\dot{V} = \frac{30 kg/s}{1.2} * \frac{836}{288} = 72.5 m^3/s$$

If smoke is at 100 C, density is 1.06 kg/m<sup>3</sup>, and adjusted volumetric flow = 80 m<sup>3</sup>/s

Even if mass flow rate is doubled to 60 kg/s, then T=428 K and V=74.3 m<sup>3</sup>/s

Design value of 80 m<sup>3</sup>/s total extraction to be used as first order approximation.\*

*\*It was noticed before thesis completion that an error exists in the above calculation, but it has been kept to demonstrate that the chosen value deviates by less than 9% from the correct value, as follows:*

$$\theta = \frac{Q_c}{m_p} = \frac{35000 * .65}{30 \frac{kg}{s} * \frac{1kJ}{kg - K}} = 758 K$$

$$T_s = 293 + 816 = 1051 K$$

$$\dot{V} = \frac{30 kg/s}{1.2} * \frac{1051}{288} = 91 m^3/s$$

*Additionally, a sensitivity study to this parameter was conducted, showing that with an extraction rate of 120 m<sup>3</sup>/s the time at which tenability was exceeded at point V3 actually decreased. See Table 5. Further uncertainties in this calculation include the combustion efficiency, chosen as .65 here to agree with the FDS model.*

## Longitudinal Ventilation (critical velocity)

Method 1 (Li, 2010)

The station grade=0

Froude Number:  $Fr_m = 4.5(1 + .0374 * \min(\text{grade}, 0)^{.8})^2 - 3 = 4.5$

Iterate the following two equations

$$V_{cr} = \left( \frac{gHQ_c}{\rho C_p A T_f F r_m} \right)^{1/3}$$

$$T_f = \frac{Q_c}{\rho C_p A V_c} + T$$

Iterate and **Vc=2.33 m/s**

This is assuming an empty station. Taking into account for the area of the carriage (subtracting carriage cross section from station cross section), the Vc would be **2.15 m/s**

Method 2: (Li, 2010)

Wu and Bakar [9] carried out another series of small-scale experiments to take varying tunnel cross-sections into account, using the hydraulic diameter instead of the tunnel height in the equation

$$\begin{aligned} V_c' &= 0.40[0.20]^{-1/3}[Q']^{1/3}, & Q' \leq 0.20 \\ V_c' &= 0.40, & Q' > 0.20 \end{aligned} \quad (6)$$

where

$$Q' = \frac{Q}{\rho_o c_p T_o g^{1/2} H^{5/2}}, \quad V_c' = \frac{V_c}{\sqrt{gH}}$$

Using this, **Vc=2.97 m/s**

Method 3 (Li, 2010)

$$\begin{aligned} V_c^* &= K_v[0.12]^{-1/3}[Q^*]^{1/3}, & Q^* \leq 0.12 \\ V_c^* &= K_v, & Q^* > 0.12 \end{aligned} \quad (5)$$

where

$$Q^* = \frac{Q}{\rho_o c_p T_o g^{1/2} H^{5/2}}, \quad V_c^* = \frac{V_c}{\sqrt{gH}}$$

Their experiments obtained values of  $K_v$ , varying with geometry and location of the fire source, of between 0.22 and 0.38.

Using this method Vc at kv=.22 is 1.57 m/s, at Kv=.38, it is **2.71 m/s**

It was decided to use the most conservative result of the three methods, 2.97 m/s, and round it to 3 m/s. This provides a starting point for critical velocity.

## Appendix C: Survey Questions

Please choose any existing subway station in the system which may be considered as representative of the others.

- 1) An important part of the fire safety of metro stations is the construction of the trains. Are the trains constructed in accordance with national or international fire safety standards? This may include interior furnishings, floor and wall coverings, electrical equipment, and other aspects of train design.
  - a. Yes
  - b. No
    - i. If Yes, in accordance with what prescriptive standards must trains be constructed in accordance with? \_\_\_\_\_
    - ii. More specifically, if applicable, to what testing standards must interior furnishings be tested in accordance with? \_\_\_\_\_
- 2) Does the subterranean station contain smoke extraction systems (either natural or mechanical)?
  - a. Yes
  - b. No

Comments: \_\_\_\_\_
- 3) In the design process of the station smoke control systems, what types of possible fire scenarios for the trains are considered?
  - a. Arson in train
  - b. Terrorism in train
  - c. Reasonable Worst Case interior fire
  - d. Fire in station platform or concourse
  - e. Other: \_\_\_\_\_
- 4) What types of smoke control systems are in place?
  - a. Transverse
    - i. Comments:
  - b. Semi-Transverse
    - i. Comments:
  - c. Longitudinal
    - i. Comments:
  - d. Overpressurization methods
    - i. Comments:
  - e. Smoke Screens.
    - i. Comments:
  - f. Natural Ventilation
    - i. Comments:
  - g. Mechanical Extraction
    - i. Comments:



h. If others, please describe:

5. If design fires are used, please describe a typical design fire on which the smoke control system is based on. Do the values for these design fires come from published literature, regulations, experimental data, or other sources?

**Response:**

6. Does the selection of design fires differ based on whether the goal of smoke control is upgrading an existing station or creating a new station?

**Response:**

7. Do mandatory national requirements exist for smoke control in new stations? If so, please elaborate.

**Response:**

## Appendix D: Relevant Statistics for Subway Fires

SFPE defines a fire risk assessment as “a process for estimation and evaluation of fire risk that addresses appropriate fire scenarios and their probabilities and consequences, using one or more acceptability thresholds.” Train fires are typically included in the design of subway station ventilation systems due to the severe consequences. Probability of such events, however, is not always considered. It would be useful to have a better idea of this probability, to assure or refute the current practice of designing for such large fires. The following section presents a small amount of relevant statistics. A full risk assessment to answer this question, however, is challenging. Some problems encountered during research of statistics included insufficient details in classifying an incident, lumping of subway fires in to broader rail categories, variation in reporting systems, and general lack of data. The following data is presented for reference.

The following table shows railway fire accidents in Korea and frequency as expressed per train kilometer. The reported frequency is  $3.58 \times 10^{-8}$  accidents/train-km. The one fire in 2003 is the Daegu Station fire, which resulted in 192 casualties. The cause of these fires were not reported, neither was the location or number of casualties.

Year	99	00	01	02	03	04	05	Average
Train Km (mil. train-km/yr)	105.5	108.4	107.9	107	108.1	113.6	111.3	108.8
No of Fire (events/yr)	8	7	7	2	1	2	0	3.86

Figure 60 - 1999-2005 Fire Incidents, Korea (Yoon, 2009)

In Singapore, no fire incidents have been reported since the first subway line was opened in 1987 (Chiam, 2005).

The US Fire Administration reported that between 1996 and 1998, there were 300 rail related fires annually (USFA, 2002). This includes fires occurring in street level stations, elevated stations, underground stations, and the trains themselves. Of the above, only 16% occurred underground (which could be either a train in a tunnel, train in a station, or a miscellaneous station fire). Finally, over 40% of those fires were a result of arson (classified as incendiary/suspicious). No distinguishment was made between which how many incidents occurred in train cars as opposed to stations. 18% of fires also were a result of smoking. Assuming 900 fires occurred over the three year span, this leads to approximately 83 fires that may have occurred underground in both the train cars and station platforms.

Between 2006-2010, at rapid transit stations in the US, each year there were an average of 490 structure fires, 40 vehicle fires, and 490 unclassified or outside fires. More details were unable to be obtained regarding the nature of the vehicle fires (Evarts, 2012).

From 2003-2007, US fire departments responded to an average of 1,290 rail vehicles annually, resulting in an average of less than one death per year. Of these fires, 3% were attributed to rapid transit or trolley cars (Ahres, 2010). Further information regarding the nature of the 3%, as well as the 10% of 'unclassified' fires, would be of benefit.

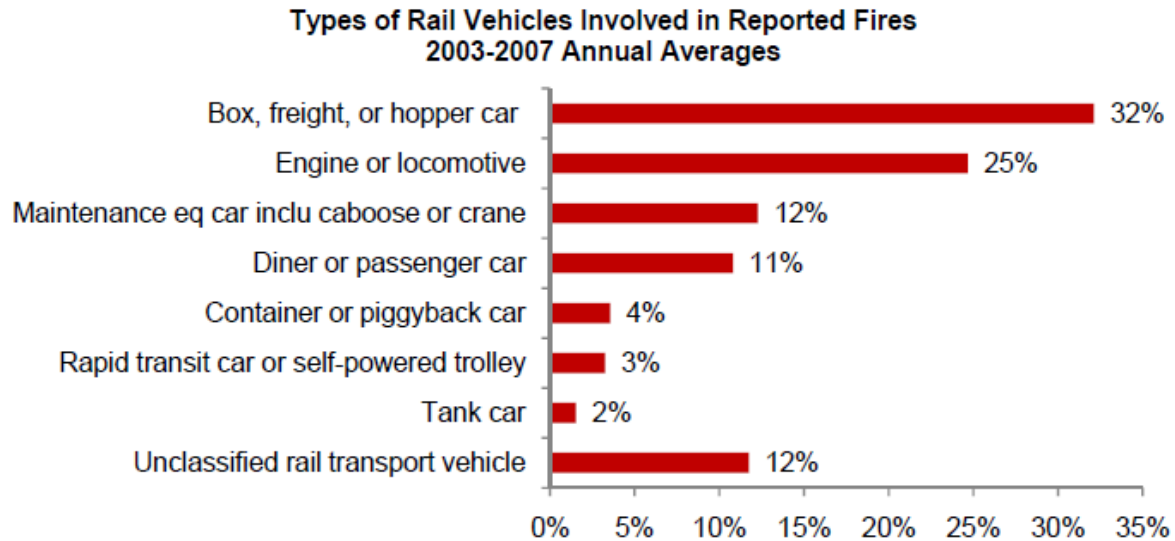


Figure 61 - Rail fires in the US -2003-2007

EU member states are required to report accidents to Eurostat [ag\*]. All rail accidents reported from 2006-2008 are shown below. Decreases in 2007 & 2008 are attributed to reporting issues in two member states [ag\*]. Reported fire incidents are 257, 122, and 105, for years 2006, 2007, and 2008.

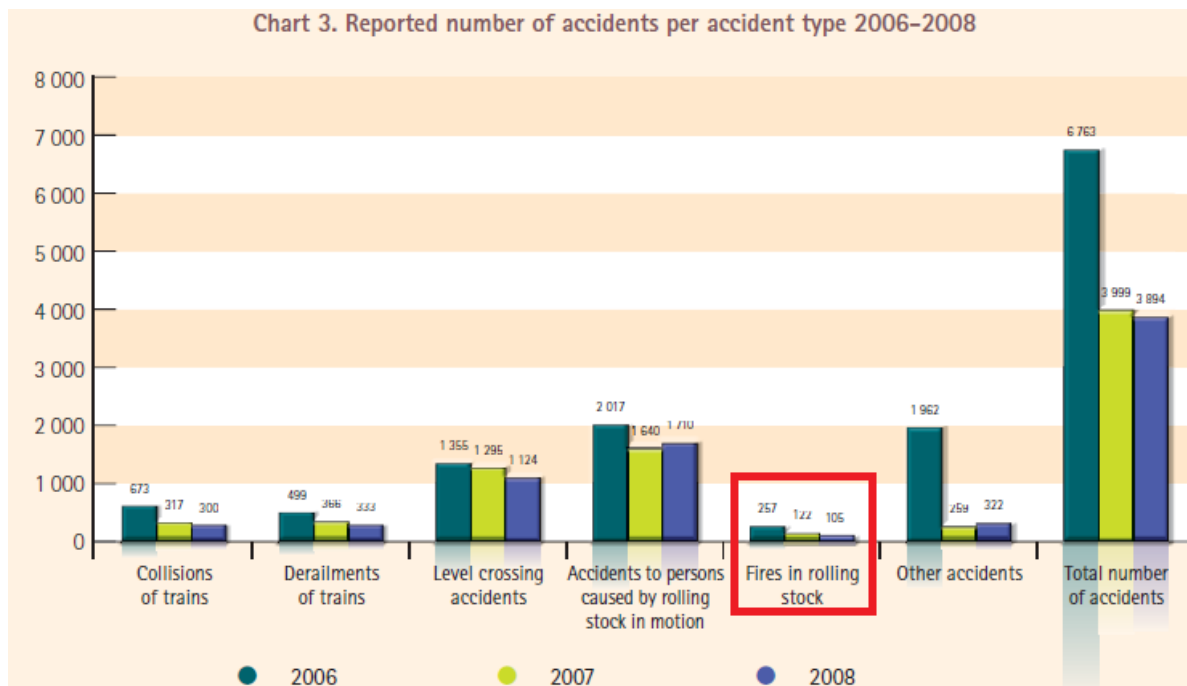


Figure 62 - Rail Accidents, 2006-2008, Europe (Agency, 2010)

In addition to incident frequency, it is important to know causes of fire. According to FIRESTARR (FIRESTARR, 2001), as a result of a survey to the major rail networks in Europe, the most probable fire scenarios in a train are due to arson, inattention, and electrical defects. Externally originating fires were, by statistical analysis, determined to be sufficiently rare to not be considered in a fire hazard analysis. In regards to arson, arson on a seat due to a cigarette lighter or a newspaper were the most common scenarios in European trains. The following statistics were compiled by Tipping on fire causes:

Cause of fire	Frequency	%
Arson fires (interior)	145	68
Electrical faults (interior)	8	4
Small Fires (interior)	2	1
Electrical faults (undercarriage)	57	27
Total	212	100

Table 6.1: Source of fire (adopted from Tipping (2004))

Figure 63 - Fire Causes (Chiam, 2005)

Chiam also analyzed a large quantity of rail fire occurrences from 1979-2003 and concluded that for interior fires, ignition sources ranged from cigarettes to flammable liquids. For exterior fires, short circuits and overheating of equipment in the undercarriage were the main source of fire (Chiam, 2005).

The following table displays rail car fires in the US from 2005-2009, on the basis of item first ignited. Statistics are not specific to subway cars, and thus include traditional rail cars (including dining cars). They also only include fires reported to municipal agencies, therefore not including incidents reported to state, federal, or private fire brigades.

TABLE X8.5 Rail Transport Vehicle Fires Reported to U.S. Municipal Fire Departments, Diner or Passenger Car Only, by Item First Ignited  
Annual Average of 2005-2009 Fires (FN2)

Item first ignited	Fires	Civilian Injuries	Direct Property Damage (in Millions)
Wire or cable insulation	38 (36%)	1 (51%)	\$0.1 (36%)
Unclassified item first ignited	18 (17%)	0 (0%)	\$0.1 (19%)
Flammable or combustible gas or liquid	16 (15%)	1 (49%)	\$0.1 (22%)
Multiple items first ignited	7 (7%)	0 (0%)	\$0.0 (11%)
Upholstered furniture or vehicle seat	7 (7%)	0 (0%)	\$0.0 (7%)
Papers	2 (2%)	0 (0%)	\$0.0 (1%)
Dust, fiber, lint, sawdust or excelsior	2 (2%)	0 (0%)	\$0.0 (0%)
Non-upholstered chair, bench or vehicle seat	2 (2%)	0 (0%)	\$0.0 (0%)
Light vegetation including grass	1 (1%)	0 (0%)	\$0.0 (0%)
Tire	1 (1%)	0 (0%)	\$0.0 (0%)
Box, carton, bag, basket or barrel	1 (1%)	0 (0%)	\$0.0 (0%)
Railroad tie	1 (1%)	0 (0%)	\$0.0 (0%)
Other known item first ignited	8 (8%)	0 (0%)	\$0.0 (3%)
<b>Total</b>	<b>106 (100%)</b>	<b>2 (100%)</b>	<b>\$0.3 (100%)</b>

Figure 64 - Rail Fire Sources USA, 2005-2009 (Hall, 2011)

## Appendix E: Obscuration – Visibility Calculations

The following equations are derived from (McGrattan). The conversion is made from beam detector obscuration to visibility.

- 1) Percent Obscuration=obs =  $(1 - \exp(-K_m \sum \rho_{soot} \Delta x)) * 100$
- 2) Light Extinction Coefficient  $K = K_m \rho Y_s$
- 3) Visibility =  $S = C/K$

Constants are:

$K_m$  = mass extinction coefficient = 8700 m<sup>2</sup>/kg

$\Delta x$  = beam detector path length = 1.4 m (as input to FDS) (2.0 for V6 & V7)

$Y_s$  = Soot production = .09 kg/kg (as input to FDS, not used here in calculation but used internally by FDS)

C=3 (FDS Default, for light reflecting signs)

In Equation 1),  $\rho_{soot}$  is equal to  $\rho Y_s$

K is obtained from equation 1).based on the fact that  $\rho_{soot}$  is equal to  $\rho Y_s$ . (Thus it is solved for  $\rho_{soot} K_m$ ) with obs known as FDS output.

$$\rho_{soot} K_m = \rho Y_s K_m = K = \frac{\ln(1 - \frac{obs}{100})}{-1.4m}$$

Visibility =  $C/K = 3/K$

## Appendix F: Literature Review of Window Failure

In the full scale subway carriage test in the EUREKA fire tests, windows were heard to be broken as early as 2 minutes into the test, continuing through to 42 minutes. Windows were polycarbonate (Beyler). In (Strege, 2003), polycarbonate train windows were tested to determine fallout times. For a .0125 m thick window, of dimensions .6 m high x 1.37 m wide, exposed to a line fire producing a heat flux of 25-30 kW/m<sup>2</sup>, window fallout times were 6 minutes. When the single sheet was replaced by two sheets of smaller area (.6 x .68 m each), the fallout time was 12.2 minutes. In (Beyler), simulations were conducted which indicated that window fallout in a rail or subway carriage would lead to a large increase in HRR (between 3 & 27 MW), depending upon fuel availability.

Shields (Shields T. S., 1998) conducted testing on a full scale office. The windows in the unit were large and double glazed. At 675 °C, the window began to fracture and fall off.

The temperature difference between glass sides exposed to fire and unexposed has been found in a number of studies to be a determining factor in glass cracking. The NRCC conducted tests in room fire conditions. They found that tempered glass shattered upon initial cracking. An exposed temperature of 290-380 °C, was recommended, with an unexposed side of 100 °C. Plain glass (unspecified thickness), was found to 'break' when the exposed side reached 150-175 °C and the unexposed between 75-150 °C. (Brabrauskas).

The Building Research Institute of Japan conducted a series of tests allowing a probability distribution of glass fallout to be reached. The charts are shown below. The tested windows were 3 mm single pane glass. The mean glass pane temperature at fallout was 240 °C with a standard deviation of 50 °C, while the mean gas temperature was 360 °C, also with a standard deviation of 50 °C (Brabrauskas).

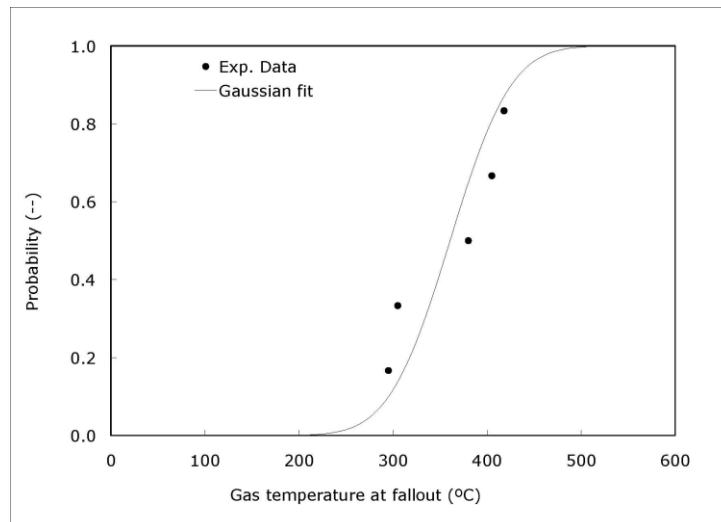
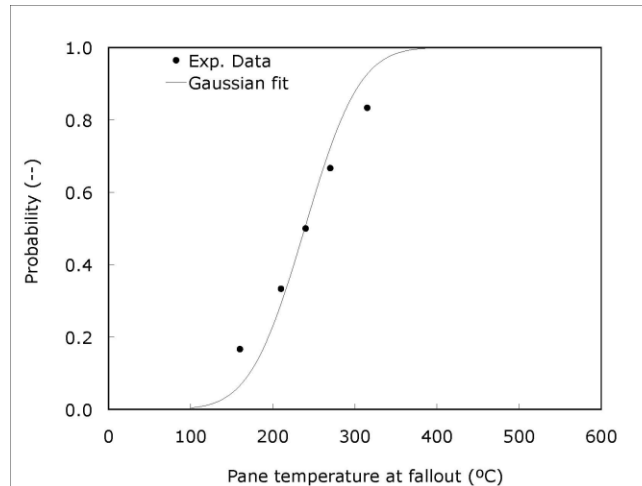


Figure 65 - Gas Temperature at Fallout (Brabrauskas)



**Figure 66 - Pane Temperature at Fallout (Brabrauskas)**

Tests were conducted by Shields, Silcock, and Hassani, on 6mm thick double glazed windows. While gas temperatures in the room reached up to 750 °C, no glass fallout occurred. In only one of the three tests did window fallout occur, happening as temperatures were declining. In this test, the inner pane fell out at a temperature of 500 °C (Shields T. S., 1997/1998).

The Loss Prevention Council of the UK conducted room fire tests using double glazed windows, each of 6 mm thickness. Using a 3 MW crib fire, the glass started to fall out at 600 °C, after 8 to 10 minutes at this temperature. When the same test was conducted in a fully furnished room, the glass also began to fall out at 600 °C, but this occurred immediately (Brabrauskas). This could be due to differences in pressure rise or rate of temperature rise caused by a 3 MW crib fire verse a fully furnished room.

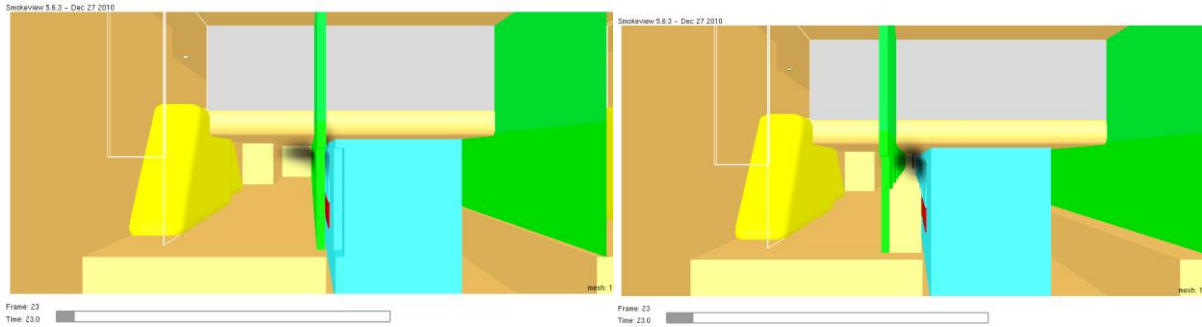
It is also recognized that various other factors outside of temperature may control window failure, from incident heat flux, to the method of installation & sealing. For the station being simulated in this project, double glazed windows are installed in the carriages. The guidelines suggested by the Loss Prevention Council of the UK will be followed, with window breakage occurring at 600 °C



## Appendix G: Effect of PSD design on smoke spread

The following illustrates the effect of platform screen door design on ability to limit smoke spread. With screens placed further from the platform, the buoyancy of the hot smoke can be utilized.

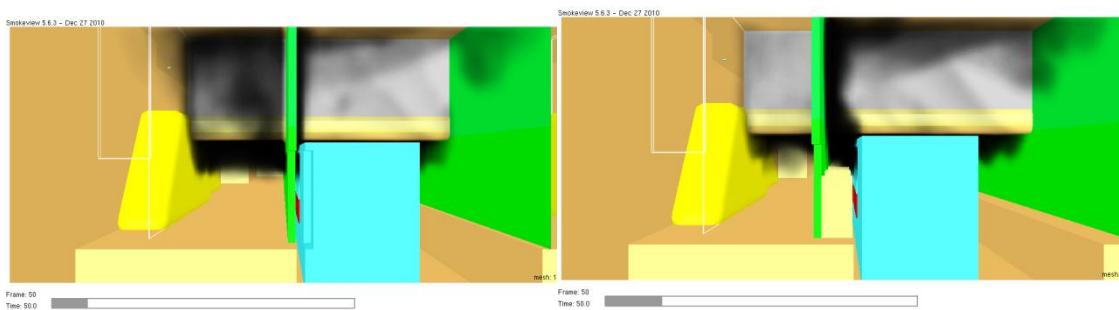
*23 Seconds (original design on left, revised on right)*



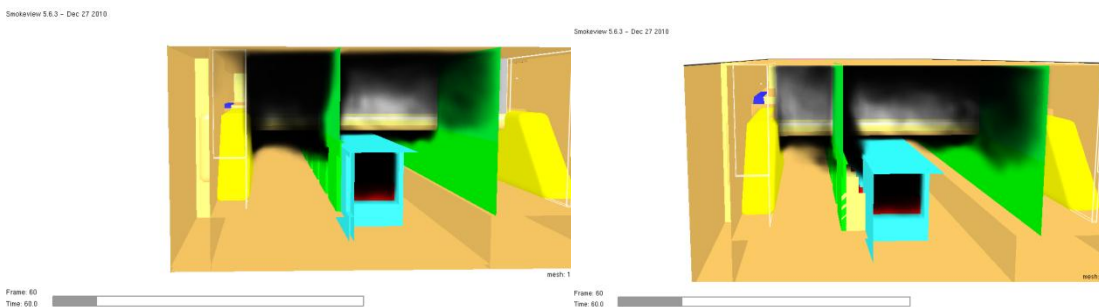
*30 Seconds (more smoke clearly being caught within PSDs in the right image):*



*50 seconds*



*60 Seconds*



Even at 300 seconds, the opposing platform is kept clear (assuming doors are left closed, no leaks occur, and glass does not break). The platform level is shown below with the revised platform screen doors:

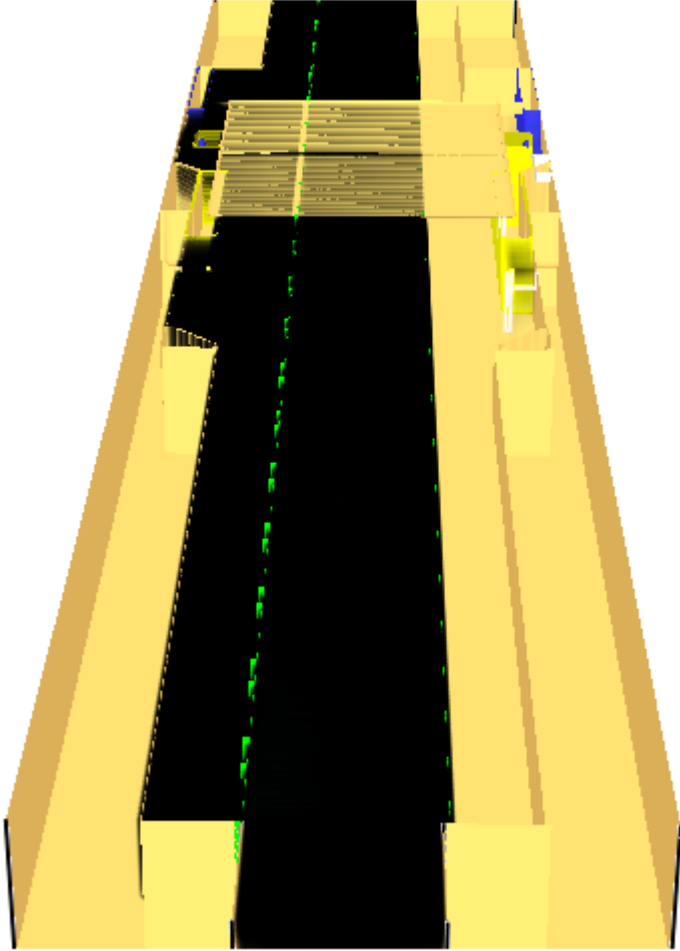
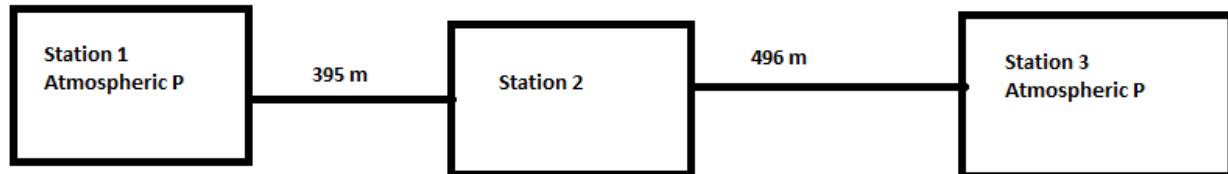


Figure 67 - Revised PSD, 300 seconds, platform B clear

## Appendix H: Calculations for Dynamic Pressure Boundaries

These pressure loss calculations assume that the previous and subsequent stations in the subway system are at atmospheric pressure. The inherent assumption is that some type of ventilation is present in these stations, for example for everyday ventilation or for cooling the tracks, such that ambient pressure results. Pressure loss occurs from through the tunnel lengths. The change in elevation between stations 1 and 2 is approximately 5.6 meters, and 9.2 meters between 2 and 3.



### Method 1:

Equation taken from (Colella, 2010). The pressure loss approximation is based on experimental data from several road tunnels.

$$\Delta p \approx 0.4\Delta z$$

Where  $z$  represents the altitude difference between portals.

$$1-2: \Delta p \approx 0.4 * 5.6 = 2.24 \text{ Pa}$$

$$3-2: \Delta p \approx 0.4 * 9.2 = 3.68 \text{ Pa}$$

### Method 2

Using the Darcy-Weisbach equation:

$$\Delta p = f \frac{L}{D} \frac{\rho V^2}{2}$$

Assuming that  $V = 1 \text{ m/s}$  (here we are looking at velocity induced in absence of forced ventilation)

$$\text{Hydraulic Diameter } D = 4A/P = (4*6*8)/(6+6+8+8) = 6.85 \text{ m}$$

$$\text{Air density } = \rho = 1.2 \text{ kg/m}^3$$

$$f = \text{friction factor} = \frac{1}{\left(2 \log\left(\frac{3.7}{\epsilon_t}\right)\right)^2} \text{ for fully rough flow (Reynolds number} = 437317 \text{ at this velocity)}$$

$$\text{Where } \epsilon_t = \frac{\epsilon_t}{D}$$

$\epsilon_t$ =tunnel wall absolute roughness = .085 m (taken for concrete from (Montecinos, 2010))

$$\text{Thus } \epsilon_t = \frac{\epsilon_t}{D} = \frac{.085}{6.85} = .012$$

$$\text{Therefore friction factor } = f = \frac{1}{\left(2 \log\left(\frac{3.7}{.012}\right)\right)^2} = .041$$

This value is doubled, to take into account obstructions and tunnel objects such as cables. Therefore, a value of .085 is used.

$$: \Delta p_{1-2} = f \frac{L}{D} \frac{\rho V^2}{2} = .082 \frac{395}{6.85} \frac{1.2 * 1^2}{2} = 2.82 \text{ Pa}$$

$$\Delta p_{3-2} = f \frac{L}{D} \frac{\rho V^2}{2} = .082 \frac{496}{6.85} \frac{1.2 * 1^2}{2} = 3.56 \text{ Pa}$$

The resulting pressure drops from methods one and two are fairly similar. Therefore, the values for method two were used as dynamic pressure boundaries in FDS at the respective tunnel portals.

# Appendix I: Visibility Comparison, Stairwell Pressurization vs. Push-Pressurization

It is seen that when smoke is pushed, the left side of the station at platform is kept clear, but the concourse becomes flooded with smoke much quicker. Taken at 180 seconds.

Smokeyview 5.6.3 - Dec 27 2010

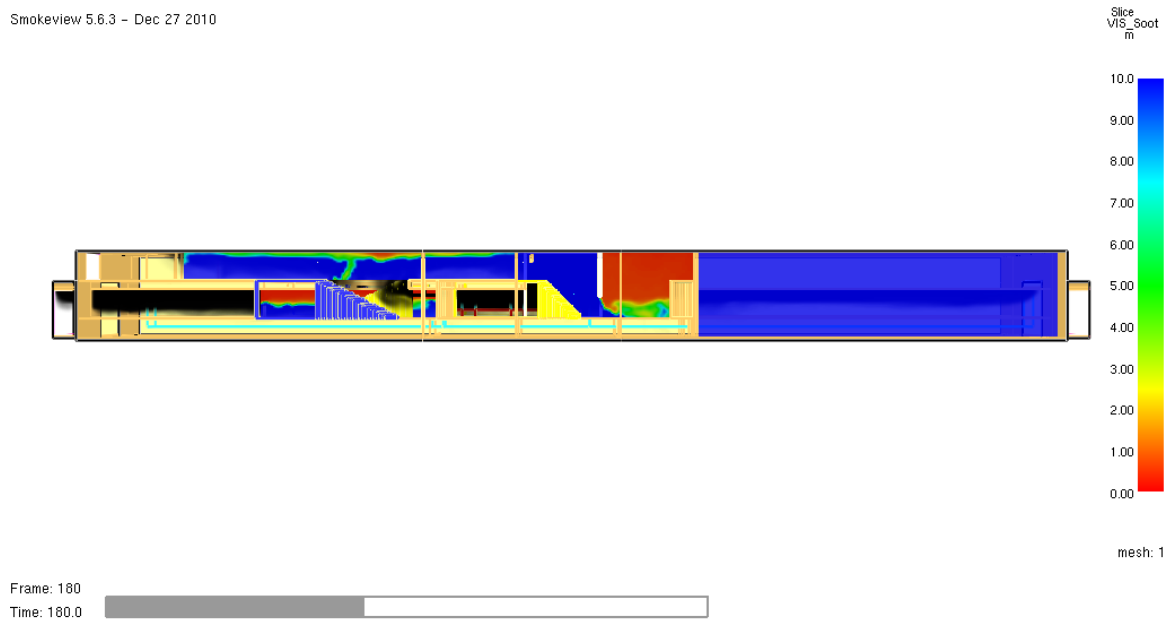


Figure 68 - Smoke Spread and visibility at X=2.6 m. Stairwell pressurization only, 180 seconds

Smokeyview 5.6.3 - Dec 27 2010

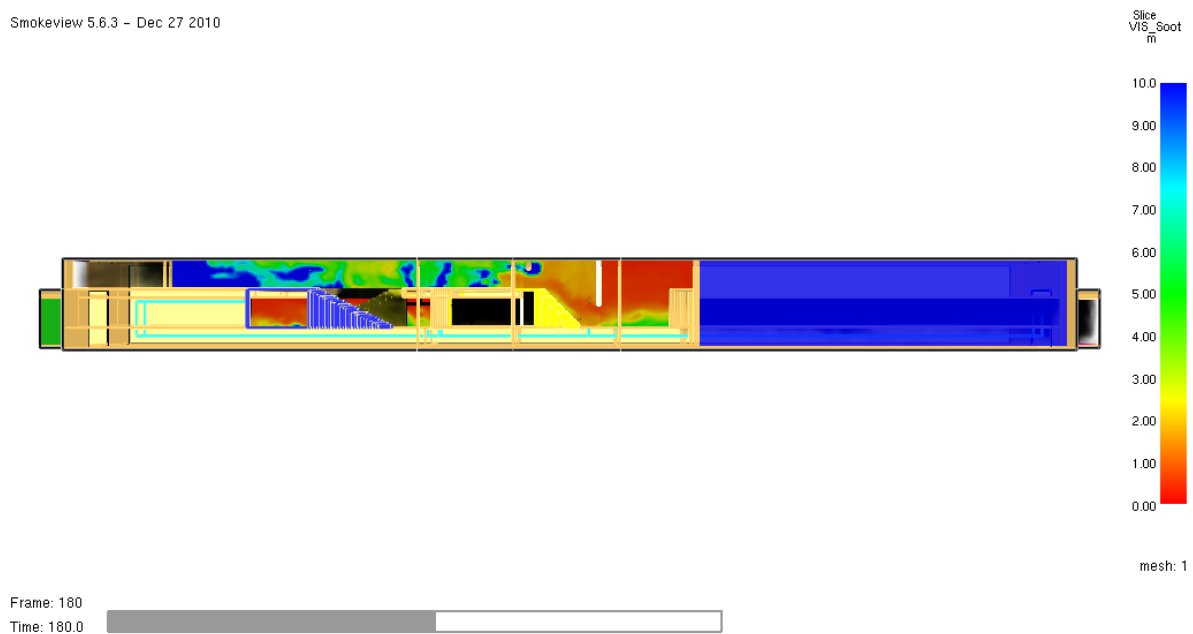


Figure 69 - Smoke Spread and visibility at X=2.6 m. Stairwell Pressurization + Push of 3 m/s from left tunnel portal., 180 seconds Less smoke spread seen at platform level, more spread at concourse level.

## Appendix J: Slices of specific cases and miscellaneous images

review 5.6.3 – Dec 27 2010

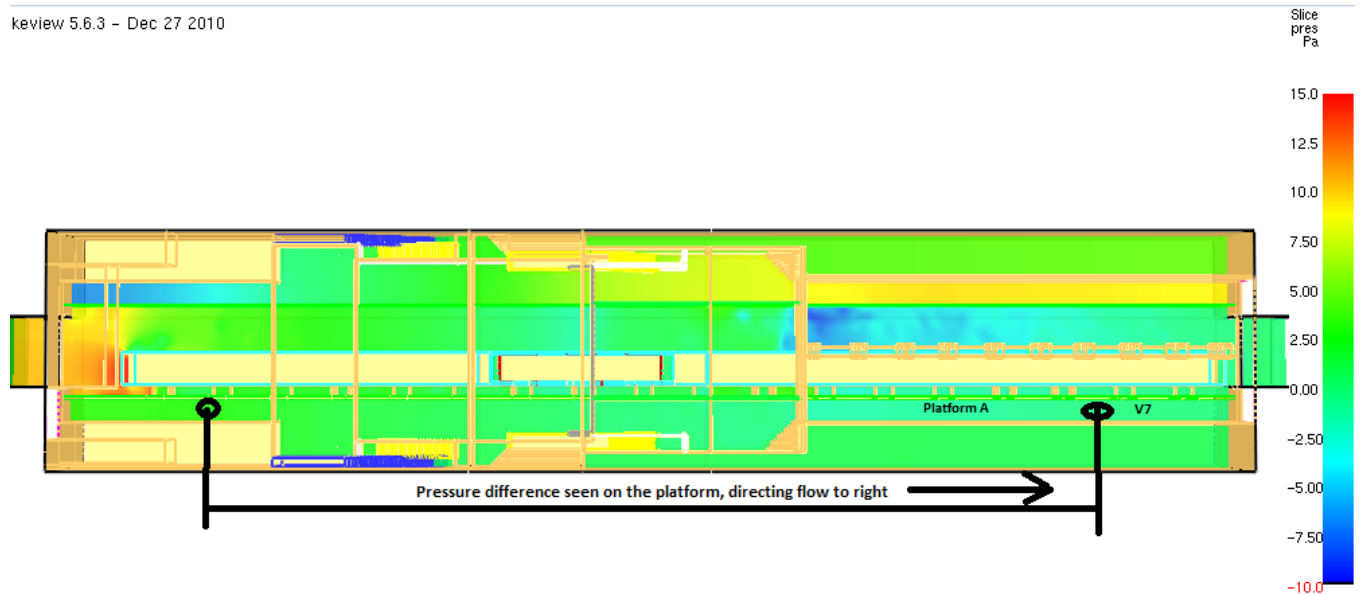


Figure 70 – Pressure slice. For Push, Ceiling Exhaust, Revised PSD, Stairs Enclosed configuration. Top view. Z=3 (.8 meters above platform height). Time=30 seconds Pressure difference seen on platform which drives flow to right. Causing V7 to be exceeded quicker and V1 and V3 (not shown, at concourse level) to be tenable for much longer.

review 5.6.3 – Dec 27 2010

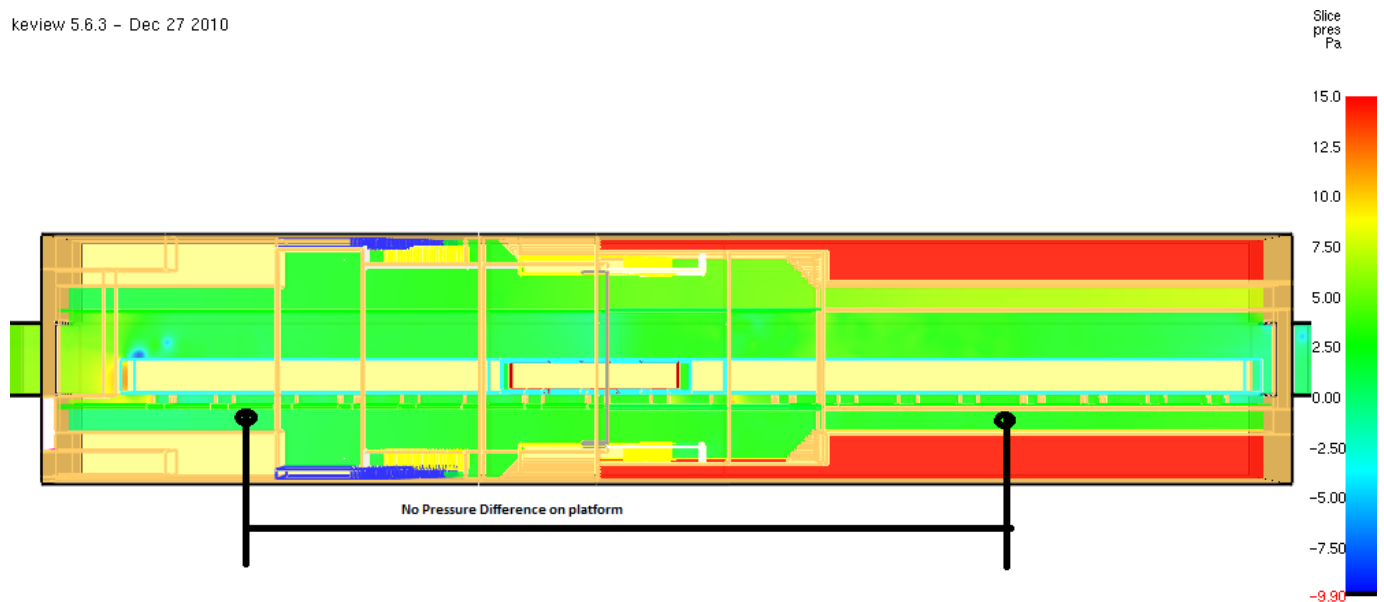


Figure 71 - Pressure slice for push, side exhaust, revised PSD, stairs enclosed configuration. Top View Z=3 (.8 meters above platform height). Time=30 seconds. Little pressure difference seen, therefore flow is not directed to the right as much and thus smoke flow occurs quicker to V1/V3 on the concourse.

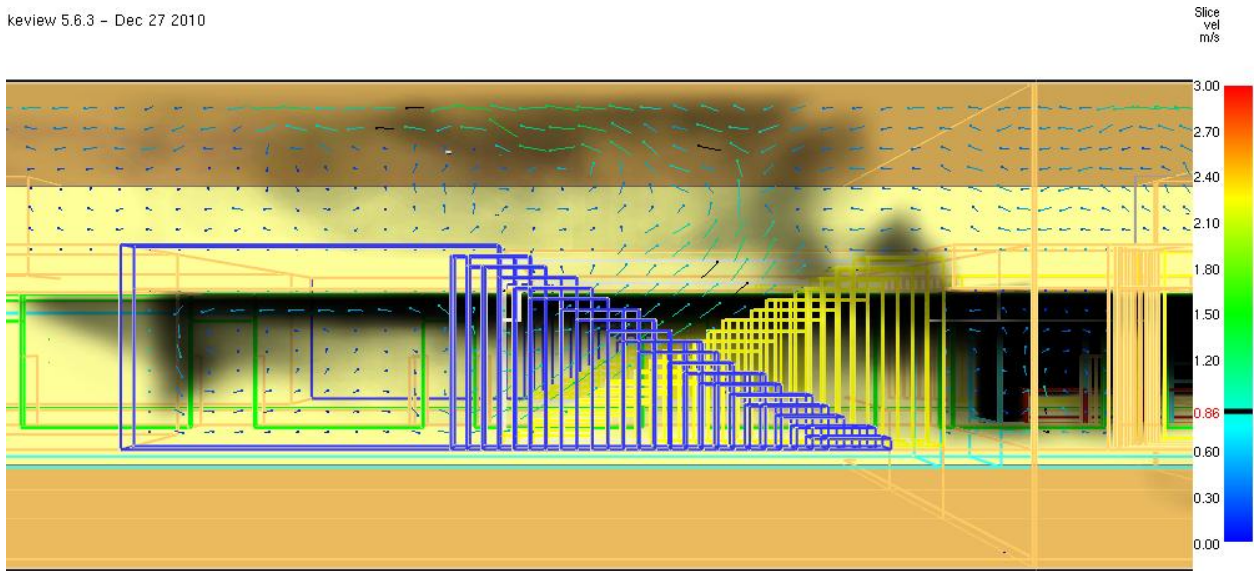


Figure 72 - Velocity vectors stairwell 2. Side view. Push, Side Exhaust, Revised PSD, Stairs Enclosed. It is seen that velocity vectors move from platform to concourse, allowing smoke spread. Time=83 seconds.

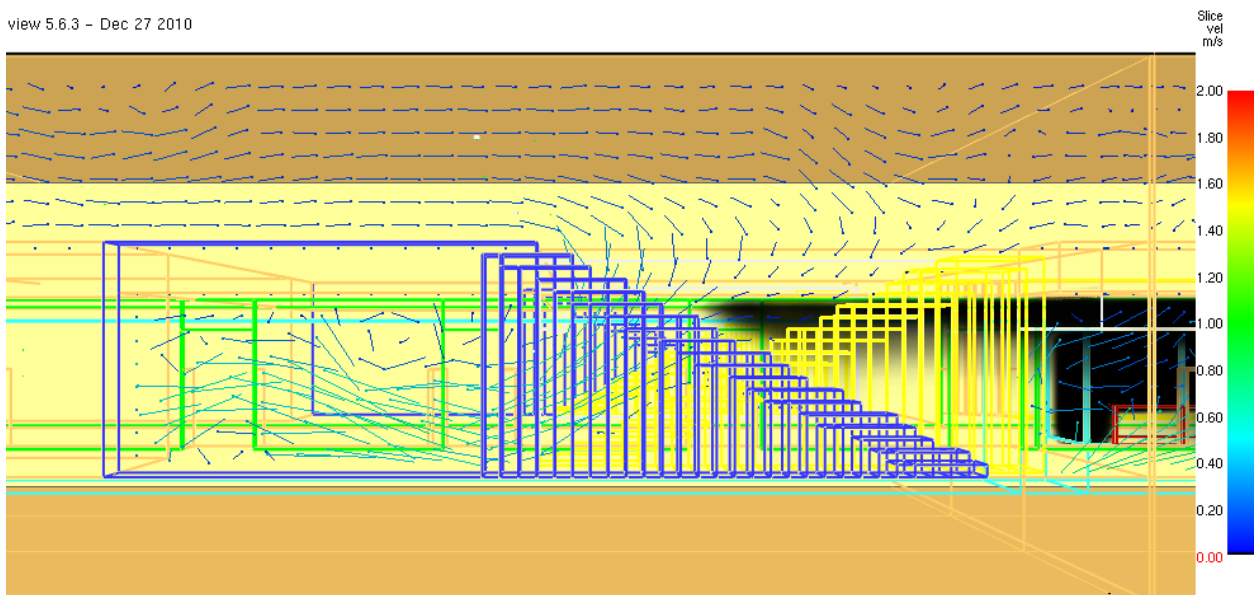
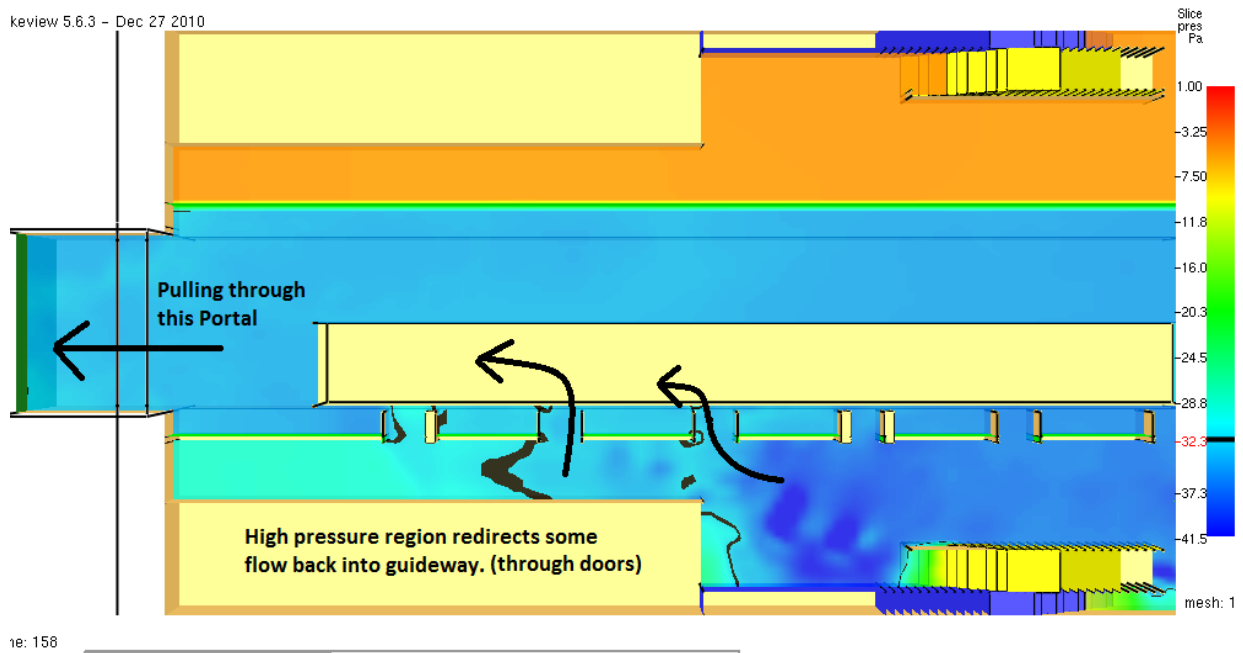


Figure 73 -Velocity vectors stairwell 2. Side view. Push, Ceiling Exhaust, Revised PSD, Stairs Enclosed. It is seen that velocity vectors move from concourse to platform, delaying smoke spread to concourse. Time=83 seconds.



re: 158

Figure 74 - Pull - Pull with PSD Revised. Left tunnel portal shown. Top-view shows platform level only. Visibility maintained in higher pressure region on platform (corresponding to where V6 is located). Time=160 seconds. Concourse visibility also maintained due to make-up air entering from concourse level.

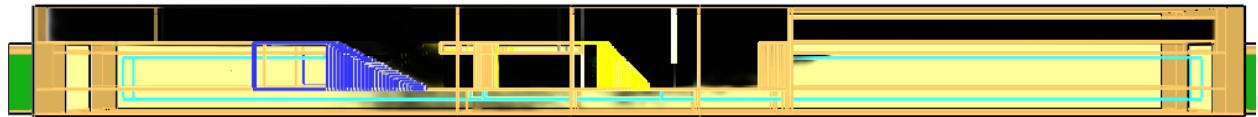


Figure 75 - Push-Push Side Exhaust Stairs Enclosed. Smoke Spread. Platform ends kept clear. Shot at 240 seconds

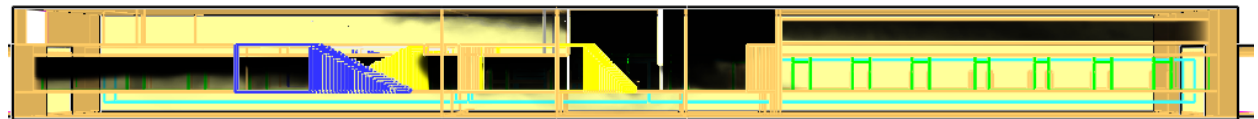


Figure 76 -Side View of smoke spread. 500 kW Fire. 420 Seconds. Side Exhaust, Revised PSD, Stairs Enclosed.



Figure 77 - Top View of smoke spread. 500 kW Fire. 420 Seconds. Side Exhaust, Revised PSD, Stairs Enclosed



## Appendix K: Temperature plots

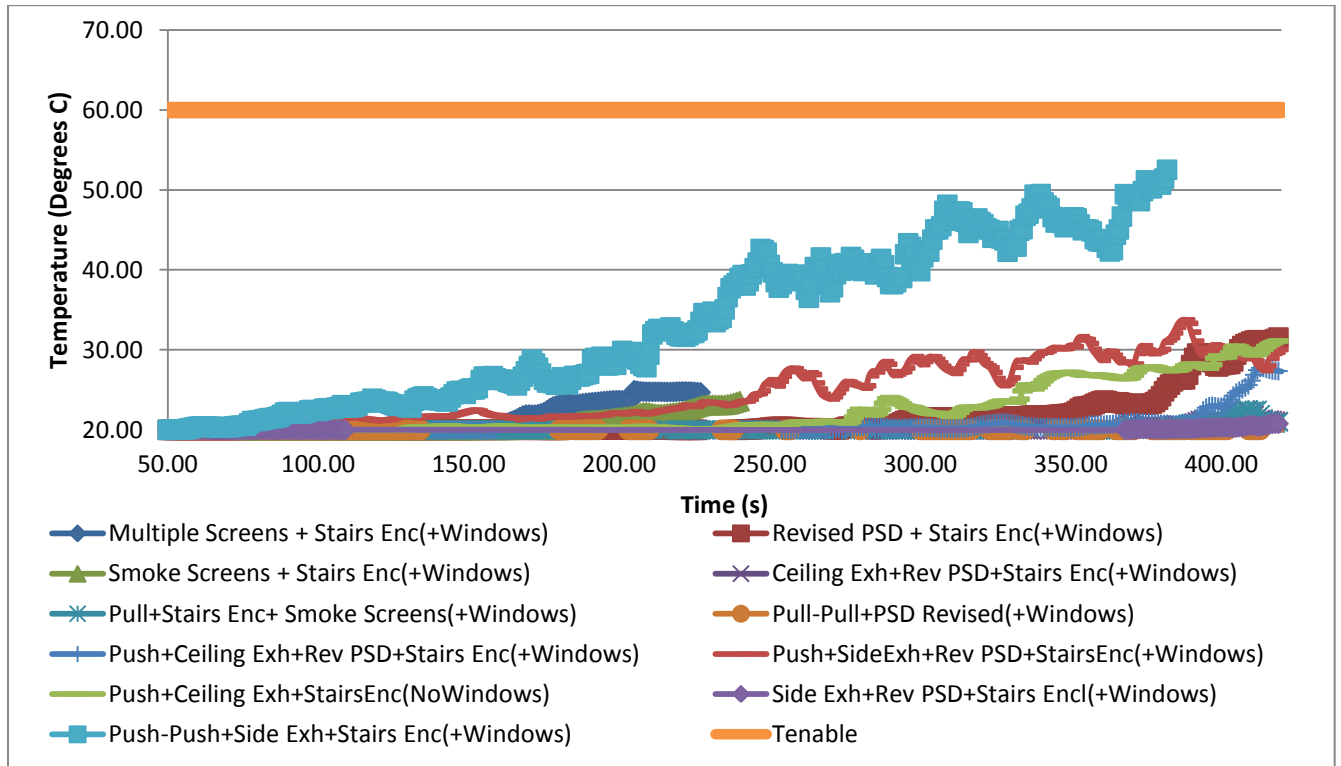


Figure 78 - Temperature vs Time at point T3. No case exceeds 60 degrees Celsius.

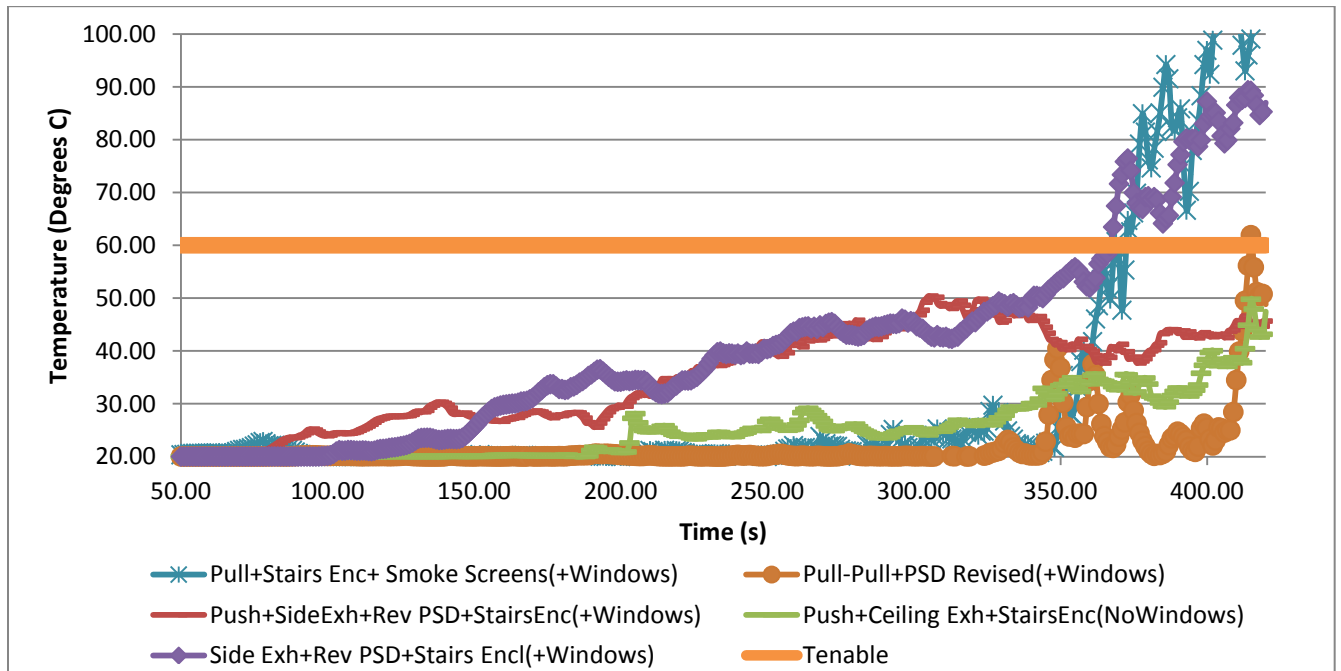


Figure 79 - Figure 76. Temperature vs Time at point T5 (half of the cases from Table 6 shown)

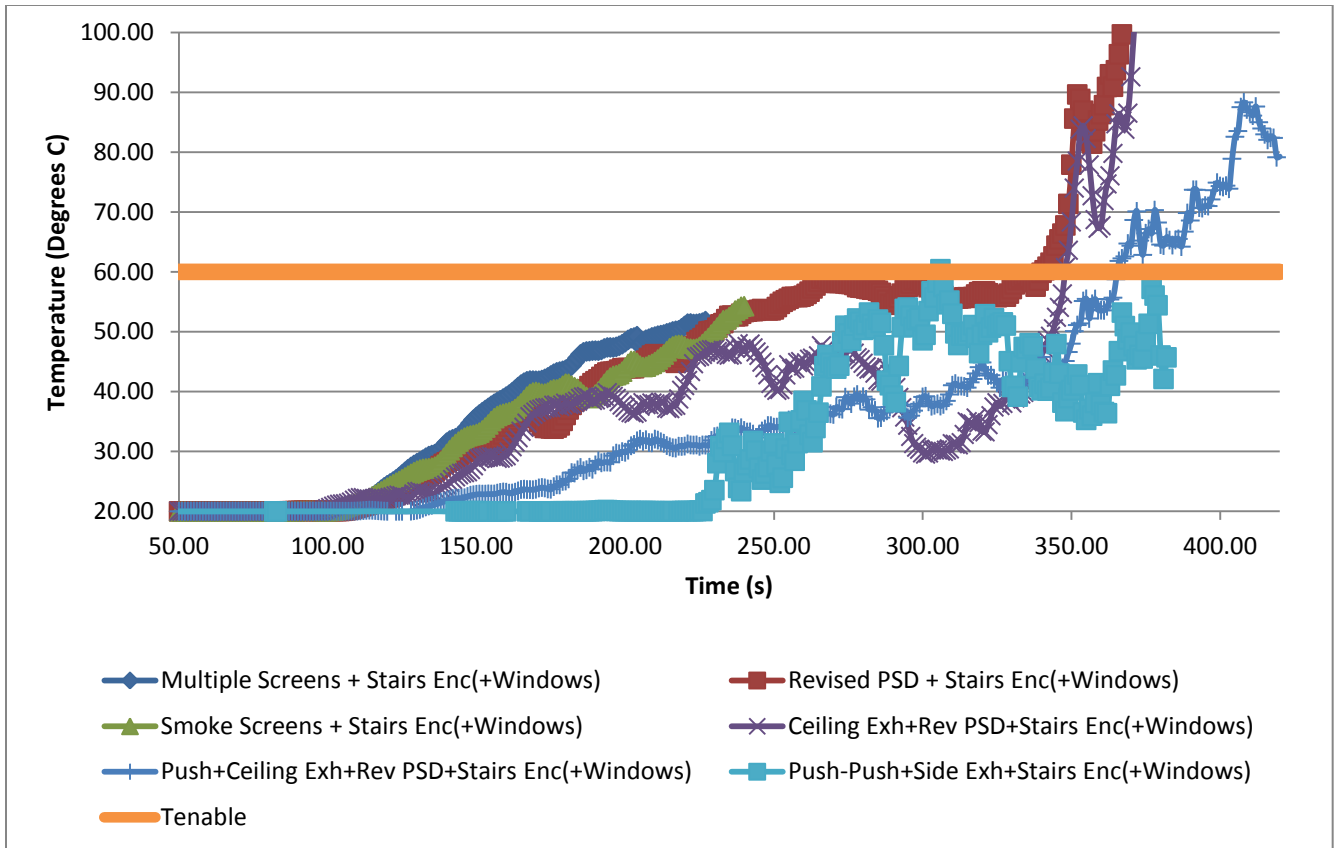


Figure 80 - Temperature vs Time, Point T5. Half of the cases from Table 6

## Appendix L: Screen shots of Case V and II

Case V (pull-pull revised PSD stairs enclosed): Best performing case. Concourse, platform B, and V6 maintained tenable at 4 minutes.



Figure 81 - Smoke spread at 4 minutes. Case V. Side view.

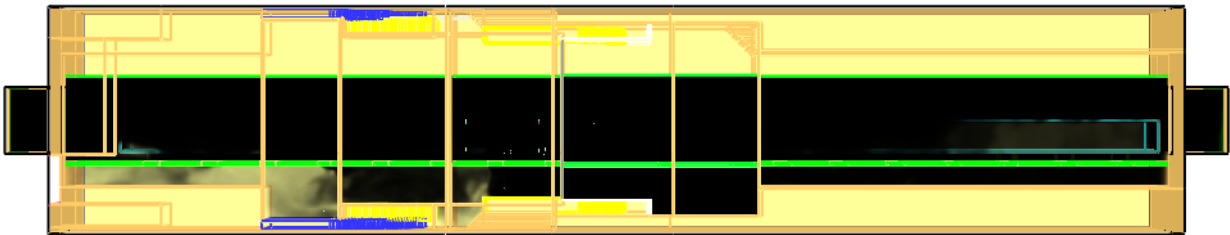


Figure 82 – Smoke spread at 4 minutes. Case V. Top View

Case II (side exhaust, revised PSD, stairs enclosed), maintains tenable conditions at 4 minutes on the concourse, right side of platform(V7), and platform B. Visibility is lost quicker on the concourse than Case V as well as at V5 and V6, therefore the ranking is lower.

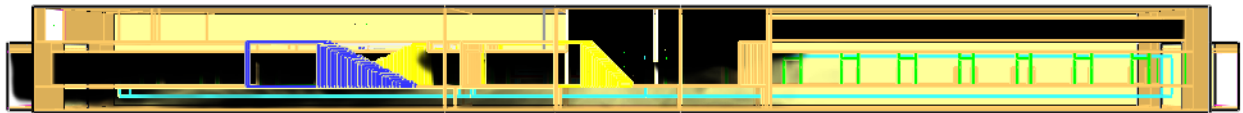


Figure 83 – Smoke spread at 4 minutes. Case II. Side view.

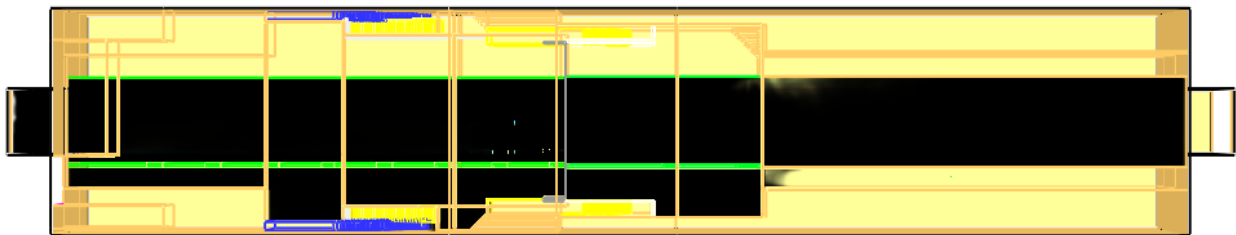


Figure 84 - Smoke spread at 4 minutes, Case II. Top view.